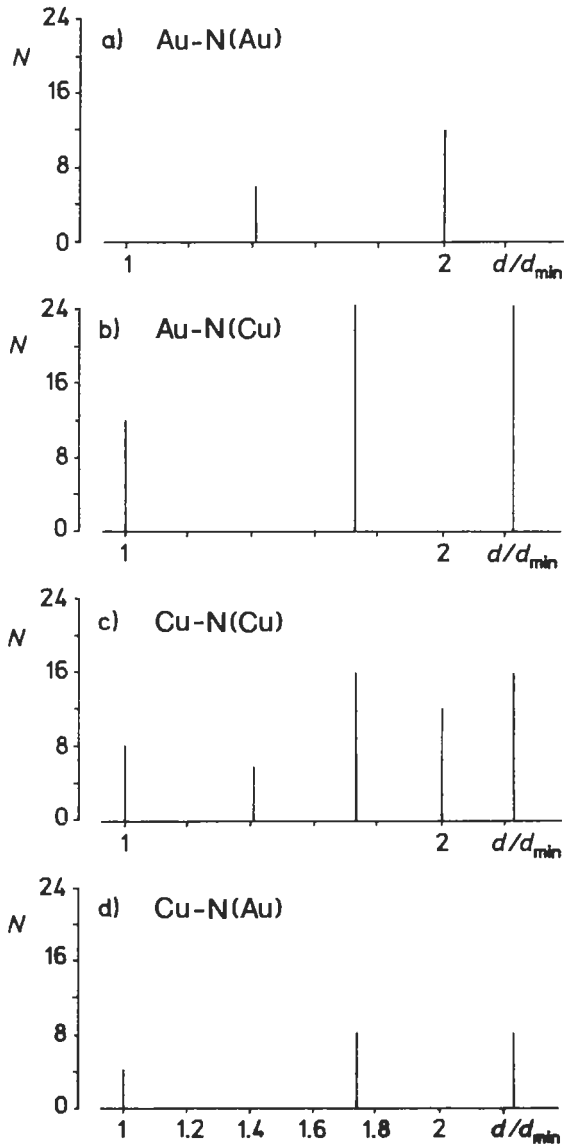

Fig. 15. cP4–$AuCu_3$ type structure. Coordinations and distances. For each type of coordination the numbers (N) of near-neighbours atoms are plotted as a function of their distances from the central atom. (Relative values of the distances, d/d_{min}, have been used. In these histograms and in the subsequent ones d_{min} is the shortest interatomic distance observed in the structure. For details see the comments reported in sec. 3.5.5.)

distance d = 592.7 pm, $d/d_{min} = 2.236$, etc. The corresponding coordination histogram is presented in fig. 15d.

References: p. 363.

Lists of coordinating atoms (with distances from the references atom), coordination polyhedra, and next-neighbor histograms are presented systematically by DAAMS *et al.* [1991]. They, however, use a more compact representation giving for each atom in a given site the histogram corresponding to the total coordination. In our case, for Au the sum of the two histograms reported in figs. 15a and b and for Cu the sum of the histograms of figs. 15c and d. (Compare with fig. 25). For the different structures, moreover, the distances are related by Daams et al. to the d_{min} observed in each coordination group instead of to the d_{min} of the overall structure as adopted here.

As a conclusion to the *description* of the different *coordinations* we may observe that those corresponding to the first distance sets are summarized in the symbol $3\overset{3}{\underset{3}{3}}[A_{6/6}][B_{8/8}]_{12/4}$. ($3\overset{3}{\underset{3}{3}}[Au_{6/6}][Cu_{8/8}]_{12/4}$ for the prototype). In terms of *polyhedra packing*, therefore, this structure may be described as a tridimensional arrangement of cubooctahedra (see sec. 3.5.3.).

Fig. 16, on the other hand, shows how for the same structure, alternative descriptions (*layer stacking sequence descriptions*) may be obtained and, according to Pearson, symbolized. In this figure the structure (viewed along the cube diagonal) is presented as a *stacking sequence* of *triangular* and *kagomé nets*. It corresponds to the symbol $Au_0^A\, Cu_0^\alpha\, Au_{1/3}^C\, Cu_{1/3}^\gamma\, Au_{2/3}^B\, Cu_{2/3}^\beta$ (In the symbol we have the same number of triangular (A,B,C) Au atom nets and of kagomé (α,β,γ) Cu atom nets. These two net types are characterized by the presence of 1 and 3 points in the unit cell (see figs. 8 and 10). This, of course, corresponds to the total 1:3 stoichiometric ratio). The same structure, viewed along the unit cell edge direction, corresponds to a *square net stacking sequence* (see fig. 13). The stacking symbol is $Au_0^1 Cu_0^4 Cu_{1/2}^5$ (These different symbols may be useful when comparing this structure with other structural types: for instance, the cF4–Cu type, sec. 6.2.1., tP2–AuCu(I) type, sec. 6.2.4., etc.).

With reference to a description in terms of *lattice complex combination*, we may

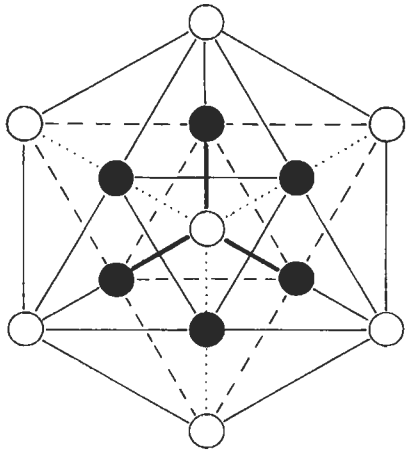

Fig. 16. cP4–$AuCu_3$ type structure. The unit cell is viewed along its diagonal. (Au atoms white, Cu black). The triangular arrangements of the atoms around the cube diagonal are evident.

finally note that the $AuCu_3$ type structure corresponds to a combination of P and J complexes (**Au**Cu_3: **P** + J; see sec. 3.1.). According to HELLNER [1979] this structure may be considered as pertaining to a F-family as a consequence of a particular splitting of the points of the F complex.

A few other comments on the $AuCu_3$ type structure and some remarks on the relationship with other structural types will be reported in the following sec. 6.2.3.).

4. Relationships between structures and structure "families"

As clearly pointed out, for instance, by BÄRNIGHAUSEN [1980] (see sec. 4.6.), one of the main objectives of crystal chemistry is to order the profusion of structure types and to show the general principles involved. To this end relations between cognate structures evidently play an important role.

The structures corresponding to different types may often be interrelated on the basis of some transformation schemes. These schemes can be used as criteria for classifying structure types and showing structural relationships.

A few selected groups of interrelated structural types will be presented in the following sections.

4.1. Degenerate and derivative structures, superstructures (defect, filled-up, derivative structures)

An important and general scheme of structure transformation and interrelation is that described, for instance, by PEARSON [1972], by means of the concept of *derivative structures* and *degenerate structures.*

A *derivative structure* can be considered being obtained from a reference structure by ordered atomic substitution, subtraction or addition processes or by unit cell distortions (or both). The opposite kinds of transformation correspond to the so-called *degeneration processes.* A derivative structure has fewer symmetry operations than the reference structure (a degenerate one has more). A derivative structure has either a larger cell or a lower symmetry (or both) than the reference structure.

It is possible, for instance, that a set of equipoints of a certain structure (considered as the reference structure) has to be subdivided into two (or more) subgroups in order to obtain the description of another ("derivative") structure. The structure of the Cu type (cF4-type), for instance, corresponds to 4 Cu atoms in the unit cell, placed in 0,0,0; $\frac{1}{2},\frac{1}{2},0$; $\frac{1}{2},0,\frac{1}{2}$; $0,\frac{1}{2},\frac{1}{2}$, whereas in the cP4–$AuCu_3$ type structure the same atomic sites are subdivided into two groups with an ordered distribution of the two atomic species (1 Au atom in 0,0,0, and 3 Cu atoms in $\frac{1}{2},\frac{1}{2},0$; $\frac{1}{2},0,\frac{1}{2}$; $0,\frac{1}{2},\frac{1}{2}$). The $AuCu_3$ type structure can, therefore, be considered as a derivative structure of the Cu type. On the other hand, if we consider the $AuCu_3$ type as the reference structure, we may describe the Cu type as a degenerate structure.

The aforementioned subdivision of a set of equipoints in more groups can be described in this case in terms of similar cubic cells (both of the original and of the derivative structures). Notice, however, that in the case of Cu the conventional cubic cell

is face-centered. It is not primitive: it corresponds to 4 (rhombohedral) primitive cells, whereas, in the case of $AuCu_3$ the primitive unit cell is larger and it is identical to the cube. Because of the observation that these ordering processes may lead to a cell *multiple* of the original one, they are also referred to as forming *superstructures* (also called *superlattices*) (BARRETT and MASSALSKI [1966]) of the original structure. An example where, due to ordering, we observe, perhaps in a more evident immediate way, the increase of the unit cell size (formation of a multiple cell) may be the structure of $MnCu_2Al$ type (see fig. 24 and sec. 6.1.3) which can be considered a derivative structure (*superstructure*) of the cP2–CsCl type structure (which in turn is a superstructure of the W-type structure, corresponding to a, non-primitive cubic, cI2 cell).

Notice that the ordering may not lead to a multiple cell, if the symmetry of the ordered structure is reduced, relative to the original one. Nevertheless the name *superstructure* is generally used especially when we have the formation of a disordered solid solution regardless of whether there is multiplication of the edges of the cell.

A contribution to the study of *order-disorder interrelations between structures* and to their *classification into two groups on the basis of the presence/absence of a difference in the translational symmetry* (unit cell edge variations) has been given by WONDRATSCHEK and JEITSCHKO [1976] and by ALBERING *et al.* [1994]. (The detectability of the two types of ordering by means of X-ray diffraction studies has been also discussed).

ALBERING *et al.* [1994] especially studied the hP3–AlB_2 type structure and its derivatives. A few of these are presented in fig. 17. A detailed description is given in sec. 6.5.6. Main features of several deformation and substitution derivatives of the AlB_2-type were discussed by GLADYSHEVSKII *et al.* [1992].

A more complex case of structure interrelation which can be presented in terms of (even if "formal") substitution is that which can be exemplified by considering structures such as those of NaCl (see fig. 18 and a detailed description in sec. 6.4.1.) and FeS_2 or CaC_2. These structures may be compared: the cP12–FeS_2 type may be described as having Fe atoms in the sodium ion positions and the centers of the discrete S_2 dumb-bell groups at the chlorine ion positions. The passage from a structure containing spherical atoms to another one in which atomic groups substituted single atoms will generally result in a symmetry reduction. A clear example may be given by the tI6–CaC_2 type which can also be compared with the NaCl type: Ca is in the sodium positions and the C_2 group in the chlorine positions. In this case, however, the long axes of the C–C groups are all aligned in one direction so that the unit cell is tetragonal instead of cubic. (See fig. 4 and a description of this structure and a comparison with the $MoSi_2$-type in sec. 3.2.). In a similar way, we may, for instance, consider the K_2PtCl_6 structure essentially the same as the CaF_2–antitype: the K ions are in the F ion positions and the centers of the $PtCl_6$ octahedral groups in the Ca ion positions.

Derived structures may also be formed with the *ordered introduction of vacant sites*. As an example we may consider the hP3–CdI_2 type structure (see sec. 6.5.2) which can be related to the hP4–NiAs type structure in which the set of equivalent points 0,0,0 and $0,0,\frac{1}{2}$ is considered as being subdivided into two groups (each of 1 site) 0,0,0, (occupied by 1 atomic species) and $0,0,\frac{1}{2}$ (vacant). We can, therefore, regard the hP3–CdI_2 type structure as a *defect derivative* form of the hP4–NiAs type.

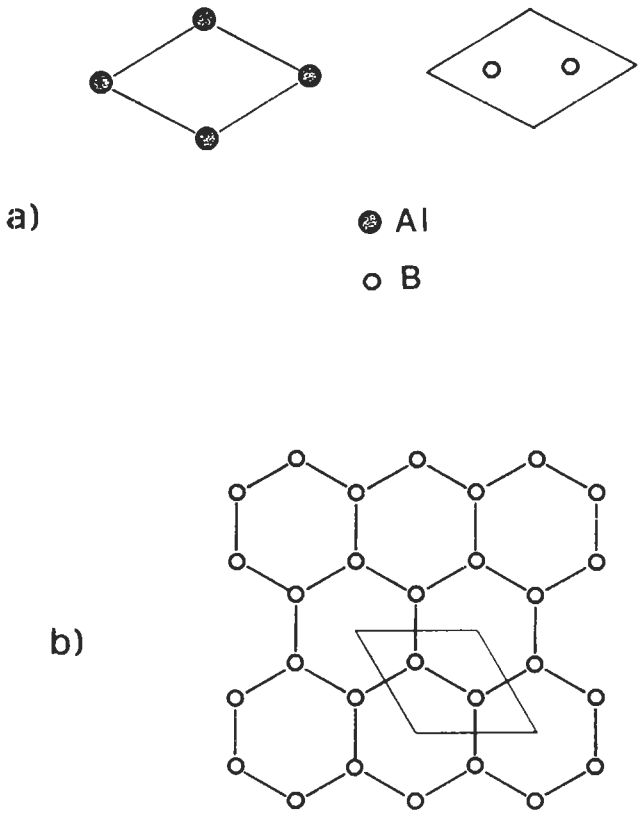

Fig. 17a,b. AlB_2–type and derivative structures.

a) Two sections of the hP3–AlB_2 unit cell are presented at the height $z=0$ (Al atoms) and $z=\frac{1}{2}$ (B atoms), respectively.

b) The corresponding hexagonal net of B atoms in AlB_2 is shown (a projection of the unit cell is superimposed. (Compare with fig. 9). The Al atoms (at the cell origin) are surrounded by 12 B, arranged in a hexagonal prism, and the B atoms are in sixfold coordination with Al, in the center of an Al trigonal prism.

Similar considerations may be extended to include (besides substitution and subtraction) *ordered addition of atoms*. In this case *stuffed* or *filled-up derivative structures* are considered in which extra atoms have been added in an ordered way, on sites unoccupied in the reference structure. An example is the hP6–Ni_2In structure, which is a stuffed derivative structure of the previously mentioned NiAs structure.

Another interesting example may be the fcc-derivative *interstitial cP5 Fe_4N phase*. It may be described as corresponding to the following atomic positions in the $Pm\bar{3}m$ (or $P\bar{4}3m$) space group:

1 Fe in a): 0,0,0; 1 N in b): $\frac{1}{2},\frac{1}{2},\frac{1}{2}$ and 3 Fe in c): $0,\frac{1}{2},\frac{1}{2}$; $\frac{1}{2},0,\frac{1}{2}$; $\frac{1}{2},\frac{1}{2},0$.

References: p. 363.

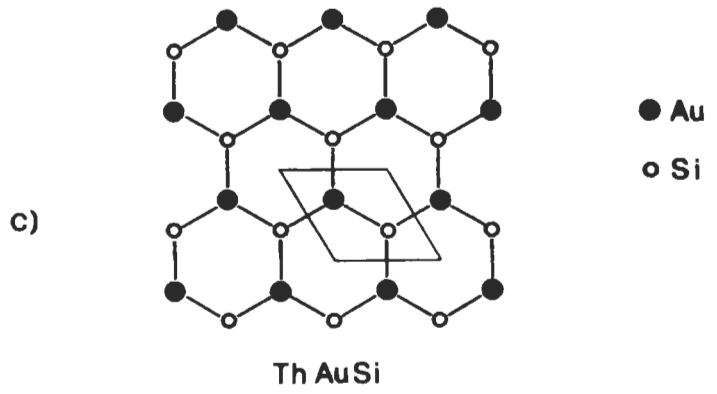

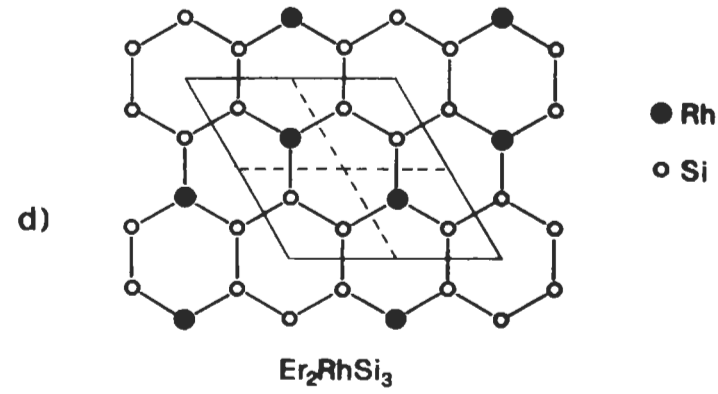

Fig. 17c, d. AlB_2–type and derivative structures.
c) and d) Hexagonal nets observed in AlB_2 derivative structures. In c) the AuSi net of the ThAuSi type structure and in d) the $RhSi_3$ net of the Er_2RhSi_3 structure are shown. In c) and d) the Th and Er positions, corresponding to those of Al in AlB_2, are not shown. The projections of the unit cells are presented: notice the larger cell of the Er_2RhSi_3 structure.

This filled-up superstructure may therefore be described in terms of the occupation by N of an interstice (centered in $\frac{1}{2},\frac{1}{2},\frac{1}{2}$) of a Cu-type (or $AuCu_3$-type) structure. The N atom results octahedrally surrounded by 6 Fe atoms. This structure could also be described as a deficient NaCl-type derivative structure (see sec. 6.4.1.): the Fe atoms are in the same positions as the Na atoms in NaCl and one out of the four Cl positions is occupied by the N atoms.

(For a description and a classification of the "holes", octahedral and tetrahedral, in

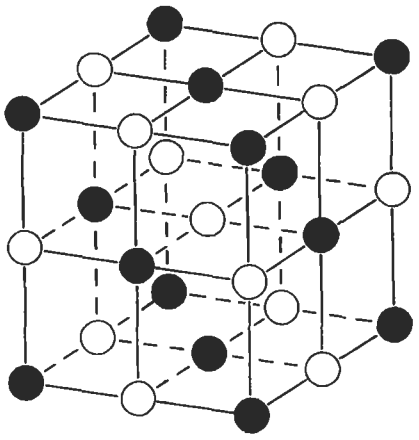

Fig. 18. NaCl-type structure (see sec. 6.4.1.). The positions in the unit cell of the two types of atoms are indicated.

closed packed structures see sec. 6.2.2, see also Hägg phases in sec. 3.4.).

As a footnote to these observations, we have also to mention that frequently structural distortions (axial ratio and/or interaxial angle variations) accompany the formation of derivative structures (especially because of the ordered distribution of atoms of different sizes or of vacant sites).

4.1.1. Ordering-disordering transformation

In a number of metal systems for a given range of compositions depending, for instance, on the temperature, it is possible to observe alloys having both a certain degenerate structure and a corresponding (more or less) ordered derivative structure. The transformation from one structure to the other corresponds to a real process (*ordering–disordering transformation*). A large number of solid solutions become ordered at low temperature.

In the specific case, for instance, of the Au–Cu system an alloy with the $AuCu_3$ composition at high temperature, has the (disordered) cF4–Cu type structure. The two atomic species are equally distributed in the four atomic sites (which are therefore equivalent: each one is occupied by Au with a 25% probability and by Cu with a 75% probability). This random distribution may be also related to the possibility of gradually changing the overall composition of the alloy maintaining the same structure and giving the formation of *solid solutions*. For the Cu–Au alloys we have, at high temperature, a continuous solid solution ranging from Cu to Au (both having the same cF4–Cu type structure): in all the intermediate alloys we have the equivalence of all the atomic sites whose occupation gradually changes from pure Cu to pure Au. By lowering the temperature we have ordering processes corresponding to a change from a nearly random distribution of atoms among the structure sites into more ordered arrangements where certain sites are predominantly occupied by one kind of atom. In the specific case of the

$AuCu_3$ composition we have the transformation from the cF4–Cu type into the described, derivative type (cP4–$AuCu_3$ type) structure.

Typical examples of ordering processes are also the transformation from the β to β' phases in the Cu–Zn system (from cI2–W type to cP2–CsCl type) and the ordering of the FeAl phase in the CsCl type structure (see sec. 6.1.2.). Notice that, ordering in these metallic phases, may be an extremely complex sluggish process requiring slow cooling and/or long annealing of the alloys. Alloy samples with different degrees of ordering can be obtained by quenching at various cooling times. As a consequence the effects of ordering on a number of properties have been studied. Alloys such as Cu_3Au and Fe_3Al have been the subject of many of these studies.

The Au–Cu system, in particular, is one of the earliest systems for which order-disorder type transformations were established. As a result, a very large volume of work has been carried out on the ordered AuCu and $AuCu_3$ phases. The description of the gold–copper system, reported by OKAMOTO and MASSALSKI [1987], may be considered as a reference to the review and to the assessment, not only for the specific system, but also for the investigation methods and discussion criteria of general interest. The following topics have been considered:

Au–Cu phase diagram, Au_3Cu, AuCu, $AuCu_3$ ordered phases (phase boundaries determination by X-ray studies, electrical resistometry, electron microscopy), crystal structure determination (by X-ray and electron diffraction methods), nature of ordering transformation in AuCu, short range order, anomalous behaviour in $AuCu_3$ at high temperatures (specific heat, thermal expansion measurements, etc.). Kinetic studies carried out by measuring gradual shift and intensity variation of the X-ray lines from a disordered to an ordered (superlattice) structure on samples after different quenching and annealing are reported.

For a review on site preference of substitutional additions to CsCl type intermetallic compounds see KAO *et al.*[1994]. In this work dilute additions to NiAl, FeAl and CeAl are especially discussed. As another example we may mention that the addition of a third element to ordered Ni_3Al (cP4–$AuCu_3$ type) occurs in different ways (OCHIAI *et al.* [1984]). For instance Sb, Si, Ge and Ga atoms replace preferably Al, while Cu and Co replace Ni.

As a conclusion to this section, we may mention that a systematic description of ordering processes in alloys and of the superstructures which can be generated has been presented, for instance, by KHACHATURYAN [1983] in the framework of a theoretical treatment of structural transformation in solids. *Two groups of superstructures* have been specially considered: *substitutional and interstitial.*

a) Examples of substitutional superstructures.

tI10–$MoNi_4$: a = 572.0, c = 356.4 pm. Space group I4/m, N.87.

2 Mo in a): 0,0,0; $\frac{1}{2},\frac{1}{2},\frac{1}{2}$.

8 Ni in h): x,y,0; −x,−y,0; −y,x,0; y,−x,0; $\frac{1}{2}+x,\frac{1}{2}+y,\frac{1}{2}$;
$\frac{1}{2}-x,\frac{1}{2}-y,\frac{1}{2}$; $\frac{1}{2}-y,\frac{1}{2}+x,\frac{1}{2}$; $\frac{1}{2}+y,\frac{1}{2}-x,\frac{1}{2}$, with $x \approx 0.2$, $y = 0.4$.

This superstructure is based on a fc cubic pseudocell. The atoms form close packed layers stacked in a 15 layer close packed repeat sequence.

oI6–$MoPt_2$: a = 276.5, b = 829.6, c = 393.8 pm. Space group Immm, N.71.
2 Mo in a): 0,0,0; $\frac{1}{2},\frac{1}{2},\frac{1}{2}$.
4 Pt in g): 0,y,0; 0,−y,0; $\frac{1}{2},\frac{1}{2}+y,\frac{1}{2}$; $\frac{1}{2},\frac{1}{2}-y,\frac{1}{2}$, with y = 0.353.
It is a close packed superstructure based on a fc cubic pseudocell. Distorted close packed triangular layers are stacked in close packed ABC sequence.

tI8–$TiAl_3$: a = 383.6, c = 857.9 pm, c/a = 2.236. Space group I4/mmm, N.139.
2 Ti in a): 0,0,0; $\frac{1}{2},\frac{1}{2},\frac{1}{2}$.
2 Al in b) 0,0,$\frac{1}{2}$; $\frac{1}{2},\frac{1}{2}$,0.
4 Al in d): 0,$\frac{1}{2},\frac{1}{4}$; $\frac{1}{2}$,0,$\frac{1}{4}$; $\frac{1}{2}$,0,$\frac{3}{4}$; 0,$\frac{1}{2},\frac{3}{4}$.
The superstructure may be described in terms of two, distorted, $AuCu_3$ type subcells stacked one above the other.

tI16–$ZrAl_3$: a = 400.5, c = 1728.5 pm, c/a = 4.316. Space group I4/mmm, N.139.
4 Al in c): 0,$\frac{1}{2}$,0; $\frac{1}{2}$,0,0; $\frac{1}{2}$,0,$\frac{1}{2}$; 0,$\frac{1}{2},\frac{1}{2}$.
4 Al in d): 0,$\frac{1}{2},\frac{1}{4}$; $\frac{1}{2}$,0,$\frac{1}{4}$; $\frac{1}{2}$,0,$\frac{3}{4}$; 0,$\frac{1}{2},\frac{3}{4}$.
4 Al in e): 0,0,z; 0,0,−z; $\frac{1}{2},\frac{1}{2},\frac{1}{2}+z$; $\frac{1}{2},\frac{1}{2},\frac{1}{2}-z$; with z = 0.361.
4 Zr in e): 0,0,z; 0,0,−z; $\frac{1}{2},\frac{1}{2},\frac{1}{2}+z$; $\frac{1}{2},\frac{1}{2},\frac{1}{2}-z$; with z = 0.122.
This structure may be considered another, more complex, superstructure based on close packing. The height of the superstructure cell in the c direction corresponds to four cubic pseudocells. Fig. 19 gives a comprehensive presentation of some structural features of the $MoNi_4$, $MoPt_2$, $TiAl_3$ and $ZrAl_3$ structural types.

Fe_3Al, cF16–Li_3Bi type structure: This structure may conveniently be described as derived from bcc solid solution (see in sec. 6.1. the interrelated types *cI2–W*, the previously mentioned types *cP2–CsCl*, *cF16–$MnCu_2Al$ and cF16–Li_3Bi*; see also fig. 24). The Li_3Bi-type structure, however, may be also considered as composed of four interpenetrating fc cubic arrays of atoms with Bi (or Al) at the cell corners and face centers and Li (or Fe) in the centers of the interstices.
tP2–AuCu(I), cP4–$AuCu_3$ and tP4–Ti_3Cu: These structures described in the following sections, 6.2. and in fig. 20, can be considered fcc based substitutional ordered superstructures.
hR96–CuPt(I): The equilibrium phase diagram of the Cu–Pt system shows the fcc continuous solid solution stable at high temperature and a number of ordered superstructure phases (with composition ranges) stable at lower temperatures. CuPt(I) is a complex, slightly distorted superstructure built up by 8 face centered cubic pseudocells. In the same Cu–Pt system other superstructures have been described for compositions around Cu_3Pt_5 (rhombohedral CuPt(II) type), $CuPt_3$ and $CuPt_7$.
hP8–Ni_3Sn: This structure may be considered an example of a superstructure based on the hexagonal close packed structure. In the same way as by ordering the Cu-type structure the $AuCu_3$ type may be obtained, the Ni_3Sn-type may be derived from the Mg type. Details of the structure are given in sec. 6.2.7.

b) Examples of interstitial superstructures
tP3–FeNiN: a = 283.0, c = 371.3 pm, c/a = 1.312. Space group P4/mmm, N.123.
1 Fe in a): 0,0,0; 1 N in c): $\frac{1}{2},\frac{1}{2}$,0 and 1 Ni in d): $\frac{1}{2},\frac{1}{2},\frac{1}{2}$.

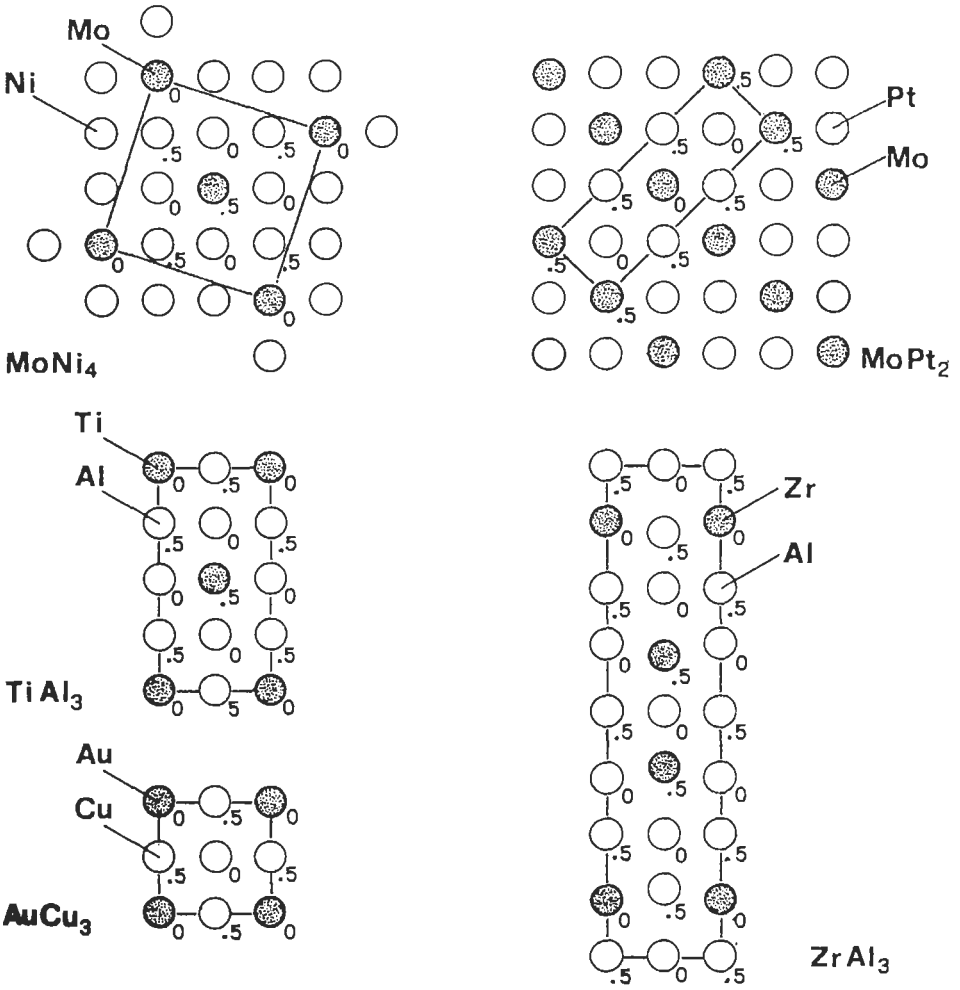

Fig. 19. Examples of face centered based, substitutional superstructures. The unit cells of a few selected superstructures are shown by means of their projection on a convenient plane and compared with a similar projection of the cP4–$AuCu_3$ type cell (on the face a,a): tI10–$MoNi_4$ (on the face a,a), oI16–$MoPt_2$ (a,b), tI8–$TiAl_3$ (a,c) tI16–$ZrAl_3$ (a,c). (The values of the coordinate along the third axis are indicated).

This structure can be considered a superstructure of the AuCu(I) type, with 1 N atom inserted in an octahedral interstitice. This structure, as the previously described *cP5–Fe_4N type*, can be considered an interstitial ordered phase. The *oP5–Ta_4O* phase and the *tI8–Fe_8N* phase are examples of bcc-based interstitial ordered phases.

oP5–Ta_4O: a = 719.4, b = 326.6, c = 320.4 pm. Space group Pmmm, N.47.

1 Ta in a): 0,0,0; 1 Ta in b): $\frac{1}{2}$,0,0; 1 O in h): $\frac{1}{2},\frac{1}{2},\frac{1}{2}$; 2 Ta in l): $x,\frac{1}{2},\frac{1}{2}$; $-x,\frac{1}{2},\frac{1}{2}$ (with x = 0.225).

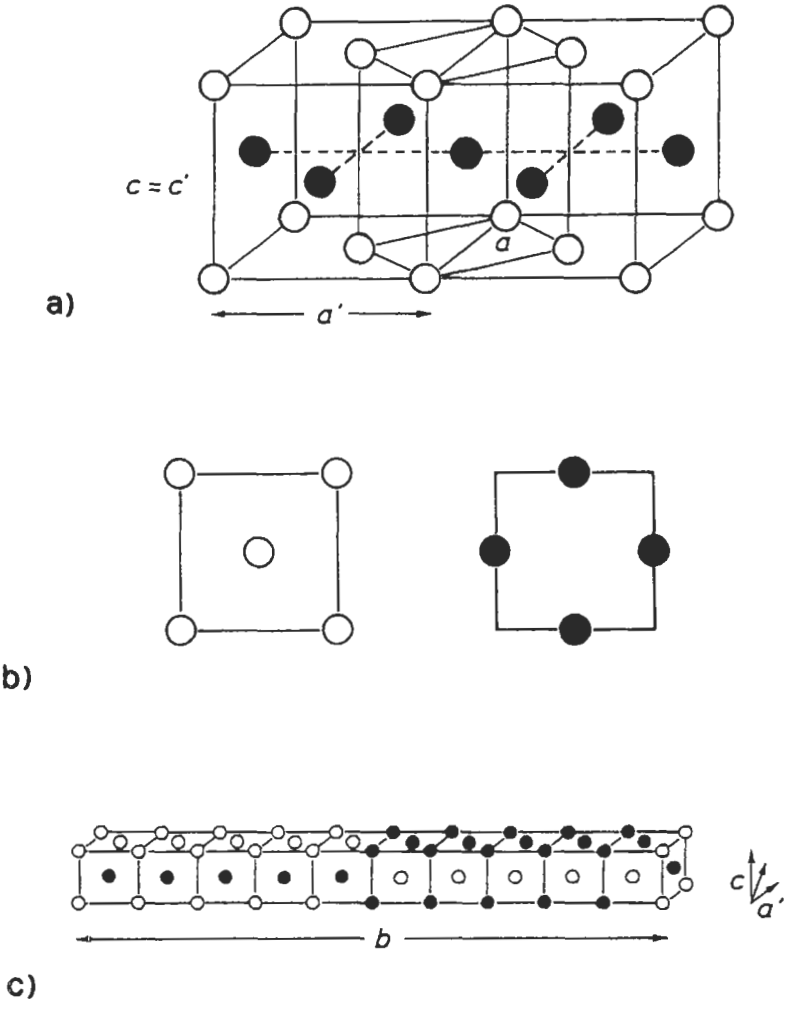

Fig. 20. AuCu type structures. The two types of atoms are shown.

a) AuCu(I) type structure. Both the tP2 cell (a and c edges) and a tP4 pseudocell (a′ and c edges) are shown. (The tetragonal pseudocell is shown in order also to make easier the comparison with the cubic, Cu-type, structure).

b) Sections of the large tP4–pseudo-cell. (Compare with fig. 13.)

c) oI40–AuCu(II) type structure.

The cell can be described as formed by two superimposed slightly distorted bcc subcells of the metal atoms. The O atom is surrounded by a (slightly compressed) Ta atom octahedron.

4.2. Antiphase domain structures

A special case of superstructures may now be considered. A typical example can be observed in the oI40–AuCu(II) type structure (fig. 20 and sec. 6.2.4.). We first have to mention that ordering of the Au–Cu face-centered cubic (cF4–Cu type) solid solution, having a 50–50 atomic composition, distributes Cu and Au atoms alternatively on two layers, resulting in a tetragonal structure, tP2–AuCu(I)) with the c axis perpendicular to the layers (see fig. 20a). The more complex structure, oP40–AuCu(II) type, is obtained by a *long-period ordering* which results in an orthorhombic cell containing 10 (slightly distorted) AuCu(I) pseudocells (fig. 20b). This ordering corresponds to a periodic shift (every 5 cells along the orthorhombic *b* axis) of the structure by $\frac{1}{2}$ (a′ + c) in the a′,c plane. This out-of step shift corresponds to a "so-called" *antiphase boundary*. An *antiphase domain* may correspondingly be defined; in this case it contains 5 AuCu(I) type pseudocells. Several examples of one-dimensional long period structures found in 1:1 and 1:3 alloys and of two-dimensional long period structures (characterized by two different domain periods and two steps-shifts) found in 1:3 alloys have been presented by PEARSON [1972]; the role of the valence-electron concentration in defining the superstructure period has also been discussed. A general presentation of several antiphase boundaries (not only planar, but also cylindrical) and related structure groups may be found in the book of HYDE and ANDERSSON [1989].

It may be useful to mention here that antiphase domain boundaries play an important role in phase changes and microstructural stability of ordered alloys and intermetallics as well as affecting mechanical behaviour. The origin of antiphase domain boundaries has been examined and discussed by MORRIS [1992], emphasis has been given to the differences between a sharp boundary, as produced by crystal shear, and a relaxed fault structure. The kinetics of relaxation of shear produced fault have examined and it was shown by MORRIS [1992] that fast relaxation may affect the movement of dislocation by creating locking stresses as well as affecting cross slip behaviour significantly affecting mechanical properties. An important point in this study, as far as the origin of the antiphase domain boundaries are concerned, is the principle that a disordered crystal exists initially which subsequently becomes ordered. According to CAHN [1987], the observation of grown-in domain network is proof that the material existed, even if momentarily, in a disordered crystalline state before becoming ordered. In agreement with this, domain networks are commonly observed in weakly ordered alloys, for example $AuCu_3$, $FeNi_3$ and sometimes FeAl, but not in strongly ordered intermetallics such as Ni_3Al and TiAl. A review on the interactions of ordering and recrystallization has been published by CAHN [1990]. Aspects of recovery and recrystallization in the $L1_2$ $(Co_{0.78}V_{0.22})_3V$ ordered alloy have been reported by GIALANELLA and CAHN [1993].

4.3. Homeotect structure types (polytypic structures)

According to PARTHE [1964], two different structure types of the same formula X_mY_n are called *homeotect structure types*, if every X atom has the same number of nearest X neighbours and the same number of nearest Y neighbours, and, conversely, if every Y

atom has the same number of nearest X and Y neighbour atoms. It is possible for several structure types to show this feature.

All the different structure types of equal composition, which have (for corresponding atoms) the same kind of surroundings, form a *set of homeotect structure types* (the term *polytypic structures* is also used to denote the relationships observed with homeotect structures).

According to PARTHE [1964] all structure types which belong to a homeotect set can be described as different stacking variants of *identical structural unit slabs* ("*minimal sandwiches*"). All structure types of a set are constructed by stacking identical unit slabs one on top of another. The various types differ only in the relative horizontal displacement of these units. (The vertical unit cell edges of the different types are integer multiples of a common unit which is the height of the unit slab characteristic for the homeotect structure type set). All structure types which belong to a homeotect set have the same space-filling curve. (See sec. 7.2.4.)

A few important examples of groups of homeotect structure types will be described in the following sections. A short index of the same is the following list (in which the Jagodzinski–Wyckoff notation of the stacking pattern has been inserted, according to the indications given in sec. 3.5.2.).

— *Close-packed element structure types* (see sec. 6.2.): Mg-type (h), Cu-type (c), La-type (hc), Sm-type (hhc).
— *Equiatomic tetrahedral structure types (Carborundum Structure types)* (see sec. 6.3.): Wurtzite-type (h), Sphalerite-type (c), SiC polytypes (hc, hcc, hccc, hcchc, ..$(hcc)_5(hccc)(hcc)_5$hc ... $(hchcc)_{17}(hcc)_2$, .. $(hcc)_{43}$hc...).
— *Laves phases* (see sec. 6.6.4.): hP12 $MgZn_2$-type (h), cF24 Cu_2Mg-type (c), hP24 Ni_2Mg-type (hc), Laves polytypes (hhc, hhccc, etc.).

Other important sets of homeotect structure types are those related to disilicide structure types ($MoSi_2$, $CrSi_2$, etc.), cadmium halide structure types, etc. (See PARTHE [1964], HYDE and ANDERSSON [1989]), or presented by certain groups of compounds such as rare earth trialuminides (VAN VUCHT and BUSCHOW [1965]).

From a general point of view, *polytypism* may be considered a special case of polymorphism: the two-dimensional translations within the layers are (essentially) preserved whereas the lattice spacings normal to the layers vary between polytypes and are indicative of the stacking period (GUINIER *et al.* [1984]). As evidenced by ZVYAGIN [1987], we may distinguish various forms of polytypic structures, including (besides close-packing of like and unlike atoms) polytypes of tetrahedral, octahedral and prismatic layers packed according to the laws of closest packings. Complex silicate structures, for instance, may be considered which are characterized by much variety in the orientations and displacements of the layers and also structures in which two-dimensional layers are conjoined with one-dimensional band and island groups.

The aforementioned papers (GUINIER *et al.* [1984], ZVYAGIN [1987]) contain also suggestions and recommendations on the nomenclature and symbolism for use in the general case of either simple or complex polytypic structures.

Another method for discussing polytypic structures has been suggested by BOKII and

References: p. 363.

LAPTEV [1994]. The polytypic structures, described by means of special unit cell diagrams and crystal-chemical formulae, are distinguished by the number and type of Wyckoff positions.

4.4. Chimney-ladder structures (structure commensurability, structure modulation)

In the cases of ordered alloys, described in the foregoing sections, long period structures were considered in which the near-neighbour coordination of the atoms remains essentially unchanged between one structural modification and another.

More complex cases can, however, be considered. As an introduction to this point, we may remember that it is often convenient to describe structures as consisting, for instance, of two interpenetrating substructures (two different atom sets).

As an example, an interesting group of phases T_nX_m may be considered which are tetragonal and are formed between transition metals T and p-block elements X (of the Ga and Si groups). In these phases, along the *c* axis, the unit cell (superstructure cell, supercell) contains *n* pseudocells of T atoms and *m* interpenetrating pseudocells of X atoms. These phases (*Nowotny phases or "chimney-ladder" structures*) contain rows of atoms X (the "ladder"), with variable interatomic spacing from one compound to another, which are inserted into channels ("chimneys") in the T array. The T metals in all of the superstructures form a βSn–like array with the number of T metal atoms in the formula of the compound corresponding to the number of βSn–like pseudocells stacked in the *c* direction of the supercell (see sec. 6.3.1.). The arrangement of the atoms in these phases can be compared to that found in the structure of $TiSi_2$.

The following is a list of some chimney-ladder phases (phases containing as many as 600 atoms in the unit cell have been described):

tP20 Ru_2Sn_3 ($a = 617.2$ pm, $c = 991.5$ pm, $c/(2a\sqrt{2}) = 0.568$)
The Ru atoms form a βSn–like array with two pseudocells along the *c* direction of the supercell).
tP32 Ir_3Ga_5 ($a = 582.3$ pm, $c = 1420$ pm, $c/(3a\sqrt{2}) = 0.575$)
tP36 Ir_4Ge_5 ($a = 561.5$ pm, $c = 1831$ pm, $c/(4a\sqrt{2}) = 0.576$)
...
tP192–$V_{17}Ge_{31}$ ($a = 591$ pm, $c = 8365$ pm, $c/(17a\sqrt{2}) = 0.589$)
(In $V_{17}Ge_{31}$, for instance, there are 17 βSn like pseudocells of V atoms and 31 Ge pseudocells stacked along the *c* axis).

The atomic arrangements in a few chimney-ladder phases are shown in fig. 21 and compared with that found in $TiSi_2$. (This structure corresponds to the orthorhombic cell oF24–$TiSi_2$-type with $a_0 = 826.7$ pm, $b_0 = 480.0$ pm, $c_0 = 855.1$ pm. It can be approximately described in terms of a smaller body-centered tetragonal pseudocell, shown in fig. 21a, having $a' \approx a_0/\sqrt{2} \approx c_0/\sqrt{2}$; $c' = b_0$ and $c'/a_0 \approx 0.58$ (close to the "ideal" value $1/\sqrt{3} = 0.577...$).

The electron concentration appears to play some role in control of this family of structures as noted by Nowotny (SCHWOMMA *et al.* [1964a, 1964b], FLIEHER *et al.* [1968a, 1968b]), JEITSCHKO and PARTHE [1967] and PARTHE [1969] and reported by PEARSON [1972].

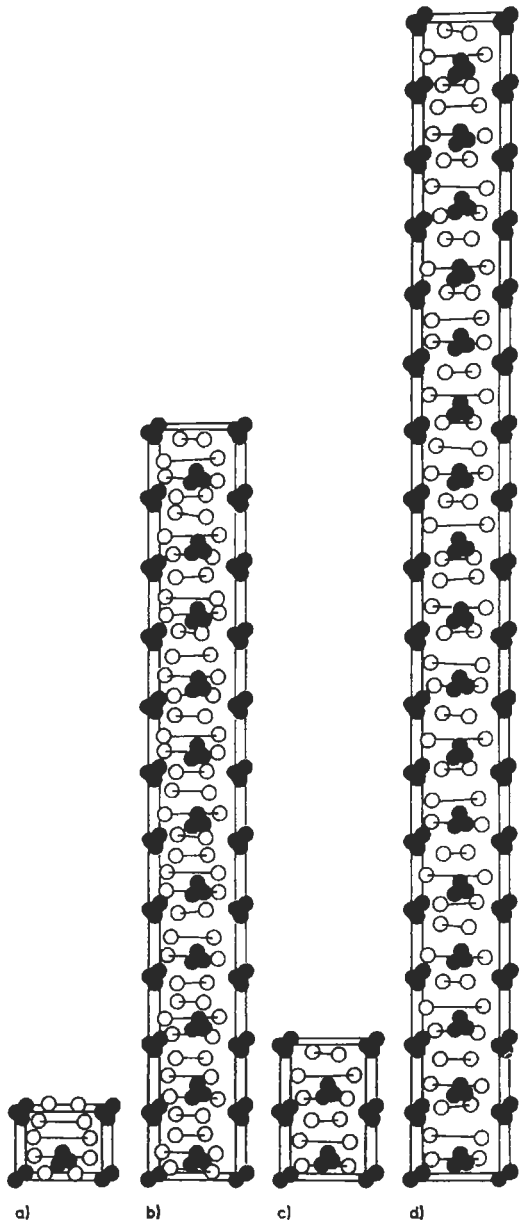

Fig. 21. Nowotny phases, chimney-ladder structures (JEITSCHKO and PARTHE [1967]).

a) The reference oF24–$TiSi_2$ type structure presented in terms of a tetragonal pseudo-cell (12 atoms in the pseudo-cell).

b) tP120–$Mn_{11}Si_{19}$; c) tP20–Ru_2Sn_3 and d) tI156–$Rh_{17}Ge_{22}$ phases.
(Notice that the metal atoms, black circles, form sequences of β-Sn like cells; compare with fig. 32 below).

References: p. 363.

In the book of HYDE and ANDERSSON [1989], the Nowotny phases are presented as a special case of a group of "*one-dimensional, columnar misfit structures*" which also include compounds such as $Ba_m(Fe_2S_4)_n$ and other complex sulphides. *Layer misfit structures*, such as those of some oxide-fluorides, arseno-sulphides, etc., are also presented and classified with reference to a concept of *structure commensurability* based on the recognition that (along one or more axes) the ratios between the different repeat units of various interpenetrating substructures can (or cannot) be represented as ratios between integer numbers.

The *coexistence of different kinds of periodicity* has also to be considered in the description of a quite different type of structure which is becoming increasingly common. In this, some atomic parameters (and/or the partial occupancy of some sites) vary in a periodic way through the structure. The periodicity may or may not be commensurate with the unit cell of the basic structure. (The ratio between the repetition length of this parameter and the lattice constant may or may not correspond to the ratio between two integer numbers). Structures having these characteristics are often termed *modulated structures* (HYDE and ANDERSSON [1989]). Several non-stoichiometric compounds present such modulations (FeS_x, Yb_3S_4, etc.). Various modulated structures have also been considered, for instance, for the NiAs-type structure (see sec. 6.5.1.).

An interesting case of *magnetic modulated structure* is that reported for $EuCo_2P_2$ (REEHUIS *et al.* [1992]). The *positional structure* of the atoms (of the atomic nuclei, nuclear structure) corresponds to the tI10–$ThCr_2Si_2$ type (see sec. 6.5.9). A magnetic structure has been also determined, which is related to the ordering of the magnetic moments of the Eu atoms. These moments are oriented perpendicular to the *c* axis and form an incommensurate spiral with the turning axis parallel to the *c* axis. The magnetic moments lie in the basal planes and they order parallel within these planes. Along the *c* axis, from one basal plane to the next one, there is a periodic rotation of the moments. The ratio, along the *c* axis, of the characteristic lengths of the magnetic and nuclear structures, is slightly dependent on temperature. At 64 K it is close to 5/6 (that is: there are 5 translation lenghts of the magnetic cell for 6 translation lengths of the nuclear structures). At 15 K the ratio was found to be close 6/7. If this magnetic structure is maintained at still lower temperatures, it may correspond to the exact 6/7 value. The ground state may then be called a commensurate structure with this ratio.

4.5. Recombination structures, intergrowth structure series

Some of the previously reported relationships between structures may be included in the general term "*recombination*" *structures*. Such structures (see LIMA DE FARIA *et al.* [1990]) are formed when topologically simple parent structures are periodically divided into blocks, rods or slabs (that is structure portions which are finite or infinite in one or two dimensions, respectively) which are recombined into derivative structures by means of one or more structure building operations. The most important operations are: *unit cell twinning*, *crystallographic shear planes*, *intergrowth* of blocks, rods or slabs of different structural types (for instance, intergrowth of cF24–$MgCu_2$ type and hP6–$CaCu_5$ type slabs to obtain the hP36–Ce_2Ni_7 type structure), *periodic out-of-plane*, antiphase boundaries

(AuCu(II), as an example), *rotation* of rods or blocks. The frequency of structure building operators (and, therefore, the size of undisturbed structure portions) can vary by well defined increments, so that many phases may occur as members of homologous series.

A few considerations about possible schemes of relationships between inorganic crystal structures based on a systematic "construction" of complex structural types by means of a few operations (symmetry operations, topological transformations) applied to some building units (point systems, clusters, rods, sheets), have been previously reported in sec. 3.5.4, following criteria suggested, for instance, by HYDE and ANDERSSON [1989] and by ZVYAGIN [1993].

We may add here that, within the "recombination" scheme, a very interesting method of describing, interpreting and interrelating complex structures is that based on the aforementioned "*intergrowth*" *concept* (KRIPYAKEVICH *et al.* [1972, 1976, 1979], GRIN′ *et al.* [1982, 1990], PARTHE *et al.* [1985], LIMA DE FARIA [1990], PANI and FORNASINI [1990]). According to this concept, selected structure types may be considered as belonging to certain intergrowth structure series. *The different structure types of an intergrowth series are described as being constructed from structure segments of more simple structures (the so-called "parent structures").*

In an other way, we may say that, according to this approach, the *construction modules* instead of being defined on a mere geometrical basis, are *selected* with reference to specific *crystallochemical criteria*. To this end, groups (series) of similar complex structures are analysed in order to recognize "fragments" which could be identified as structure segments of more simple structural types.

The structure series are then classified according to the *kind of fragments* and the *method of construction*. On the basis of the kind of fragments the structure series is described as homogeneous or inhomogeneous: *the homogeneous intergrowth structures* consist of identical fragments, the *inhomogeneous intergrowth structures* consist of segments (differing in composition and/or coordination) belonging to different parent structures. According to the method of construction, the intergrowth structure series can be classified into *one-dimensional* (linear), *two-* or *three-dimensional series*. In a *linear series* we have the one-dimensional stacking (along one direction) of two-dimensional, infinite segments (slabs) of the parent structures. The different structures of a *two-dimensional intergrowth series*, on the other hand, are built up by aggregations of several one-dimensional fragments (infinite rods, columns). Finally, the structures of a *three-dimensional intergrowth series* are constructed from (zero-dimensional, finite) parent structure blocks stacked in three dimensions.

It has been pointed out (GRIN′ [1992]) that slicing the parent structure into segments can be done in different ways. For a segment to be used in a particular structure series, for the members of which we are interested in predicting composition and symmetry, a number of requirements should be fulfilled. The segments should contain certain symmetry elements (in a linear series, for instance, all the segments used for the description usually contain some symmetry elements, mostly parallel to the stacking direction, which are retained in any stacking sequence, and represent the "minimal symmetry" of the series). The segments interfaces necessarily pass through atom centers.

References: p. 363.

(The composition of the segment is proportional to the stoichiometry of the parent structure: by addition it is possible to obtain the compositions of all possible structures of the series). The segments, moreover, selected from different parent structures, must have, at least, one topologically equal interface in order to make the intergrowth possible. Additional requirements are necessary when the atomic arrangement on the interface permits more than one possibility of intergrowing and when more complex (two-, three-dimensional) series are studied.

Considering, for instance, the particular case of the "linear intergrowth structure series", we may mention that many, binary and ternary, intermetallic phases can be considered members of those series (both homogeneous and inhomogeneous).

A representative of a structure belonging to a linear inhomogeneous series is presented in fig. 22. In this case, the parent structures are the oC8–CrB and oC12–UPt_2 types. The intergrowth structure presented is the oC28–W_3CoB_3 (or Y_3Co_3Ga) type. Its unit cell contains a segment arrangement corresponding to two repetition of a sequence containing a UPt_2 fragment followed by two CrB-type fragments. A simple code of this structure may be $(2_{CrB}1_{UPt2})_2$. Other members of the series have been described, for instance:

$1_{CrB}1_{UPt2}$ (corresponding to the oI10–W_2CoB_2 type);
$3_{CrB}1_{UPt2}$ (corresponding to the mC18–Y_4Co_4Ga type);
$(4_{CrB}1_{UPt2})_2$ (corresponding to the oC44–Y_5Co_5Ga type).

It is interesting to observe that many real representatives of this series may be found in the Y–Co–Ga system. This may be considered an example of the fact that, often, *several members* of a *certain intergrowth series* have representatives in the *same* (binary and ternary) *alloy system*. In the same system (or in chemically analogous systems) representatives of the parent structures may also be found (in the example reported, for instance, YCo has the CrB type structure). The interest of a crystallochemical description based on the intergrowth concept is thus evident.

As a further simple example, we may mention the structure of the oC16–$NdNiGa_2$ type belonging to the series $BaAl_4$–AlB_2. Its unit cell contains indeed two $BaAl_4$-type segments and two AlB_2-type segments. The simple code, previously considered, will be $(1_{BaAl4}1_{AlB2})_2$. (Notice, however, that in a more complex and detailed notation, superscripted indexes may be added to the formulae of the segments in order to specify, for instance, their symmetry (GRIN′ *et al.* [1982], PARTHE *et al.* [1985]).

General compositional formulae are often used for representing a series (GRIN′ [1992]). $Me_{m+n}X_{5m+3n}Y_{2n}$, for instance, may be the overall formula of a series consisting of intergrown $CaCu_5$-type and $CeCo_3B_2$-type slabs. (For the hP6–$CaCu_5$ type and its ordered variant hP6–$CeCo_3B_2$ type structures, see sec. 6.2.8.). Members of this series are the following structure types: hP12–$CeCo_4B$ (corresponding, in the aforementioned formula, to m = 1, n = 1), hP18–$Ce_3Co_{11}B_4$ (m = 1, n = 2), hP24–$Ce_2Co_7B_3$ (m = 1, n = 3), hP18–$Nd_3Ni_{13}B_2$ (m = 2, n = 1) and hP30–$Lu_5Ni_{19}B_6$ (m = 2, n = 3). We may notice in this case too, the close chemical analogy among the alloy systems (rare earth, nickel or cobalt, borides) forming structures corresponding to the different members of a given series.

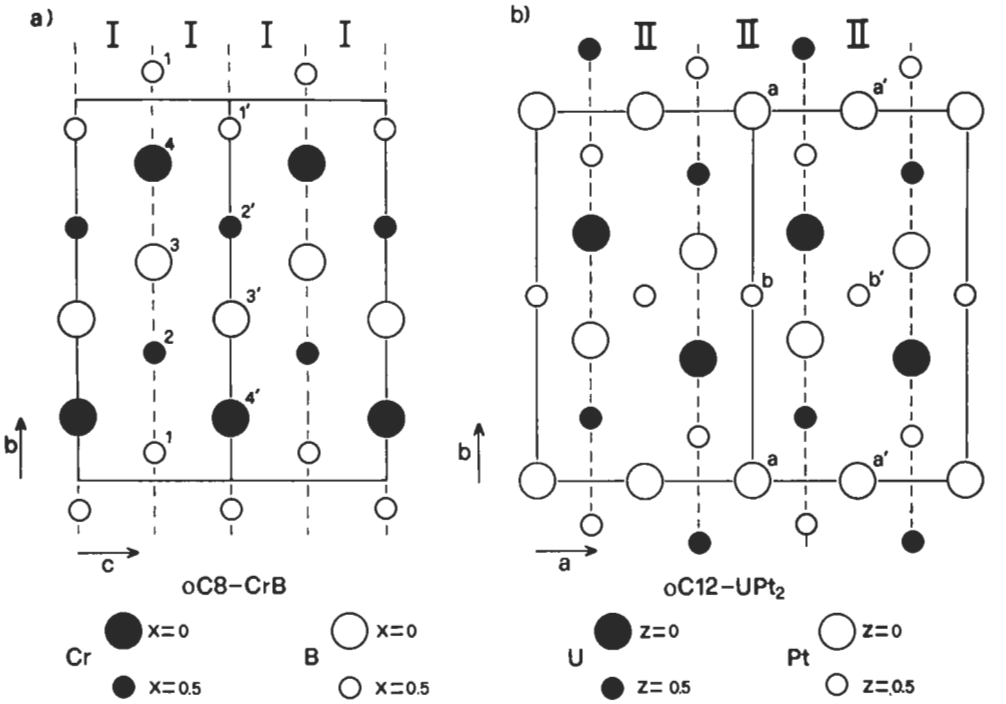

Fig. 22a, b

4.6. Group-subgroup relations for the representation of crystal-chemical relationships

According to the presentation given by BÄRNIGHAUSEN [1980], if two structures are topologically equivalent their interrelation may be conveniently expressed by *group–subgroup* relations between their space groups. Graphic representation of these relations leads to hierarchic ordering resembling a "*family tree*". At the top of the tree there is the so-called "*aristotype*" (a highly symmetrical structure). From the aristotype the other structures of the tree may be derived along specific routes of symmetry reduction. In order to obtain a well-defined description, the symmetry reduction is presented in terms of *minimal steps* (that is a given structure is followed by another whose space group is a so-called maximal subgroup (M) (see HAHN [1989]) of the space group (G) of the former structure). The minimal steps of symmetry reduction are characterized by the terms *lattice-equivalent* (M contains all the translations of G, the crystal class of M is of lower symmetry than that of G), or *class-equivalent* (M and G have the same crystal class but belong to different space-group types: M has lost translational symmetry, that is the primitive cell corresponding to M is larger than that of G) or *crystallographically-equivalent* (G and M belong to the same space group type, that is, as in the previous case, M has lost translational symmetry).

References: p. 363.

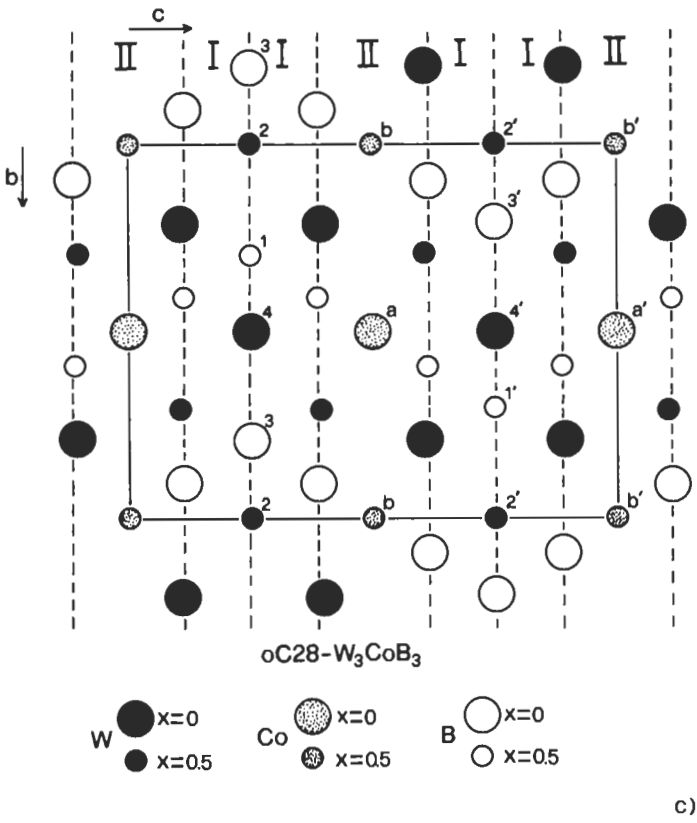

Fig. 22. An example of the application of the intergrowth concept. In a) and in b) two "parent" structures (CrB and UPt_2) are presented. The projections of a few unit cells (defined by the continuous lines) on the b,c and a,b planes respectively are shown. The structure segments which have been correspondingly identified are shown by dotted lines. In c) a member (W_3CoB_3 type structure) of the linear inhomogeneous series CrB-UPt_2 is presented (the sequence of parallel building segments is indicated). The segments characteristic of the CrB and UPt_2 structures have been indicated by I and II. In order to make easier the comparison, a few atoms with similar environments have been marked by the same numbers (or letters) in the parent and in the derived structures.

5. *Elements of systematic description of structure types. General remarks and references*

By means of the considerations previously presented some typical structures will be described in the following sections. On the basis of somewhat arbitrary criteria (such as high frequency of the structural type, existence of phases of considerable practical importance, possibility of presenting some features of general interest, etc.) the types to be described have been selected and presented in a few sections. This description, therefore, should be considered as only an initial introduction to a vast subject. As

already mentioned, complete and updated descriptions may be found in some reference books such as: LANDOLT–BÖRNSTEIN (HELLWEGE [1971], PREDEL [1991]), VILLARS and CALVERT [1985, 1991], MASSALSKI [1990] and DAAMS *et al.* [1991] that report (in alphabetical order) all the known binary systems. They can be considered complete riformulation of "classic" books such as: HANSEN [1936], HANSEN and ANDERKO [1958], ELLIOTT [1965], SHUNK [1969], MOFFATT [1986]. Phase diagrams are presented and discussed; crystal structure data of the intermediate phases, moreover, are systematically given. A similar lay-out has been adopted in the Monograph Series on Alloy Phase Diagrams published by ASM International. The book of VILLARS and CALVERT [1991] consists of an "*Handbook of Crystallographic Data*" (in 4 volumes); DAAMS *et al.* [1991] published an "*Atlas of Crystal Structure Types*" (in 4 volumes). The "Handbook" reports all the data available for binary (and complex) intermetallic phases. The "Atlas" describes the different structural types presenting (both by using tables and drawings) atomic coordinates, interatomic distances and coordination polyhedra.

For a general presentation of the Inorganic Crystallochemistry, see, for instance, WELLS [1970].

For a *systematic classification* of the *intermetallic structure types*, the *following monographs* may be consulted.

SCHUBERT [1964] in his book "*Kristallstrukturen Zweikomponentiger Phasen*" (Crystal Structures of Binary Phases) described a few hundred structural types. In this book, Schubert paid great attention to chemical criteria for the description, classification and discussion of the properties of the different phases. The position of the elements involved in the Periodic Table was considered particularly relevant. For this purpose, the elements were considered by Schubert to be subdivided into the following families: A-metals (elements of the s-block of the periodic table), T-metals (transition metals), B-elements (elements of the p-block of the Periodic Table). The different structural types were then described according to the following chapter subdivision:

Brass-type alloys and *close-packed* sphere stacking and superstructure variants: $AuCu_3$, AuCu, $SrPb_3$, $ZrAl_3$, $ZrGa_2$, Nb_5Ga_{13}, etc.; Mg-type structure and superstructures Ni_3Sn, etc.; body-centered sphere packing W structure and derivatives Fe_3Si, CsCl, NaTl, Cu_5Zn_8, Ni_2In, etc.

T–T phases (among which the T element structures of the so-called Cr_3Si family such as the βU, cI58–αMn, hR39–W_6Fe_7, Th_6Mn_{23}, etc., and then the Laves phase structures).

B–B phases (structures considered as deformation variants of close-packed structures, such as Zn, In, etc., structures of B, graphite, structures of the diamond-family, of the P and As families, etc.).

A–B phases (several types partly classified according to the stoichiometry: Li_3Bi, Mg_2Sn, Mg_3Sb_2, NaCl, etc.).

T–B phases (T-rich borides, carbides, nitrides, oxides and hydrides, $CuAl_2$, $MoSi_2$, NiAs, FeS_2 structures and their variants).

PEARSON [1972], in his book "*The Crystal Chemistry and Physics of Metals and Alloys*", discussed the characteristics and specific features (coordination, stability, relationships

with other structures, etc.) of about a thousand structure types. He was able to classify all these structures in 12 different families. The most important 10 are summarized here below.

1) *Valence compounds of non-metals* (semiconducting compounds with anions forming close packed arrays, polyanionic compounds, polycationic compounds, group IV, V and VI elements and IV-VI and V-VI compounds, etc.).
2) *Metastable phases, interstitial phases, martensite* (in this group of phases the Hägg interstitial phases formed by transition metal and small non-metal atoms such as H, B, C, N have been especially considered: in these phases the non-metals occupy the interstices, generally the octahedral ones of the close-packed structures of the transition metals).
3) *Structures based on the close packing of the 3^6 close-packed nets* (Cu and Mg structures and their derivative structures $AuCu_3$, AuCu, Ti_3Cu, $TiAl_3$, $ZrGa_2$, $MoNi_4$, etc.).
4) *Structures derived by filling tetrahedral, octahedral (and other) holes in close-packed arrays of atoms* (sphalerite structure and derivative structures oP12–CuAsS, tI16–$FeCuS_2$, tI16–Cu_3AsS_4, etc., wurtzite structure and derivative structures, oP16–$CuSbS_2$, oP16–Cu_3AsS_4, hP30–In_2Se_3, etc.; CaF_2 structure and distorted, defective, superstructures of CaF_2; NaCl structure and derivative structures of the NaCl type; NiAs structure, etc.).
5) *Structure types dominated by triangular prismatic arrangements* (hP2–WC, hR9–MoS_2, tI8–NbAs, tP6–Cu_2Sb, oP36–Ta_2P, hP3–AlB_2, hP6–$CaIn_2$, hP6–Ni_2In and their variants, are examples of structure types included in this group).
6) *Structures based on simple cubic and body centered cubic packing* (in this group the structure types cI2–W, tI2–Pa, martensite, cP6–Cu_2O, cP2–CsCl, tP4–TiCu, cF16–Li_3Bi, cF16–NaTl, cF16–$MnCu_2Al$, tP3–$FeSi_2$, cI52–Cu_5Zn_8 and several variants are considered. In this structure family the Nowotny chimney-ladder phases are also included).
7) *Structures generated by square-triangle nets of atoms: cubes and cubic antiprisms* (for instance tI12–$CuAl_2$, oP24–$AuSn_2$, mC12–PdP_2, oC20–$PtSn_4$, tP10–U_3Si_2, tP40–$FeCu_2Al_7$, oP16–ThNi, oI20–UAl_4, etc.)
8) *Structures generated by alternate stacking of triangular and kagomé nets.* (The structures of hP6–$CaCu_5$, tI26–$ThMn_{12}$, hP38–Th_2Ni_{17} and their variants are included in this family. The Laves phases cF24–Cu_2Mg, hP12–$MgZn_2$ and hP24–Ni_2Mg types and several variants are considered in this family. However, they are also described, as Frank–Kasper structures, in the subsequent group).
9) *Structures in which icosahedra and CN 14, 15 and 16 polyhedra play a dominant role.* (Laves phases, μ phases: hR39–W_6Fe_7; P phases: oP56–Mo-Cr-Ni phase, (which, at a composition corresponding to 42 at% Mo and 18 at% Cr, has a unit cell containing 56 atoms in partial substitutional disorder); R phases: hR159–Mo-Co-Cr, etc. are included in this family, as well as a number of intermetallic phases with giant cells such as the cF1124–Cu_4Cd_3, cF1192–$NaCd_2$, cF1832–Mg_2Al_3 types studied by SAMSON [1969].

10) *Structures with large coordination polyhedra.* (Structures are presented in which large coordination polyhedra are contained: for instance cP36–$BaHg_{11}$ in which Ba is surrounded by 20 Hg, tI92–Ce_5Mg_{41}, tI48–$BaCd_{11}$, cF112–$NaZn_{13}$ in which coordination polyhedra corresponding to coordination numbers (CN) 20, 22 and 24 are present respectively).

As a comment to the Pearson's classification and description of structure types we may mention a paper by PEARSON [1985b] himself on the classification of the crystal structures of intermetallic phases according to building principles and properties. Five groups of phases have been evidenced:

1) Phases based on geometrical packings;
2) Phases in which the band-structure energy is an unusually large fraction of the total energy;
3) Valency compounds;
4) Framework structures;
5) Hybrid framework structures with geometrical packings.

A substantially geometrical approach has been adopted in their book "*Inorganic Crystal structures*", by HYDE and ANDERSSON [1989] who presented and discussed the structure of more than a thousand inorganic compounds, explicitly ignoring "the artificial barrier between inorganic and mineral structures on the one hand and metallurgical structures (intermetallic compounds, borides, carbides, etc.) on the other." In their treatment and classification of the structural types, they generate complex structures starting with relatively few basic structures and applying to segments of such structures, one or more of a few geometrical operations that are essentially symmetry operators. The "segments" or building units considered may be blocks (or clusters, bounded in 3 dimensions), rods, (or columns, bounded in 2 dimensions, infinite in the third), slabs (or lamellae, sheets, layers, the latter bounded in 1 dimension and infinite in the other two).

6. *Description of a few selected structural types*

The selected structural types which will be presented in the following sections arranged in a few groups according to their crystallochemical interrelations are also alphabetically summarized, for reader convenience, in Appendix 1: "Gazetteer of Intermetallic Phases".

For the different phases described, the values of the lattice parameters have been generally reported: this may indeed be useful in comparing different structures and in order to get a better idea of the real atomic packing. Notice, however, that, generally, for the various phases, several slightly different values have been reported in the literature (owing to different preparation and measurement techniques and/or to the existence of certain, often not well-defined, homogeneity ranges). The reader interested in accurate values of the lattice parameters should therefore consult the original literature.

References: p. 363.

6.1. bcc W-type structure and derivative structures

In this section a few structural types are presented which can be described as related to the simple body-centered cubic structure, cI2–W type. For some of them, fig. 23 shows the normalized interatomic distances and the corresponding numbers of equidistant atoms.

6.1.1. Structural type: cI2–W

Body-centered cubic, space group $Im\bar{3}m$, No. 229.
Atomic positions:
2 W in a) 0,0,0; $\frac{1}{2},\frac{1}{2},\frac{1}{2}$
Coordination symbol: $\overset{3}{\underset{\infty}{}}[W_{8/8}]$
Layer stacking symbols:
Triangular (T) nets: $W^{A}_{0}W^{B}_{1/6}W^{C}_{1/3}W^{A}_{1/2}W^{B}_{2/3}W^{C}_{5/6}$
Square (S) nets: $W^{1}_{0}W^{4}_{1/2}$
For the prototype itself, W, a = 316.5 pm.

This structure can be compared with the CsCl type structure (which can be obtained from the W type by an ordered substitution of the atoms) and the $MnCu_2Al$ type structure ("ordered" superstructure of the CsCl type): see fig. 24a and 24b and notice the typical 8 (cubic) coordination.

The W-type structure is shown by a number of unary systems: Li, Na, K, Rb, Ba, Cr, Eu, Cr, Mo, V, Ta, W, etc., (as the only form or the room temperature stable form), Be, Ca, Sr, several rare earth elements, Th, etc., (as a high temperature form) and α and δ Fe forms.

The same structure is formed in a number of binary (or ternary) phases, for which a random distribution of the two (or three) atomic species in the two equivalent sites is possible. Typical examples are the β-Cu–Zn phase (in which the equivalent 0,0,0; $\frac{1}{2},\frac{1}{2},\frac{1}{2}$ positions are occupied by Cu and Zn with a 50% probability) and the β-Cu–Al phase having a composition around Cu_3Al (in which the two crystal sites are similarly occupied, on average by Cu, with a 75% occupation probability, and by Al, with a 25% occupation probability). A number of these phases can be included within the group of the "Hume–Rothery" phases (see sec. 3.4.). In the Villars–Calvert compilation 380 phases (about 1.5% of the total number of phases considered) are listed under this structural type (which is the 11th in the frequency order).

6.1.2. Structural type: cP2–CsCl

Cubic, space group $Pm\bar{3}m$, No.221.
Atomic positions:
1 Cs in a) 0,0,0
1 Cl in b) $\frac{1}{2},\frac{1}{2},\frac{1}{2}$
Coordination formulae:
$\overset{3}{\underset{\infty}{}}[CsCl]_{8/8}$ or $\overset{3}{\underset{\infty}{}}[CsCl]_{8cb/8cb}$ (ionic description)
$\overset{333}{\underset{\infty}{}}[X_{6/6}][Y_{6/6}]_{8/8}$ or $\overset{333}{\underset{\infty}{}}[X_{6o/6o}][Y_{6o/6o}]_{8cb/8cb}$ (metallic description)

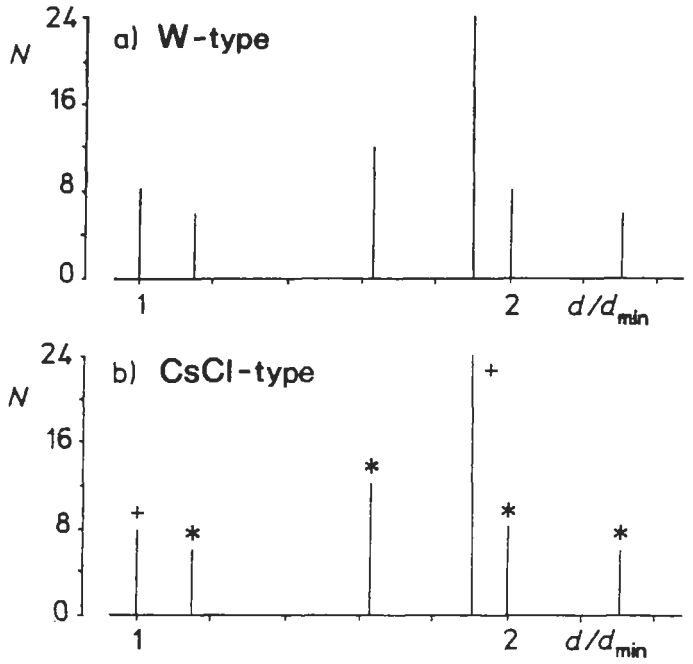

Fig. 23a,b. Trends of interatomic distances and coordinations in a group of closely interrelated structures.
a) cI2–W type structure: coordination around W.
b) XY compounds of cP2–CsCl type structure:
(+) X–Y (or Y–X) coordination.
(*) X–X (or Y–Y) coordination.

Layer stacking symbols:
Triangular (T) nets: $Cs_0^A Cl_{1/6}^B Cs_{1/3}^C Cl_{1/2}^A Cs_{2/3}^B Cl_{5/6}^C$
Square (S) nets: $Cs_0^1 Cl_{1/2}^4$
For the prototype itself, CsCl, a = 411.3 pm.

See also fig. 3. The 8 coordination (cubic) of the two atomic species is apparent.

The normalized interatomic distances and numbers of equidistant neighbours are shown in fig. 23. In the same figure data are also reported for the W type structure, which can be considered a degenerate structure of the CsCl type structure (in the W type structure the two atomic sites are equivalent) and of the derivative (superstructure) $MnCu_2Al$ type.

The CsCl type structure is adopted by many of the 1:1 intermetallics and by a few halide and chalcogenide 1:1 (ionic) compounds (for which, however, it is in competition with the NaCl type structure (see sec. 6.4.1)). Of the monohalides only CsCl, CsBr, CsI, TlCl, TlBr and TlI (and of the monochalcogenides only, ThTe) have the CsCl type structure, while the rest with a lower atomic (ionic) ratio have the NaCl type structure (corresponding to a lower coordination, 6 instead of 8).

References: p. 363.

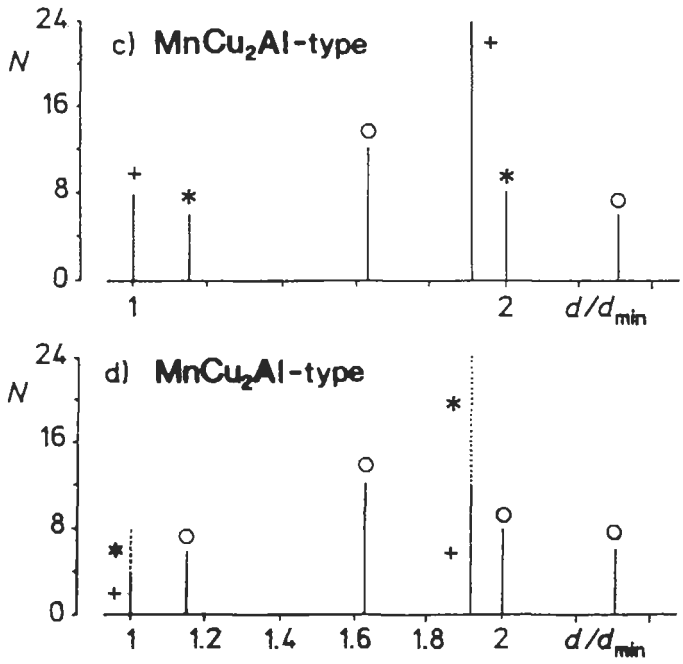

Fig. 23c,d. Trends of interatomic distances and coordinations in a group of closely interrelated structures.
c) cF16–$MnCu_2Al$ type structure: coordination around Al (or Mn)
(+) Al–Cu (or Mn–Cu); (*) Al–Mn (or Mn–Al);
(o) Al–Al (or Mn–Mn).
d) cF16–$MnCu_2Al$ type structure: coordination around Cu
(+) Cu-Mn; (*) Cu–Al; (o) Cu–Cu.

As for the intermetallics, in the Villars-Calvert compilation, about 460 compounds (≈ 1.8% of the total number of phases considered) are listed under this structural type (7th in the frequency rank order); about 300 phases are binary, the others are (more or less disordered) ternary phases. Among the binary phases we may mention 1:1 compounds such as those of alkaline earth and rare earth elements with Mg, Zn, Cd, Hg (and often with In, Tl, Ag, Au), those of Al and Ga with Fe and Pt group metals. The β' Cu–Zn phase (stable at room temperature) belongs to this structural type; at higher temperature it undergoes the order–disorder transformation into the disordered cI2–W-type, β phase. FeAl also is an example of a phase having this (more or less) ordered structure. It corresponds to a solid solution range from ≈ 23 to ≈ 55 at% Al. It forms through ordering of the α Fe, cI2–W type, phase which has a solubility range from 0 to ≈ 45 at% Al.

Other interesting phases belonging to this structural type are:

Ni_xAl_{1-x} (homogeneous between 42 and 69 at% Ni) with good mechanical and oxidation resistance properties. (By quenching from high temperatures the formation of an ordered martensite is obtained which can be considered for shape memory behaviour).

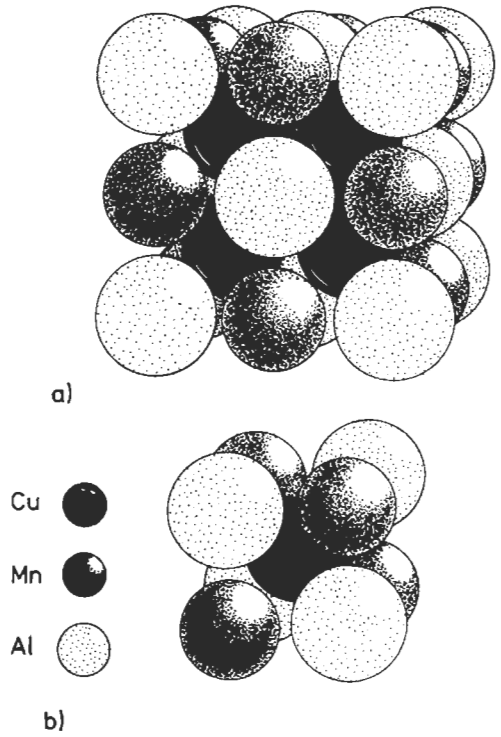

Fig. 24. cF16–$MnCu_2Al$ type structure. The unit cell is shown in a). This structure degenerates in the Li_3Bi type if the Cu and Mn positions become equivalent. The small cube presented in b) corresponds to $\frac{1}{8}$ of the $MnCu_2Al$ unit cell and degenerates into a CsCl type cell if the atoms at the vertices (Mn + Al positions) are equal. Moreover a further degeneration in the W type will be obtained if all the atoms are equal.

Co_xAl_{1-x} (≈ 48 to 79 at% Co), Co_xBe_{1-x} (26 to 53 at% Co), Ni_xBe_{1-x} (≈ 25 to 52 at% Ni), PdBe (≈ 50 at% Pd), Cu_xBe_{1-x} (≈ 51 to 53 at% Cu), etc.

For a discussion on substitutional additions to CsCl type alloys (site preference for dilute additions to NiAl, FeAl, CoAl, etc.) see KAO *et al.* [1994].

Finally, we may mention Ti_xPd_{1-x} (47 to 53 at%Pd) and Ti_xPt_{1-x} (46 to 54 at% Pt) which have the CsCl type structure at high temperature and the oP4–AuCd structure at low temperature.

6.1.3. Structural type: cF16–$MnCu_2Al$

Face-centered cubic, space group $Fm\bar{3}m$, No. 225.

Atomic positions:

4 Al in a) 0,0,0; $\frac{1}{2},\frac{1}{2},0$; $\frac{1}{2},0,\frac{1}{2}$; $0,\frac{1}{2},\frac{1}{2}$

4 Mn in b) $\frac{1}{2},\frac{1}{2},\frac{1}{2}$; $0,0,\frac{1}{2}$; $0,\frac{1}{2},0$; $\frac{1}{2},0,0$

8 Cu in c) $\frac{1}{4},\frac{1}{4},\frac{1}{4}$; $\frac{3}{4},\frac{3}{4},\frac{1}{4}$; $\frac{3}{4},\frac{1}{4},\frac{3}{4}$; $\frac{1}{4},\frac{3}{4},\frac{3}{4}$; $\frac{3}{4},\frac{3}{4},\frac{3}{4}$; $\frac{1}{4},\frac{1}{4},\frac{3}{4}$; $\frac{3}{4},\frac{1}{4},\frac{1}{4}$; $\frac{1}{4},\frac{3}{4},\frac{1}{4}$

Coordination formula:
$^{3}_{\infty}[AlCu_{8/4}Mn_{6/6}]$

For the layer stacking symbols, the data are reported in the next section in comparison with the Li_3Bi and NaTl type structures.

For the prototype itself, $MnCu_2Al$, a = 596.8 pm.

The structure is shown in fig. 24. In this figure a comparison is also made with the CsCl type structure. It is apparent that if the two a) and b) sites are occupied by the same atomic species, the cell degenerates into a block of 8 equal cells (of the CsCl-type). We may also observe that, on the contrary, if a single atomic species were assigned to the b) and c) sites, another ordered structure would be obtained, corresponding to the 1:3 stoichiometric ratio (Li_3Bi-type or BiF_3-type).

In the Villars–Calvert compilation the phases belonging to the $MnCu_2Al$ and Li_3Bi types are listed together. (See also sec. 6.1.3. and 6.1.4.). They are about 380 (≈ 1.5% of the total number of phases considered and 12th in the frequency rank order).

Among the ternary alloys, we may mention several $Me'Me''Me'''_2$ phases (with Me′ = Al, Ga, Ge, Sn; Me″ = Ti, Zr, Hf, V, Nb, Mn, etc. and Me‴ = Co, Ni, Cu, Au, etc.). The compounds which crystallize with the $MnCu_2Al$ type structure (and particularly the magnetic compounds having this structure) are called *Heusler Phases*. In the specific case of the Al–Cu–Mn system this phase is ferromagnetic and stable above 400°C, but it can be frozen by quenching to room temperature. It is assumed that its whole moment is due to the spin moment of Mn which has an unfilled d shell (5 electrons). Magnetic properties of Heusler phases are strongly dependent on the ordering of the atoms.

6.1.4. Structural types: cF16–Li_3Bi and cF16–NaTl

cF16–Li_3Bi type is face-centered cubic, space group $Fm\bar{3}m$, No. 225.
Atomic positions:
4 Bi in a) 0,0,0; $\frac{1}{2},\frac{1}{2},0$; $\frac{1}{2},0,\frac{1}{2}$; $0,\frac{1}{2},\frac{1}{2}$
4 Li in b) $\frac{1}{2},\frac{1}{2},\frac{1}{2}$; $0,0,\frac{1}{2}$; $0,\frac{1}{2},0$; $\frac{1}{2},0,0$
8 Li in c) $\frac{1}{4},\frac{1}{4},\frac{1}{4}$; $\frac{3}{4},\frac{3}{4},\frac{1}{4}$; $\frac{3}{4},\frac{1}{4},\frac{3}{4}$; $\frac{1}{4},\frac{3}{4},\frac{3}{4}$; $\frac{3}{4},\frac{3}{4},\frac{3}{4}$; $\frac{1}{4},\frac{1}{4},\frac{3}{4}$; $\frac{3}{4},\frac{1}{4},\frac{1}{4}$; $\frac{1}{4},\frac{3}{4},\frac{1}{4}$
Coordination formula:
$^{3}_{\infty}[BiLi_{8/4}Li_{6/6}]$ (ionic description)
For the layer stacking symbols, see under the following description of the NaTl type.
For the prototype itself, Li_3Bi, a = 672.2 pm.

This structure (or BiF_3 structure) could also be described as derived from a cubic close-packed array of atoms (Bi atoms) by filling all the tetrahedral and octahedral holes with Li (or F) atoms.

The *cF16–NaTl type* structure is face-centered, cubic, space group $Fd\bar{3}m$, No. 227.
Atomic positions:
8 Tl in a) 0,0,0; $0,\frac{1}{2},\frac{1}{2}$; $\frac{1}{2},0,\frac{1}{2}$; $\frac{1}{2},\frac{1}{2},0$; $\frac{3}{4},\frac{1}{4},\frac{3}{4}$; $\frac{3}{4},\frac{3}{4},\frac{1}{4}$; $\frac{1}{4},\frac{1}{4},\frac{1}{4}$; $\frac{1}{4},\frac{3}{4},\frac{3}{4}$.
8 Na in b) $\frac{1}{2},\frac{1}{2},\frac{1}{2}$; $\frac{1}{2},0,0$,; $0,\frac{1}{2},0$; $\frac{1}{2},\frac{1}{2},0$; $\frac{1}{4},\frac{3}{4},\frac{1}{4}$; $\frac{1}{4},\frac{1}{4},\frac{3}{4}$; $\frac{3}{4},\frac{3}{4},\frac{3}{4}$; $\frac{3}{4},\frac{1}{4},\frac{1}{4}$.
For the prototype, NaTl, a = 747.3 pm.

LiZn, LiCd, LiAl, NaIn have this structure.

This structure may be regarded as a completely filled-up fcc arrangement in which each component occupies a diamond like array of sites (see sec. 6.3.1. and, in sec. 3.4., "Zintl Phases".)

The structure may thus be presented as **NaTl**: **D** + D′ (see the descriptions in terms of combination of invariant lattice complexes reported in sec. 3.1.).

The coordination formula is $^{33}_{\infty}Na[Tl_{4/4}]_{4/4}$.

All the three cF16–NaTl, Li_3Bi and $MnCu_2Al$ types, which may also be considered as composed of four interpenetrating face centered cubic arrays (F + F′ + F″ + F‴), correspond to the same space filling as in 8 b.c. cubic (or in 8 CsCl type) cells (see fig. 24).

The layer stacking symbols of the NaTl structure are here reported in comparison with those of the cF16–Li_3Bi and cF16–$MnCu_2Al$ types.

Triangular (T) nets:

NaTl type:

$Na_0^A\ Tl_{1/12}^B\ Tl_{1/6}^C\ Na_{1/4}^A\ Na_{1/3}^B\ Tl_{5/12}^C\ Tl_{1/2}^A\ Na_{7/12}^B\ Na_{2/3}^C\ Tl_{3/4}^A\ Tl_{5/6}^B\ Na_{11/12}^C$

Li_3Bi type

$Bi_0^A\ Li_{1/12}^B\ Li_{1/6}^C\ Li_{1/4}^A\ Bi_{1/3}^B\ Li_{5/12}^C\ Li_{1/2}^A\ Li_{7/12}^B\ Bi_{2/3}^C\ Li_{3/4}^A\ Li_{5/6}^B\ Li_{11/12}^C$

$MnCu_2Al$ type

$Al_0^A\ Cu_{1/12}^B\ Mn_{1/6}^C\ Cu_{1/4}^A\ Al_{1/3}^B\ Cu_{5/12}^C\ Mn_{1/2}^A\ Cu_{7/12}^B\ Al_{2/3}^C\ Cu_{3/4}^A\ Mn_{5/6}^B\ Cu_{11/12}^C$

Square (S) nets:

NaTl type:

$Na_0^1\ Na_0^4\ Tl_0^5\ Na_{1/4}^6\ Tl_{1/4}^7\ Tl_{1/2}^1\ Tl_{1/2}^4\ Na_{1/2}^5\ Tl_{3/4}^6\ Na_{3/4}^7$

Li_3Bi type

$Bi_0^1\ Bi_0^4\ Li_0^5\ Li_{1/4}^6\ Li_{1/4}^7\ Li_{1/2}^1\ Li_{1/2}^4\ Bi_{1/2}^5\ Li_{3/4}^6\ Li_{3/4}^7$

$MnCu_2Al$ type:

$Al_0^1\ Al_0^4\ Mn_0^5\ Cu_{1/4}^6\ Cu_{1/4}^7\ Mn_{1/2}^1\ Mn_{1/2}^4\ Al_{1/2}^5\ Cu_{3/4}^6\ Cu_{3/4}^7$

6.1.5. Comments on the bcc derivative structures

In the family of bcc derivative structures we may include several other structural types.

As an important *defect superstructure* based on the bcc structure we may mention the **cP52–Cu_9Al_4** type structure (Ag_9In_4, Au_9In_4, Pd_8Cd_{43}, Co_5Zn_{21}, Cu_9Ga_4, $Li_{10}Pb_3$ can be considered reference formulae of selected solid solution phases having this structure). The large cell (a = 870.4 pm in the case of Cu_9Al_4) can be considered to be obtained by assembling 27 CsCl type pseudocells with two vacant sites. One vacant site occurs on each sublattice $Al_{16}Cu_{10}\square$ and $Cu_{26}\square$.

The **γ-brass, cI52–Cu_5Zn_8**-type structure can be similarly described as a distorted defect superstructure of the W type structure, in which 27 pseudocells are assembled together with two vacant sites (corner and body center of the supercell). In this case, however, the atoms, are considerably displaced from their ideal sites. The structure could also be described as built up of interpenetrating, distorted, icosahedra (each atom being sur-

rounded by 12 neighbours). This description applies also to the cP52–Cu_9Al_4 type structure. (Ag_5Cd_8, Li_7Ag_3, Ag_5Zn_8, V_5Al_8, Au_5Cd_8, Au_5Hg_8, Fe_3Zn_{10}, $NiGa_4$, V_6Ga_7, Ni_2Zn_{11}, etc. crystallize in the cI52–Cu_5Zn_8 structural type).

Martensite. The iron-carbon martensite structure can be considered a tetragonal distortion of the body-centered cubic cell of Fe (a = 285 pm, c = 298 pm at ≈ 1 mass% C (≈ 4.5 at%), in comparison to a = 286.65 pm for α-Fe, cI2–W type). Carbon is randomly distributed in the octahedral holes having coordinates $0,0,\frac{1}{2}$ and $\frac{1}{2},\frac{1}{2},0$. Typically an occupancy of these sites of only a few % has to be considered. For a 100% occupancy the structure of the tI4–CoO type (low-temperature form) is obtained with 2 Co in a) $0,0,0$; $\frac{1}{2},\frac{1}{2},\frac{1}{2}$; and 2 O in b) $0,0,\frac{1}{2}$; $\frac{1}{2},\frac{1}{2},0$ in the space group I4/mmm, No. 139. In the martensitic cell the position parameters of the Fe atoms have a range along the fourfold axis, so there is a displacement from the cell corners and body center and an enlargement of the octahedral holes containing carbon. (Notice, however, that "*martensite*" is also a general name used by metallurgists to denote all phases formed by diffusionless shear).

Al–Cu–Ni continuous sequence of ordered structures. An interesting series of superstructures have been described by LU and CHANG [1957a, 1957b]. For an assessed description of the system and of the intermediate phases see PRINCE [1991]. They all have hexagonal unit cells (some corresponding to rhombohedral structures) based on ordered sequences of pseudo cubic subcells slightly distorted in rhombohedra having the constant a_{rhom} included between 289 and 291 pm and the interaxial angle α_{rhom} included between 90.34 and 90.10°. (These data may be compared with the values a = ≈ 288 pm and, of course, $\alpha = 90°$, for the cubic CsCl type unit cell of NiAl at the 50 at% Al composition). The hexagonal cells of the superstructures have a certain number of subcells stacked along c. Al atoms occupy the corners of the subcells and Ni,Cu (Me) atoms or vacancies (Vac) occupy the centers in ordered array, vacancies occurring along the three triad axes ($0,0,0$; $\frac{1}{2},\frac{2}{3},z$; $\frac{2}{3},\frac{1}{3},z$). All together these phases corresponds to the τ-region lying in the ternary system in a domain included between ≈ 7 and 12 at% Ni and between ≈ 27 and 38 at% Cu. The different τ_i ordered structures correspond to the stacking of i subcells centred according to a definite sequence of Vac or Me atoms.

Following stacking variants have been described:

$\tau_5 \approx (Ni,Cu)_3Al_5$, hR24, a = 411.9 pm, c = 2512.5 pm (= 5 * 502.5)
stacking sequence $VacMeMeMeVac = VacMe_3Vac$

$\tau_6 \approx (Ni,Cu)_4Al_6$, hP30, a = 411.3 pm, c = 3013.5 pm (= 6 * 502.3)
stacking sequence $VacMe_4Vac$

$\tau_7 \approx (Ni,Cu)_5Al_7$, hP36, a = 410.6 pm, c = 3493.8 pm (= 7 * 499.1)
stacking sequence $VacMe_5Vac$

$\tau_8 \approx (Ni,Cu)_6Al_8$, hR42, a = 410.5 pm, c = 3990 pm (= 8 * 498.8)
stacking sequence $VacMe_6Vac$

$\tau_{11} \approx (Ni,Cu)_6Al_{11}$, hP51, a = 411.5 pm, c = 5528.9 pm (= 11 * 502.6)
stacking sequence $VacMe_3Vac_3Me_3Vac$

$\tau_{13} \approx (Ni,Cu)_8Al_{13}$, hR63, a = 411.3 pm, c = 6517.3 pm (= 13 * 501.3)
stacking sequence $VacMe_4Vac_3Me_4Vac$

$\tau_{15} \approx (Ni,Cu)_{10}Al_{15}$, hP75, a = 409.6 pm, c = 7464.5 pm (= 15 * 497.6)
stacking sequence $VacMe_5Vac_3Me_5Vac$
$\tau_{17} \approx (Ni,Cu)_{12}Al_{17}$, hP87, a = 410.1 pm, c = 8449.9 pm (= 17 * 497.1)
stacking sequence $VacMe_6Vac_3Me_6Vac$

These structures appeared to be determined by the free electron concentration. They represent a so-called "*continuous sequence of ordered structures*" or, infinitely adaptive structures (HYDE and ANDERSSON [1989]). These structures occupy a single-phase field in the system: it has been observed that, in such cases, may be ambiguous to define a phase in terms of a unit cell of structure.

6.2. Close-packed structures and derivative structures

In this section, a few important elemental structures are described. Particularly the cubic (cF4–Cu type) and hexagonal close-packed (hP2–Mg) structures are presented. A few other stacking variants of identical monoatomic triangular nets are also reported. A group of structures which can be considered as derivative structures of Cu are also described.

Normalized interatomic distances and numbers of equidistant neighbours are shown in figs. 25 and 26.

6.2.1. Structural type: cF4–Cu

Face-centered cubic, space group $Fm\bar{3}m$, No. 225.
Atomic positions:
4 Cu in a) 0,0,0; $0,\frac{1}{2},\frac{1}{2}$; $\frac{1}{2},0,\frac{1}{2}$; $\frac{1}{2},\frac{1}{2},0$;
Coordination formula: $^{3}_{\infty}[Cu_{12/12}]$
Layer stacking symbols:
Triangular (T) nets: $Cu_0^A\, Cu_{1/3}^B\, Cu_{2/3}^C$
Square (S) nets: $Cu_0^1\, Cu_0^4\, Cu_{1/2}^5$
For the prototype itself, Cu, a = 361.46 pm.

The atoms are arranged in close packed layers stacked in the ABC sequence (see sec. 3.5.2.).

Several metals, such as Al, Ag, Au, α Ca, α Ce, γ Ce, α Co, Cu, γ Fe, Ir, β La, Pb, Pd, Pt, Rh, α Sr, α Th and the noble gases Ne, Ar, Kr, Xe crystallize in this structural type. Several binary (and complex) phases having this structure have also been reported (solid solutions with random distribution of several atomic species in the four equivalent positions).

6.2.2. Cu-derivative, substitutional and interstitial superstructures (tetrahedral and octahedral holes)

Derivative structures may be obtained from the Cu type structure by ordered substitution or by ordered addition of atoms. As examples of *derivative structures* obtained *by ordered substitution* (and/or distortion) in the Cu type we may mention the $AuCu_3$, AuCu, Ti_3Cu types, which are described here below. (In the specific case of the $AuCu_3$ type structure and the Cu–$AuCu_3$ types interrelation, see also sec. 3.5.5.). For a

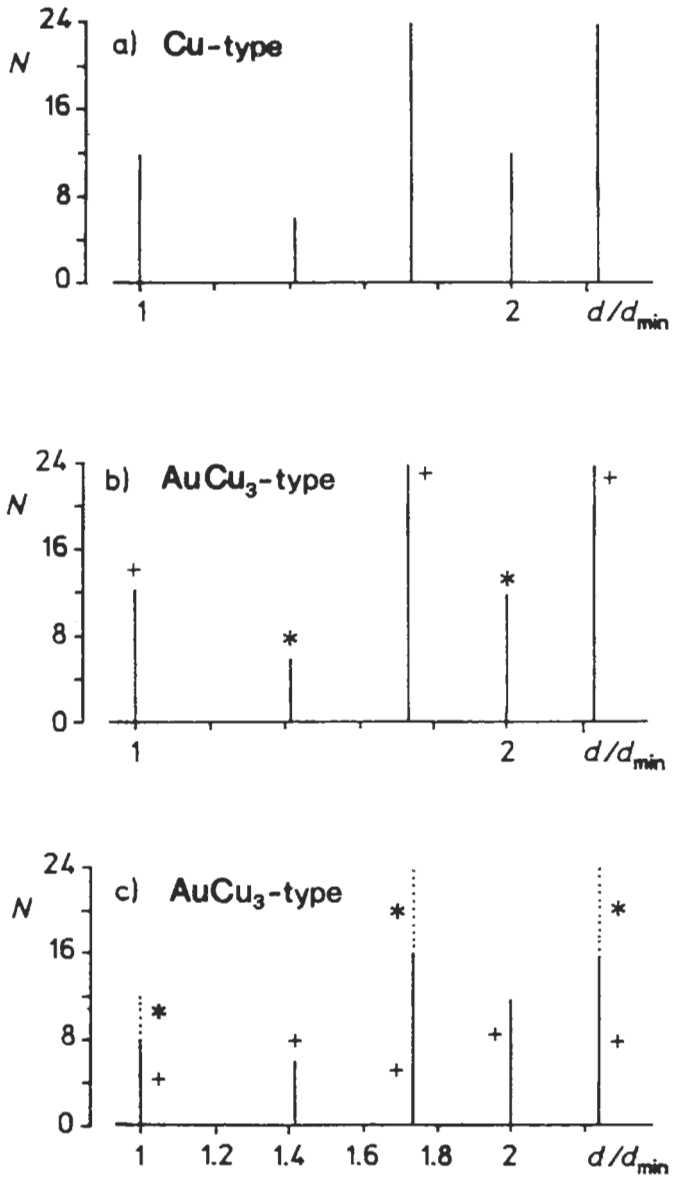

Fig. 25. Distances and coordinations in the cF4–Cu and cP4–$AuCu_3$ types structures. (Compare also with figs. 14 and 15.)

a) cF4–Cu type structure

b) cP4–$AuCu_3$ type structure: coordination around Au
(+) Au-Cu; (*) Au-Au.

c) $AuCu_3$ type structure: coordination around Cu
(+) Cu-Cu; (*) Cu-Au.

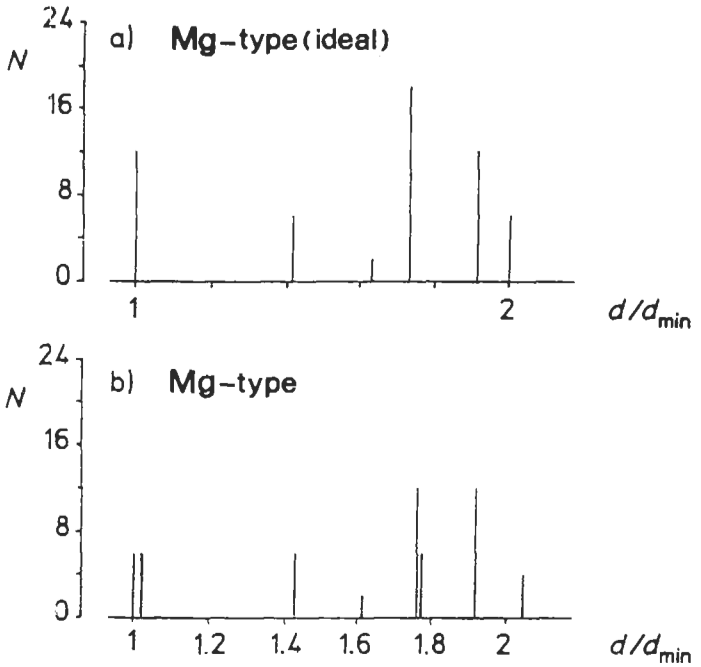

Fig. 26. Distances and coordinations in the hexagonal close-packed (Mg-type) structure.
a) Ideal structure, c/a = 1.633 (first coordination shell corresponding to 12 atoms at the same distance).
b) Mg-type structures with c/a = 1.579.
The group of the first 12 neighbours is subdivided into 6 + 6 atoms at slightly different distances.

systematic description of the *derivative structures* which may be obtained from the Cu type *by ordered filling-up* it may be useful to consider that in a closest packing of equal spheres there are, among the spheres themselves, essentially two kinds of interstices (holes). These are shown in fig. 27. The smallest holes surrounded by a polyhedral group of spheres are those marked by T. An atom inserted in this hole will have four neighbours whose centres lie at the vertices of a regular tetrahedron (*tetrahedral holes*). The larger holes (*octahedral holes*) are surrounded by octahedral groups of six spheres. In an infinite assembly of close-packed spheres the ratios of the numbers of the tetrahedral and octahedral holes to the number of spheres are, respectively, 2 and 1.

Considering the Cu type structure (in which the 4 close-packed spheres are in 0,0,0; $0,\frac{1}{2},\frac{1}{2}$; $\frac{1}{2},0,\frac{1}{2}$; $\frac{1}{2},\frac{1}{2},0$) the centers of the tetrahedral and octahedral holes have the coordinates:

4 octahedral holes in:
$\frac{1}{2},\frac{1}{2},\frac{1}{2}$; $\frac{1}{2},0,0$; $0,\frac{1}{2},0$; $0,0,\frac{1}{2}$;
2 sets of 4 tetrahedral holes in:
$\frac{1}{4},\frac{1}{4},\frac{1}{4}$; $\frac{1}{4},\frac{3}{4},\frac{3}{4}$; $\frac{3}{4},\frac{1}{4},\frac{3}{4}$; $\frac{3}{4},\frac{3}{4},\frac{1}{4}$;
and in:
$\frac{3}{4},\frac{3}{4},\frac{3}{4}$; $\frac{3}{4},\frac{1}{4},\frac{1}{4}$; $\frac{1}{4},\frac{3}{4},\frac{1}{4}$; $\frac{1}{4},\frac{1}{4},\frac{3}{4}$.

References: p. 363.

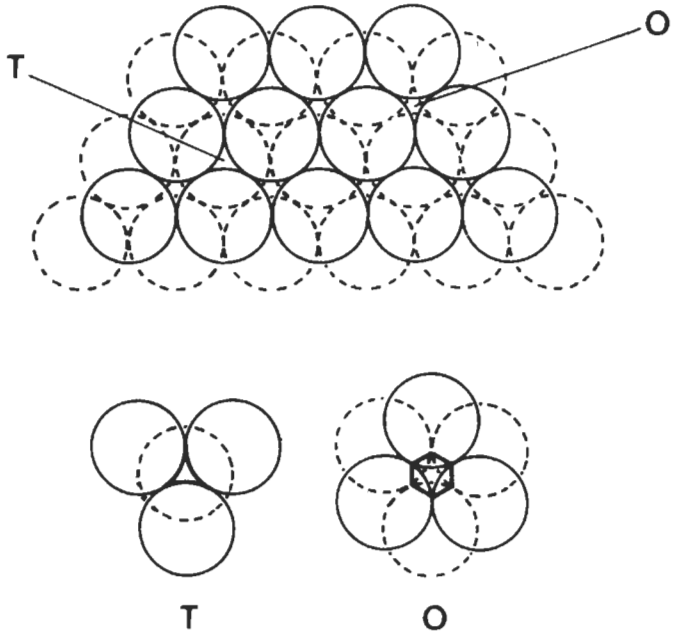

Fig. 27. Voids in the closest packing of equal spheres; tetrahedral (T) and octahedral holes (O) are evidenced within two superimposed triangular nets.

Several cubic structures, therefore, in which (besides 0,0,0; $0,\frac{1}{2},\frac{1}{2}$; $\frac{1}{2},0,\frac{1}{2}$; $\frac{1}{2},\frac{1}{2},0$) one (or more) of the reported coordinate groups are occupied could be considered as filled-up derivatives of the cubic close-packed structures. The NaCl, CaF_2, ZnS (sphalerite), AgMgAs and Li_3Bi type structures could, therefore, be included in this family of derivative structures. For this purpose, however, it may be useful to note that the radii of small spheres which fit exactly into tetrahedral and octahedral holes are 0.225... and 0.414..., respectively, if the radius of the close-packed spheres is 1.0. For a given phase pertaining to one of the aforementioned types (NaCl, ZnS, etc.) if the stated dimensional conditions are not fulfilled, alternative descriptions of the structure may be more convenient than the reported derivation schemes.

Notice, moreover, that a fc cubic cell of atoms X in which all the interstices are occupied (the octahedral by X and the tetrahedral by Z atoms) is equivalent to a block of 8 XZ, CsCl type, cells (see figs. 3 and 24). This relationships (and other ones with other structures such Li_3Bi and $MnCu_2Al$) should be kept in mind when considering, for instance, phase transformations occurring in ordering processes.

Similar considerations may be made with reference to the other simple close-packed structure, that is to the hexagonal Mg type structure. In this case two basic derived structures can be considered: the NiAs type with occupied octahedral holes and the wurtzite (ZnS) type with one set of occupied tetrahedral holes.

6.2.3. Structural type: cP4–$AuCu_3$

Cubic, space group $Pm\bar{3}m$, No. 221;

Atomic positions:
1 Au in a) 0,0,0
3 Cu in c) $0,\frac{1}{2},\frac{1}{2}$; $\frac{1}{2},0,\frac{1}{2}$; $\frac{1}{2},\frac{1}{2},0$
Coordination formula: $3^3_3\,3\,[Au_{6/6}][Cu_{8/8}]_{12/4}$
Layer stacking symbols:
Triangular, kagomé (T,K) nets:
$Au^{A}_{0}\,C^{\alpha}_{0}\,Au^{C}_{1/3}\,Cu^{\gamma}_{1/3}\,Au^{B}_{2/3}\,Cu^{\beta}_{2/3}$
Square (S) nets: $Au^{1}_{0}\,Cu^{4}_{0}\,Cu^{5}_{1/2}$
For the prototype itself, $AuCu_3$, a = 374.8 pm.
(See also sec. 3.5.5. for a detailed description of this structure.)

This structure can be considered a derivative structure (ordered substitution) of the cF4–Cu type.

A discussion of the characteristics of a number of ordered layer (super)structures involving a XY_3 stoichiometry has been reported by MASSALSKI [1989]. Sequences of layer structures (among which those corresponding to the cP4–$AuCu_3$, hP16–$TiNi_3$, hP24–VCo_3, hR36–$BaPb_3$ types) as observed in V (or Ti) alloys with Fe, Co, Ni, Cu are described. The relative stabilities of the different stacking sequences have been analyzed in terms of a few parameters which characterize the interactions between various layers.

6.2.4. Structural types: tP2–AuCu (I) and oI40–AuCu(II)

tP2–AuCu(I) is tetragonal, space group P4/mmm, No. 123;

Atomic positions:
1 Au in a) 0,0,0;
1 Cu in d) $\frac{1}{2},\frac{1}{2},\frac{1}{2}$;
For the prototype itself, AuCu(I), a = 280.4 pm, c = 367.3 pm, c/a = 1.310.

The unit cell could be considered either as a distorted CsCl type cell greatly elongated in the c direction or, better, as a deformed (and orderly substituted) Cu type cell. This is apparent from fig. 20 where the tP2 unit cell and two tP4 supercells having $a' = a\sqrt{2} = 396.6$ pm, $c' = c = 367.3$ pm are also shown. The larger cell is similar to a Cu type cell, slightly compressed ($c'/a' = 0.926$) and in which the atoms placed in the center of the sidefaces have been orderly substituted. The coordinates in the tP4 super(pseudo)cell are:

Au in 0,0,0, and $\frac{1}{2},\frac{1}{2},0$;
Cu in $\frac{1}{2},0,\frac{1}{2}$ and $0,\frac{1}{2},\frac{1}{2}$;
and the corresponding square nets stacking sequence is $Au^{1}_{0}\,Au^{4}_{0}\,Cu^{5}_{1/2}$.
The *long period superstructure of AuCu(I)*, discussed in sec. 4.2., resulting in the antiphase-domain structure of AuCu(II) is shown in fig. 20c.

6.2.5. Structural type: tP4–Ti_3Cu

Tetragonal, space group P4/mmm, No. 123;

Atomic positions:
1 Cu in a) 0,0,0
1 Ti in c) $\frac{1}{2},\frac{1}{2},0$;
2 Ti in e) $0,\frac{1}{2},\frac{1}{2}$; $\frac{1}{2},0,\frac{1}{2}$;
Coordination formula: $^{3}_{\infty}3[Cu_{6/6}][Ti_{8/8}]_{12/4}$
Layer stacking symbols:
Square (S) nets: $Cu^{1}_{0}\,Ti^{4}_{0}\,Ti^{5}_{1/2}$.
For the prototype itself, Ti_3Cu, a = 415.8 pm, c = 359.4 pm, c/a = 0.864. This structure can be described as a tetragonal distortion of the $AuCu_3$ type structure. It may also be considered a variant of the previously described AuCu(I) type (compare with its tP4 pseudocell).

6.2.6. Structural types: hP2–Mg, hP4–La and hR9–Sm

hP2–Mg type. Hexagonal, Space group $P6_3/mmc$, No. 194.

Atomic positions:
2 Mg in c) $\frac{1}{3},\frac{2}{3},\frac{1}{4}$; $\frac{2}{3},\frac{1}{3},\frac{3}{4}$;
Coordination formula: $^{3}_{\infty}[Mg_{(6+6)/(6+6)}]$ and ideally: $^{3}_{\infty}[Mg_{12/12}]$.
For the prototype itself, Mg, a = 320.89 pm, c = 521.01 pm, c/a = 1.624.
Normalized interatomic distances and numbers of equidistant neighbours are presented in fig. 26a for an "ideal" hexagonal close-packed structure ($c/a = \sqrt{8/3} = \approx 1.633$), which corresponds to 12 nearest neighbours at the same distance, and, in fig. 26b, for a slightly distorted cells.

The atoms are arranged in close-packed layers stacked in the sequence ABAB... (or BCBC... see sec. 3.5.2.). The corresponding layer symbol (triangular nets) is $Mg^{B}_{0.25}\,Mg^{C}_{0.75}$.

Several metals have been reported with this type of structure, such as: αBe, Cd, εCo, αDy, Er, Ho, Lu, Mg, Os, Re, Ru, Tc, αY, Zn, etc. Several binary (and complex) phases have also been described with this type of structure. These are generally solid solution phases with a random distribution of the different atomic species in the two equivalent positions.

Other *stacking variants* of close-packed structures are the *La type* and *Sm type structures*. Characteristic features of these types are presented here below.

hP4–La type. Hexagonal, Space group $P6_3/mmc$, No. 194.
Atomic positions:
2 La in a) 0,0,0; $0,0,\frac{1}{2}$;
2 La in c) $\frac{1}{3},\frac{2}{3},\frac{1}{4}$; $\frac{2}{3},\frac{1}{3},\frac{3}{4}$;
For the prototype itself, αLa, a = 377.0 pm, c = 1215.9 pm, c/a = 3.225.
Layer stacking symbols:
Triangular (T) nets: $La^{A}_{0}\,La^{B}_{0.25}\,La^{A}_{0.5}\,La^{C}_{0.75}$.

hR9–Sm type. Rhombohedral, space group $R\bar{3}m$, No. 166.
Atomic positions:
3 Sm in a) 0,0,0; $\frac{2}{3},\frac{1}{3},\frac{1}{3}$; $\frac{1}{3},\frac{2}{3},\frac{2}{3}$;

6 Sm in c) 0,0,z; 0,0,−z; $\frac{2}{3},\frac{1}{3},\frac{1}{3}+z$; $\frac{2}{3},\frac{1}{3},\frac{1}{3}-z$; $\frac{1}{3},\frac{2}{3},\frac{2}{3}+z$; $\frac{1}{3},\frac{2}{3},\frac{2}{3}-z$;
For the prototype itself, αSm, a = 362.90 pm, c = 2620.7 pm, c/a = 7.222 and z = 0.222.
Layer stacking symbols:
Triangular (T) nets:
$Sm_0^A\ Sm_{0.11}^C\ Sm_{0.22}^A\ Sm_{0.33}^C\ Sm_{0.45}^B\ Sm_{0.55}^C\ Sm_{0.67}^B\ Sm_{0.78}^A\ Sm_{0.89}^B$.

The La and Sm type structures belong to the same *homeotect type* set as Mg and Cu (see sec. 4.3.). All these close-packed element structures are stacking variants of identical slab types (monoatomic triangular nets).

6.2.7. Structural type: hP8–Ni_3Sn

Hexagonal, Space group $P6_3/mmc$, No. 194.
Atomic positions:
2 Sn in c): $\frac{1}{3},\frac{2}{3},\frac{1}{4}$; $\frac{2}{3},\frac{1}{3},\frac{3}{4}$;
6 Ni in h): x,2x,$\frac{1}{4}$; −2x,−x,$\frac{1}{4}$; x,−x,$\frac{1}{4}$; −x,−2x,$\frac{3}{4}$; 2x,x,$\frac{3}{4}$; −x,x,$\frac{3}{4}$.
For the prototype itself a = 527.5 pm, c = 423.4 pm, c/a = 0.802 and x = 0.833.
(A projection of the cell is shown in fig. 28 and compared with that of the hP2–Mg type).
The layer stacking symbol (triangular and kagomé nets) is:
$Sn_{0.25}^B\ Ni_{0.25}^{\beta}\ Sn_{0.75}^C\ Ni_{0.75}^{\gamma}$.
(which may be compared with the symbol $Mg_{0.25}^B\ Mg_{0.75}^C$ of the Mg type).

This type is a superstructure of the closed packed (hP2–Mg) hexagonal structure in the same way as the $AuCu_3$ type is of the close-packed cubic (cF4–Cu) structure. It can, therefore, be considered a stacked polytype of the $AuCu_3$ type.

Several phases belong to this type, for instance, Ti_3Al, Fe_3Ga, Fe_3Ge, Fe_3Sn, $ZrNi_3$, $ThAl_3$, YAl_3, etc.

In the specific case of the rare earth trialuminides $REAl_3$, the Ni_3Sn type structure has been observed for $LaAl_3$ to $GdAl_3$ (and YAl_3). For $ErAl_3$ to $YbAl_3$ and $ScAl_3$ the $AuCu_3$ type structure is formed. For the intermediate $REAl_3$, intermediate stacking variants of similar layers have been described and their relative stabilities discussed (VAN VUCHT and BUSCHOW [1965]). In fig. 28b, the oP8–β $TiCu_3$ type structure is also shown. The close relationship between the two structures may be noticed.

6.2.8. Structural type: hP6–$CaCu_5$

As another example of structures in which more complex stacking sequences can be observed we may mention here the hP6–$CaCu_5$ type structure, which is the reference type for a family of structures in which 3^6 nets (and 6^3) are alternatively stacked with 3636 (kagomé) nets of atoms.

The hP6–$CaCu_5$ structure is hexagonal, space group P6/mmm, No. 191, with:
1 Ca in a) 0,0,0,
2 Cu in c) $\frac{1}{3},\frac{2}{3},0$; $\frac{2}{3},\frac{1}{3},0$;
3 Cu in g) $\frac{1}{2},0,\frac{1}{2}$; $0,\frac{1}{2},\frac{1}{2}$; $\frac{1}{2},\frac{1}{2},\frac{1}{2}$;
For the prototype, a = 509.2 pm, c = 408.6 pm, c/a = 0.802.
The layer stacking symbol, triangular (T: A,B,C), hexagonal (H: a,b,c) and kagomé (K: α,β,γ) nets is: $Ca_0^A\ Cu_0^a\ Cu_{0.5}^{\alpha}$ (see fig. 29).

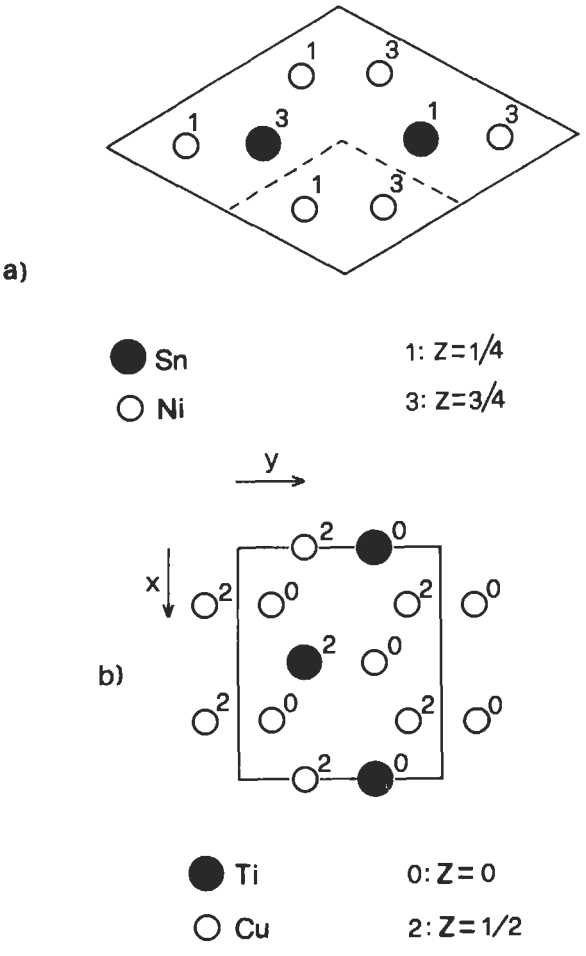

Fig. 28. hP8–Ni_3Sn type unit cell.

a) Projection of the hP8–Ni_3Sn type unit cell on the x,y plane (the values of the coordinate z are indicated). A Mg-type subcell is represented by the dotted lines.

b) Projection of the oP8–β-$TiCu_3$ type cell. Compare the similar arrangements of the atoms in the two structures.

A large coordination is obtained in this structure: Ca is surrounded by 6 Cu + 12 Cu + 2 Ca at progressively higher distances and the Cu atoms have 12 neighbours (in a non-icosahedral coordination).

Several phases belonging to this structure are known (alkali metal compounds such as KAu_5, $RbAu_5$, alkaline earth compounds such as $BaAu_5$, $BaPd_5$, $BaPt_5$, $CaPt_5$, $CaZn_5$, etc., rare earth alloys such as $LaCo_5$, $LaCu_5$, $LaPd_5$, $LaPt_5$, $LaZn_5$, etc., The compounds as $ThFe_5$, $ThCo_5$, $ThNi_5$, etc.). Ternary phases have been also described, both correspon-

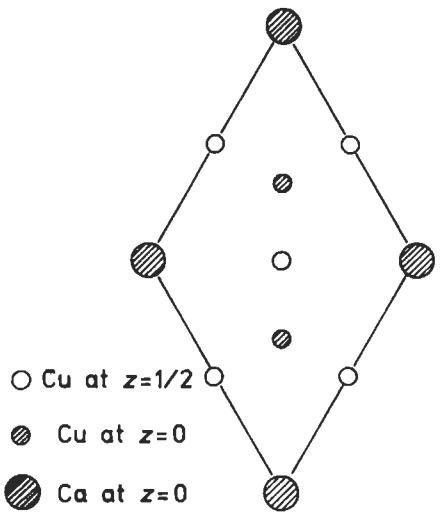

Fig. 29. Projection of the hP6–$CaCu_5$ type unit cell on the x,y plane.

ding to the *ordered derivative hP6–$CeCo_3B_2$ type* (1 Ce in a), 2 B in c) and 3 Co in g)) and to disordered solid solutions of a third component in a binary $CaCu_5$ type phase.

According to PEARSON [1972] several structures may be described as derived from the $CaCu_5$ type (for instance, the tI26–$ThMn_{12}$ type; hR57–Th_2Zn_{17} type; hP38–Th_2Ni_{17} type; etc.).

As for the building principles of the $CaCu_5$ type some analogies with the Laves phases (see sec. 6.6.4) may be noticed.

Cobalt-based rare earth alloys such as $SmCo_5$ (hP6–$CaCu_5$ type) are important materials for permanent magnets. A short review on the properties of alloys for permanent magnetic materials has been reported by RAGHAVAN and ANTIA [1994]. Complex (especially iron) alloys have been mentioned starting from the Alnico (Fe–Al–Ni–Co) alloys introduced in the thirties followed by ferrites and Co-based rare earth alloys (such as $SmCo_5$) and then by $Sm_2(Co,Fe,Cu)_{17}$ and $Nd_2Fe_{14}B$ (tP68) with a progressive decreasing of volume and weight of magnets per unit energy product.

6.3. Tetrahedral structures

This section is mainly dedicated to the presentation of a few typical so-called tetrahedral structures. For the simplest ones, normalized interatomic distances and numbers of equidistant neighbours are shown in fig. 30. The graphite structure will also be described.

6.3.1. cF8–C (diamond) and tI4–βSn structural types

cF8–C (diamond) type.

Face-centered cubic, space group $Fd\bar{3}m$, No. 227.

Atomic positions:

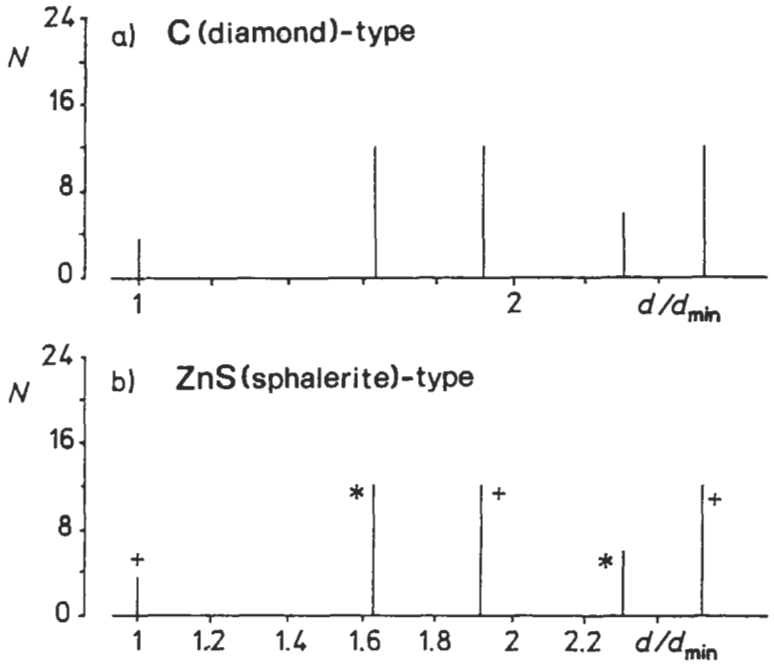

Fig. 30. Distances and coordinations in the cF8–C diamond and cF8–ZnS sphalerite type structures.
a) cF8–C (diamond) type structure.
b) XY compounds of cF8–ZnS type structure:
(+) X–Y (or Y–X) coordination.
(*) X–X (or Y–Y) coordination.

8 C in a) 0,0,0; $0,\frac{1}{2},\frac{1}{2}$; $\frac{1}{2},0,\frac{1}{2}$; $\frac{1}{2},\frac{1}{2},0$; $\frac{1}{4},\frac{1}{4},\frac{1}{4}$; $\frac{1}{4},\frac{3}{4},\frac{3}{4}$; $\frac{3}{4},\frac{1}{4},\frac{3}{4}$; $\frac{3}{4},\frac{3}{4},\frac{1}{4}$;
(This group of atomic positions corresponds to the so-called invariant lattice complex D; see sec. 3.1.).
The coordination formula is $^{3}_{\infty}[C_{4/4}]$
The layer stacking symbols are:
Triangular (T) nets: $C_0^A\, C_{1/4}^A\, C_{1/3}^B\, C_{7/12}^B\, C_{2/3}^C\, C_{11/12}^C$
Square (S) nets: $C_0^1\, C_0^4\, C_{1/4}^6\, C_{1/2}^5\, C_{3/4}^7$
For the prototype itself, C diamond, a = 356.69 pm.

The diamond structure is a 3–dimensional adamantine network in which every atom is surrounded tetrahedrally by four neighbours. The 8 atoms in the unit cell may be considered as forming two interpenetrating face centered cubic networks. If the two networks are occupied by different atoms we obtain the derivative cF8–ZnS (sphalerite) type structure. As a further derivative structure, we may mention the tI16–$FeCuS_2$ type structure (See fig. 31). These are all examples of a family of "tetrahedral" structures which have been described by Parthé and will be briefly presented in sec. 7.2.1.

Si, Ge and αSn have the diamond-type structure. The *tI4–βSn structure* (a = 583.2

pm, c = 318.2 pm) (4 Sn in a) 0,0,0; $0,\frac{1}{2},\frac{1}{4}$;; $\frac{1}{2},\frac{1}{2},\frac{1}{2}$; $\frac{1}{2},0,\frac{3}{4}$; space group $I4_1/amd$, No. 141) can be considered a very much distorted diamond type structure. Each Sn has 4 close neighbours, 2 more at a slightly larger (and 4 other at a considerably larger) distance. The βSn unit cell is reported in fig. 32.

6.3.2. Structural types: cF8–ZnS sphalerite and hP4–ZnO (ZnS wurtzite)

cF8–ZnS sphalerite

Face-centered cubic, space group $F\bar{4}3m$, No. 216.
Atomic positions:

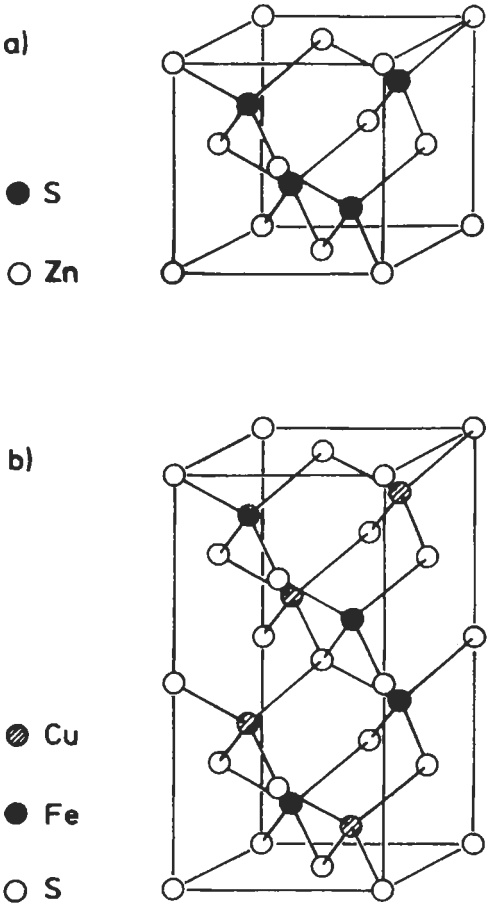

Fig. 31. a) cF8–ZnS sphalerite and b) tI16–$FeCuS_2$ (chalcopyrite) type structures.

References: p. 363.

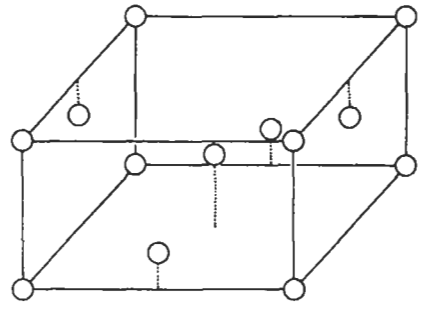

Fig. 32. tI4–βSn type structure.

4 Zn in a) 0,0,0; $0,\frac{1}{2},\frac{1}{2}$; $\frac{1}{2},0,\frac{1}{2}$; $\frac{1}{2},\frac{1}{2},0$;
4 S in c) $\frac{1}{4},\frac{1}{4},\frac{1}{4}$; $\frac{1}{4},\frac{3}{4},\frac{3}{4}$; $\frac{3}{4},\frac{1}{4},\frac{3}{4}$; $\frac{3}{4},\frac{3}{4},\frac{1}{4}$;
In terms of a combination of invariant lattice complexes (see sec. 3.1) we may therefore describe the sphalerite structure as **ZnS**: **F** + F″.
Coordination formulae:
$^{3}_{\infty}[ZnS_{4/4}]$ (ionic or covalent description)
$^{333}_{\infty}[Zn_{12/12}][S_{12/12}]_{4/4}$ (metallic description)
For the prototype itself, ZnS sphalerite, a = 541.1 pm.

Structural type ***hP4–ZnO or ZnS wurtzite***
hexagonal, $P6_3mc$, No. 186.
Atomic positions:
2 Zn in b (1) $\frac{1}{3},\frac{2}{3},z$; $\frac{2}{3},\frac{1}{3},\frac{1}{2}+z$; $(z=z_1)$
2 O or 2 S in b (2) $\frac{1}{3},\frac{2}{3},z$; $\frac{2}{3},\frac{1}{3},\frac{1}{2}+z$; $(z=z_2)$
Coordination formula: $^{3}_{\infty}[ZnO_{4/4}]$
For the prototypes themselves, ZnO: a = 325.0 pm, c = 520.7 pm, c/a = 1.602; ZnS (wurtzite): a = 382.3 pm, c = 626.1 pm, c/a = 1.638. The atomic positions correspond, for both types of atoms, to similar coordinate groups (to the same Wyckoff positions) with different values of the z parameter. For ZnO $z_{Zn}=0$, $z_O=0.382_5$ and for ZnS $z_{Zn}=0$, $z_S=0.371$.

6.3.3. General remarks on "tetrahedral structures" and polytypes. tI16–FeCuS2, hP4–C lonsdaleite, oP16–BeSiN2 types and polytypes

Compounds, isostructural with the cubic cF8–ZnS sphalerite include AgSe, AlP, AlAs, AlSb, AsB, AsGa, AsIn, BeS, BeSe, BeTe, BePo, CdSe, CdTe, CdPo, HgS, HgSe, HgTe, etc. (possibly in one of their modifications).

The sphalerite structure can be described as a derivative structure of the diamond type structure. Alternatively we may describe the same structure as a derivative of the cubic close-packed structure (cF4–Cu type) in which a set of tetrahedral holes has been filled-in. (This alternative description would be especially convenient, when the atomic diameter ratio of the two species is close to 0.225: see the comments reported in sec. 6.2.2.).

In a similar way the closely related hP4–ZnO structure can be considered as a derivative of the hexagonal close-packed structure (hP2–Mg type) in which, too, a set of tetrahedral holes has been filled-in.

Compounds, isostructural with ZnO include some forms of AgI, BeO, CdS, CdSe, CuX (X = H, Cl, Br, I), MnX (X = S, Se, Te), MeN (Me = Al, Ga, In, Nb), ZnX (X = O, S, Se, Te).

In order to have around each atom in this hexagonal structure, four exactly equidistant neighbouring atoms, the axial ratio should have the ideal value $\sqrt{8/3}$, that is ≈ 1.633. The experimental values range from 1.59 to 1.66. The ideal value of one of the parameters (being fixed at zero the other one by conventionally shifting the origin of the cell) is $z = 3/8 = 0.3750$.

The C diamond, sphalerite and wurtzite type structures are well-known examples of the "*normal tetrahedral structures*" (see sec. 7.2.1.).

Several *superstructures* and *defect superstructures* based on sphalerite and on wurtzite have been described. The *tI16–$FeCuS_2$ (chalcopyrite) type structure* (tetragonal, a = 525 pm, c = 1032 pm, c/a = 1.966) (see fig. 31b), for instance, is a superstructure of sphalerite in which the two metals adopt ordered positions. The superstructure cell corresponds to two sphalerite cells stacked in the c-direction. The c/2a ratio is nearly 1. As another example we may mention the *oP16–$BeSiN_2$ type structure* which similarly corresponds to the wurtzite type structure.

The degenerate structures of sphalerite and wurtzite (when, for instance, both Zn and S are replaced by C) corresponds to the previously described cF8–diamond type structure and, respectively, to the *hP4–hexagonal diamond or lonsdaleite* which is very rare compared with the cubic, more common, gem diamond. The unit cell dimensions of lonsdaleite (prepared at 13 GPa and 1000°C) are a = 252 pm, c = 412 pm, c/a = 1.635. (Compare with ZnS wurtzite).

While discussing the sphalerite and wurtzite type structures we have also to remember that they belong to a homeotect structure type set. (See sec. 4.3.)

The layer stacking sequence symbols (triangular nets) of the two structures are:
Sphalerite: $Zn_0^A\, S_{1/4}^A\, Zn_{1/3}^B\, S_{7/12}^B\, Zn_{2/3}^C\, S_{11/12}^C$
Wurtzite: $Zn_0^B\, S_{0.37}^B\, Zn_{1/2}^C\, S_{0.87}^C$.

In the first case we have (along the direction of the diagonal of the cubic cell) a sequence ABC of identical "unit slabs" ("minimal sandwiches") each composed of two superimposed triangular nets of Zn and S atoms. The "thickness" of the slabs, between the Zn and S atom nets is 0.25 of the lattice period along the superimposition direction (cubic cell diagonal: $a\sqrt{3}$). It is $(0.25\sqrt{3} * 541)$ pm = 234 pm. In the wurtzite structure we have a sequence BC of slabs formed by sandwiches of the same triangular nets of Zn and S atoms (their thickness is $\approx 0.37 * c = (0.37 * 626.1)$ pm = 232 pm).

With reference to the aforementioned structural unit slab the Jagodzinski-Wyckoff symbol of the two structures will be:
ZnS sphalerite: c; ZnS wurtzite: h.

In the same (equiatomic tetrahedral structure type) homeotect set many more structures occur often with very long stacking periods. Several other polytypes of ZnS itself have

been identified and characterized. The largest number of polytypic forms and the largest number of layers in regular sequence have, however, been found for silicon monocarbide. A cubic form of SiC is known and many tenths of rhombohedral and hexagonal polytypes. (In commercial SiC a six-layer structure, hcc, is the most abundant). All have the same $a_{hex} \approx 308$ pm, the c_{hex} of their hexagonal (or equivalent hexagonal) cells are all multiples of ≈ 252 pm and range from 505 pm to more than 150000 pm (up to more than 600 Si-C slabs in a regular sequence).

6.3.4. An important non-tetrahedral C structure. The hP4–C graphite

In comparison with the previously described tetrahedral structures of C we may mention here the very different structure that carbon adopts in graphite (see fig. 33).
hP4–C graphite. Hexagonal, space group $P6_3/mmc$, No. 194.
Atomic positions:
2 C in b) $0,0,\frac{1}{4}$; $0,0,\frac{3}{4}$;
2 C in c) $\frac{1}{3},\frac{2}{3},\frac{1}{4}$; $\frac{2}{3},\frac{1}{3},\frac{3}{4}$;
Coordination formula: $^{2}_{\infty}[C_{3/3}]$
The lattice parameters are $a = 246.4$ pm and $c = 671.1$ pm; $c/a = 2.724$.
Different varieties, however, of graphite may be considered: the actual structure, in fact, and unit cell dimensions and layer stacking can vary depending on the preparation conditions, degree of crystallinity, disorientation of layers, etc.

In crystalline hP4–graphite, sheets of six-membered rings are situated so that the atoms in alternate layers lie over one other, and the second layer is displaced according to the stacking symbol $C^{b}_{1/4}\,C^{c}_{3/4}$ (compare with fig. 9). Whereas in diamond the bond length is 154 pm, in graphite the C–C minimum bond lenght is 142 pm in the sheets and 335 pm between sheets. This may be related to the highly anisotropic properties of this substance. (It may be said, for instance, that properties of graphite in the sheets are similar to those of a metal while perpendicularly are more like those of a semiconductor).

In conclusion, notice also that in terms of combinations of invariant lattice complexes the positions of the atoms in the level $\frac{1}{4}$ may be represented by $\frac{2}{3},\frac{1}{3},\frac{1}{4}$ G and those in the level $\frac{3}{4}$ by $\frac{1}{3},\frac{2}{3},\frac{3}{4}$ G (where G is the symbol of the "graphitic" net complex, here presented in non-standard settings by means of shifting vectors; see sections 3.1. and 3.5.2.).

6.4. cF8–NaCl, cF12–CaF_2, and cF12–AgMgAs types

In this section the NaCl type, CaF_2 type (and the related AgMgAs type) structures are described.

In fig. 34 the normalized interatomic distances and the equidistant neighbours are shown for the NaCl and CaF_2 structures.

6.4.1. cF8–NaCl type structure and compounds

Face-centered cubic, space group $Fm\bar{3}m$, No. 225.
Atomic positions:
4 Na in a) $0,0,0$; $0,\frac{1}{2},\frac{1}{2}$; $\frac{1}{2},0,\frac{1}{2}$; $\frac{1}{2},\frac{1}{2},0$;
4 Cl in b) $\frac{1}{2},\frac{1}{2},\frac{1}{2}$; $\frac{1}{2},0,0$; $0,\frac{1}{2},0$; $0,0,\frac{1}{2}$;

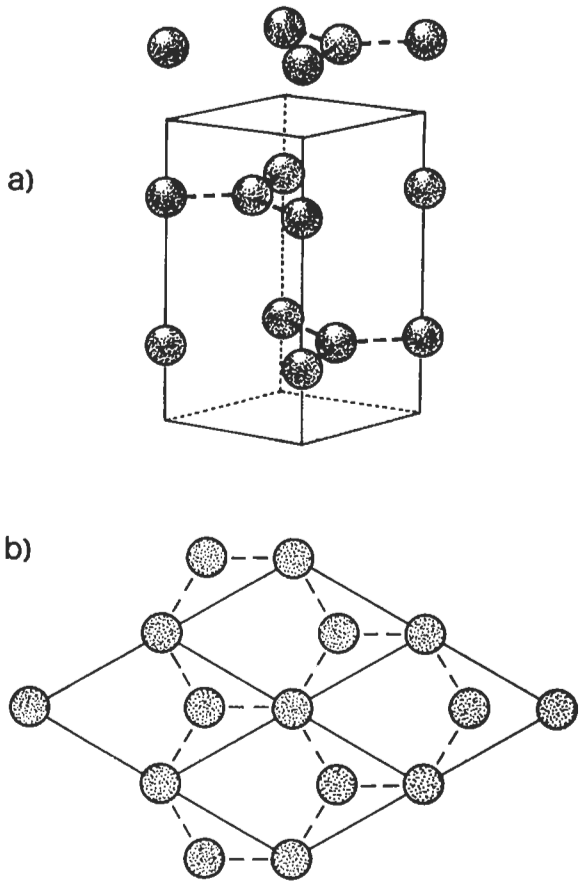

Fig. 33. Graphite structure.
a) unit cell with the indication of the atoms at the levels $z=\frac{1}{4}$ and $\frac{3}{4}$ (part of a second, superimposed cell is also shown).
b) the hexagonal net formed at level $z=\frac{1}{4}$ is shown (four adjacent cells are indicated).

Coordination formula: $^{3}_{\infty}3[Na_{12/12}][Cl_{12/12}]_{6/6}$
Layer stacking symbols:
Triangular (T) nets: $Na^{A}_{0}\,Cl^{C}_{1/6}\,Na^{B}_{1/3}\,Cl^{A}_{1/2}\,Na^{C}_{2/3}\,Cl^{B}_{5/6}$
Square (S) nets: $Na^{1}_{0}\,Na^{4}_{0}\,Cl^{5}_{0}\,Cl^{1}_{1/2}\,Cl^{4}_{1/2}\,Na^{5}_{1/2}$
For the prototype itself, NaCl, a = 564.0 pm.

(A sketch of the NaCl unit cell is shown in fig. 18.)

A large number of compounds belong to this structure type, besides several alkali metal halides, for instance, nearly all the (partially ionic covalent) 1:1 compounds formed by the rare earths and the actinides with N, P, As, Sb, Bi, S, Se, Te, Po, by the alkaline earths with O, S, Se, Te, Po, etc.

Notice that we may also describe this structure as a derivative of the cubic close-

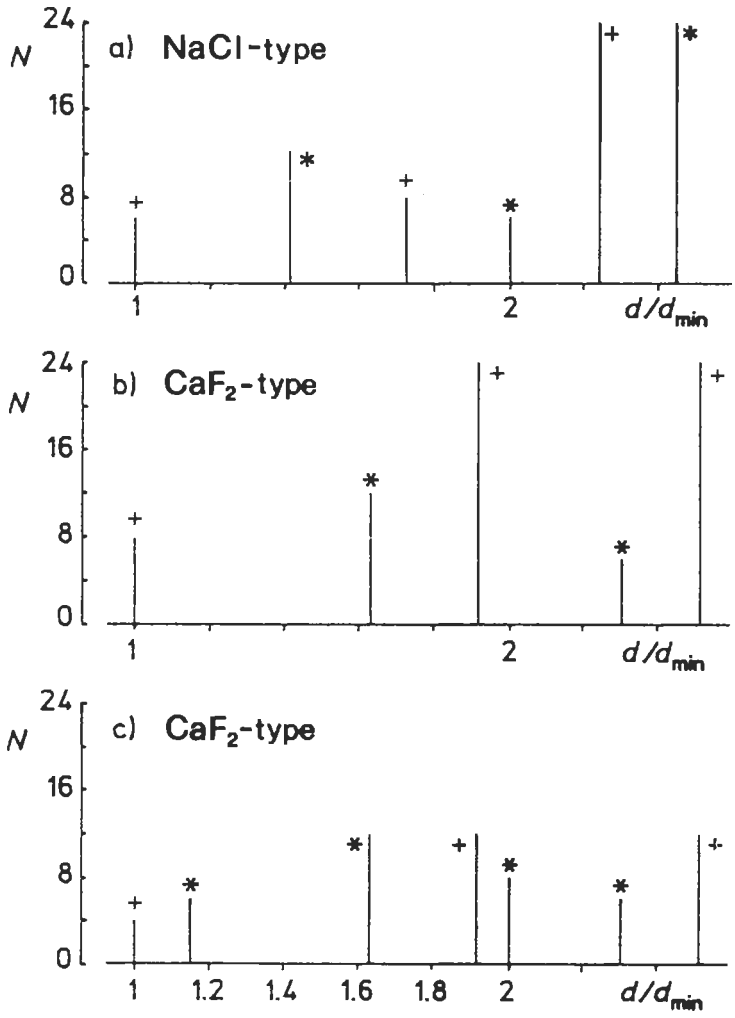

Fig. 34. Distances and coordinations in the cF8–NaCl and cF12–CaF_2 types structures.
a) XY compounds of cF8–NaCl type structure:
(*) X–X (or Y–Y) coordination.
(+) X–Y (or Y–X) coordination.
b) cF12–CaF_2 type structure. Coordination around Ca:
(*) Ca–Ca; (+) Ca–F;
c) CaF_2 type structure. Coordination around F
(*) F–F; (+): F–Ca.

packed structure (cF4–Cu type), in which the octahedral holes have been filled in. This description, however, may be specially convenient when the atomic diameter ratio between the two elements is close to the theoretical value 0.414. In this case the small

spheres will fit exactly into the octahedral holes of the close-packed arrangement of the metal atoms. (See sec. 6.2.2.). This could be the case of a number of "*interstitial compounds*". Compounds of the transition metals having relatively large atomic radii with non metals having small radii (H, B, C, N, possibly O) may be simple examples of this type. (General properties of these compounds were discussed by HÄGG [1931]).

Examples of typical phases belonging to this group may be a number of "mono" carbides, nitrides, etc.

The NaCl type structure is shown by several monocarbides MeC (or more generally MeC_{1-x}) such as TiC_{1-x} (homogeneous in the composition range ≈ 32–49 at% C), ZrC_{1-x} (≈ 33–50 at% C), HfC_{1-x} (≈ 33–50 at% C) and ThC_x (with a very large homogeneity range at high temperature). All the aforementioned monocarbides are stable from room temperature up to the melting points (which are among the highest known: ≈ 3500°C for ZrC and ≈ 4000°C for HfC). The carbides VC_{1-x} (37–48 at% C), NbC_{1-x} (40–50 at% C) are stable only at high temperature: at lower temperature, transformations associated with C-atom ordering have been reported, resulting in the formation of V_8C_7, V_6C_5, Nb_6C_5 structures. WC_{1-x} is a NaCl type high temperature phase homogeneous between 37–39 at% C. At 50 at% C another structure is formed: the hP2–WC type.

Among the NaCl type mononitrides we may mention VN_{1-x}. At high temperature (up to the melting point ≈ 2340°C) we have a large homogeneity field (≈ 33–50 at% N). The composition changes result from variation in the number of vacancies on sites in the N sublattice, with x being the fraction of sites randomly vacant. At lower temperature, in the composition range 43–46 at% N, an ordering of the N atoms has been observed, resulting in a tetragonal superstructure containing 32 V atoms and 26 N atoms in the unit cell. In the W–N system, a WN_{1-x}, NaCl type phase, has been observed in the composition range ≈ 33–50(?) at% N; hP2–WC type structure, however, has been described at 50 at% N.

As a final example, we may mention the NaCl type phases formed in the V–O and Ti–O systems. The ($VO_{1\pm x}$) phase is homogeneous in the composition range 42 to 57 at% O. Lattice parameter determination in combination with density measurements evidenced that, in the structure, vacancies occur in both V and O sub-lattices through the entire range of composition. At the stoichiometric composition VO there are ≈ 15% of sites vacant in each sublattice.

In the Ti–O system, γTiO (high temperature form, homogeneous in the composition range 35 to 55 at% O) has the NaCl type structure. (Other forms of the monooxide βTiO, αTiO, $\beta Ti_{1-x}O$, $\alpha Ti_{1-x}O$ have ordered structures based on γTiO.) In the structure there are atoms missing from some of the sites. According to what is summarized by HYDE and ANDERSSON [1989], in $TiO_{0.64}$ ≈ 36% of the oxigens are missing, in $TiO_{1.26}$ (which, of course, can be represented also with the stoichiometry $Ti_{0.79}O$) ≈ 20% of the Ti atoms are missing and in ≈ TiO both kinds of atoms are missing (≈ 15% of each): see fig. 35.

6.4.2. cF12-CaF_2 type and antitype structures and compounds

Face-centered cubic, space group $Fm\bar{3}m$, No. 225.
Atomic positions:

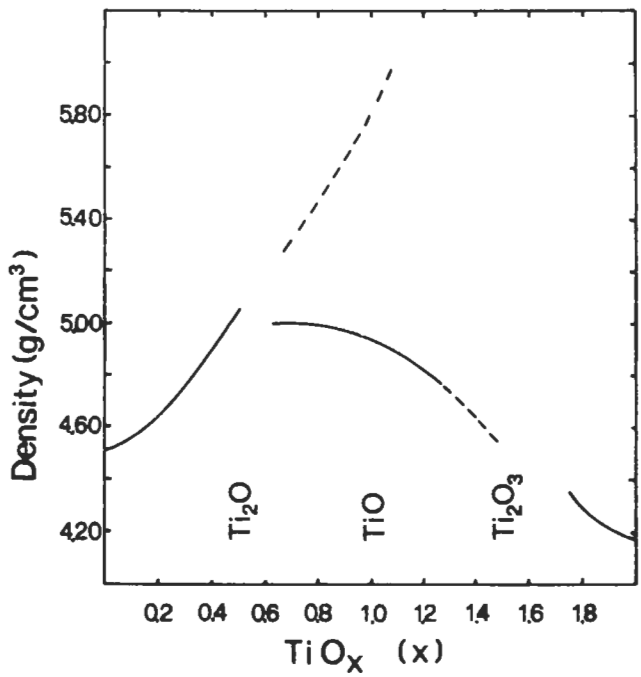

Fig. 35. Experimental densities of titanium oxides (continuous lines). The upper dotted line gives the values computed for a 100% occupancy of the cation sites in the NaCl structure type (from HYDE and ANDERSSON [1989]).

4 Ca in a) 0,0,0; $0,\frac{1}{2},\frac{1}{2}$; $\frac{1}{2},0,\frac{1}{2}$; $\frac{1}{2},\frac{1}{2},0$;
8 F in c) $\frac{1}{4},\frac{1}{4},\frac{1}{4}$; $\frac{1}{4},\frac{1}{4},\frac{3}{4}$; $\frac{1}{4},\frac{3}{4},\frac{3}{4}$; $\frac{1}{4},\frac{3}{4},\frac{1}{4}$; $\frac{3}{4},\frac{1}{4},\frac{3}{4}$; $\frac{3}{4},\frac{1}{4},\frac{1}{4}$; $\frac{3}{4},\frac{3}{4},\frac{1}{4}$; $\frac{3}{4},\frac{3}{4},\frac{3}{4}$;
Coordination formula: $3\underset{\sim}{3}3\,[Ca_{12/12}][F_{6/6}]_{8/4}$
Layer stacking symbols:
Triangular (T) nets:
$Ca_0^A\,F_{1/12}^B\,F_{1/4}^A\,Ca_{1/3}^B\,F_{5/12}^C\,F_{7/12}^B\,Ca_{2/3}^C\,F_{3/4}^A\,F_{11/12}^C$
Square (S) nets: $Ca_0^1\,Ca_0^4\,F_{1/4}^6\,F_{1/4}^7\,Ca_{1/2}^5\,F_{3/4}^6\,F_{3/4}^7$
For the prototype itself, CaF_2, a = 546.3 pm.

As pointed out in the description of the cubic close-packed structure (cF4–Cu type) this structure may be described (especially for certain values of the atomic diameter ratio) as a derivative of the Cu type structure in which two sets of tetrahedral holes have been filled in.

A ternary ordered derivative variant of this structure is the cF12–AgMgAs type.

Several (more or less ionic) compounds such as CeO_2, UO_2, ThO_2, etc. belong to this structural type.

Several Me_2X compounds, with Me = Li, Na, K, X = O, S, Se, Te), also belong to this type. In this case, however, the cation and anion positions are exchanged, Me in c) and X in a) and these compounds are sometimes referred to a *CaF_2–antitype*. Typical (more

metallic) phases having this structure are also, for instance, $AuAl_2$, $PtAl_2$, Mg_2Pb, Mg_2Sn, Mg_2Ge, Mg_2Si.

6.4.3. Structural type: cF12–AgMgAs

Face-centered cubic, space group $F\bar{4}3m$, No. 216.
Atomic positions:
4 As in a) 0,0,0; $0,\frac{1}{2},\frac{1}{2}$; $\frac{1}{2},0,\frac{1}{2}$; $\frac{1}{2},\frac{1}{2},0$;
4 Ag in c) $\frac{1}{4},\frac{1}{4},\frac{1}{4}$; $\frac{1}{4},\frac{3}{4},\frac{3}{4}$; $\frac{3}{4},\frac{1}{4},\frac{3}{4}$; $\frac{3}{4},\frac{3}{4},\frac{1}{4}$;
4 Mg in d) $\frac{3}{4},\frac{3}{4},\frac{3}{4}$; $\frac{3}{4},\frac{1}{4},\frac{1}{4}$; $\frac{1}{4},\frac{3}{4},\frac{1}{4}$; $\frac{1}{4},\frac{1}{4},\frac{3}{4}$;
Layer stacking symbols:
Triangular (T) nets:
$As_0^A\, Mg_{1/12}^B\, Ag_{1/4}^A\, As_{1/3}^B\, Mg_{5/12}^C\, Ag_{7/12}^B\, As_{2/3}^C\, Mg_{3/4}^A\, Ag_{11/12}^C$
Square (S) nets: $As_0^1\, As_0^4\, Ag_{1/4}^6\, Mg_{1/4}^7\, As_{1/2}^5\, Mg_{3/4}^6\, Ag_{3/4}^7$
For the prototype itself, AgMgAs, a = 624 pm.

In systematic investigations of MeTX ternary alloys (Me = Th, U, rare earth metals, etc., T = transition metal, X element from the V, IV main groups) several tens of phases pertaining to this structure type have been identified. For the same group of alloys, however, other structural types are also frequently found. The hP6–$CaIn_2$ type and its derivative types often represent a stable alternative. The relative stabilities of the two structures (especially as a function of the atomic dimensions of the metals involved) have been discussed, for instance, by DWIGHT [1974], MARAZZA *et al.* [1980, 1988], WENSKI and MEWIS [1986].

6.5. hP4–NiAs, cP3–CdI_2, hP6–Ni_2In, oP12–Co_2Si, oP12–TiNiSi types; hP2–WC, hP3–AlB_2, hP6–$CaIn_2$, hP9–Fe_2P types, tI8–NbAs, tI8–$AgTlTe_2$ and tI10–$BaAl_4$ ($ThCr_2Si_2$) types, tI12–$ThSi_2$ and tI12–LaPtSi types

In this section a number of important interrelated structures are presented. A first group is represented by the cP3–CdI_2, hP4–NiAs and hP6–Ni_2In types. Some comments on the interrelations between these structures have been reported in sec. 4.1. A further comparison may also be made by considering their characteristic triangular net stacking sequences:

hP3–CdI_2 $\quad Cd_0^A\, I_{1/4}^B\, I_{3/4}^C$
hP4–NiAs $\quad Ni_0^A\, As_{1/4}^B\, Ni_{1/2}^A\, As_{3/4}^C$
hP6–Ni_2In $\quad Ni_0^A\, Ni_{1/4}^C\, In_{1/4}^B\, Ni_{1/2}^A\, Ni_{3/4}^B\, In_{3/4}^C$

We see, on passing from CdI_2 to the NiAs type the insertion of a new layer at level $\frac{1}{2}$ and, from NiAs to $NiIn_2$, the ordered addition of atoms at levels $\frac{1}{4}$ and $\frac{3}{4}$.

In this section, moreover, the typical non-metal atom frameworks characteristic of the AlB_2, and derivative structures ("graphitic" layers) and of $\alpha ThSi_2$, and derivative structures ("hinged", tridimensional framework) will also be presented, compared and discussed.

The groups of more or less strictly interrelated structures which will be considered in this section are those corresponding to the hP2–WC, hP3–AlB_2, hP6–$CaIn_2$ and hP9–Fe_2P

types, and, respectively, to the tI8–NbAs, tI8–$AgTlTe_2$, tI10–$BaAl_4$ (and tI10–$ThCr_2Si_2$) types and to the tI12–α-$ThSi_2$ and tI12–LaPtSi types.

6.5.1. Structural type: hP4–NiAs

Hexagonal, space group $P6_3/mmc$, N.194,
Atomic positions:
2 Ni in a) 0,0,0; $0,0,\frac{1}{2}$;
2 As in c) $\frac{1}{3},\frac{2}{3},\frac{1}{4}$; $\frac{2}{3},\frac{1}{3},\frac{3}{4}$;
Coordination formula: $^{13}_{\infty}[Ni_{2/2}]As_{6/6}$
For the prototype itself, a = 361.9 pm, c = 504 pm, c/a = 1.393.

According to HYDE and ANDERSSON [1989], the data reported have to be considered as corresponding to an average slightly idealized structure, corresponding for several compounds to the form which is stable at high temperature. At room temperature, in the real structure, there are very small displacements of both Ni and As from their ideal average positions. The structure should, therefore, be better described by:

2 Ni in a) 0,0,z; $0,0,\frac{1}{2}+z$; $(z=0)$
2 As in b) $\frac{1}{3},\frac{2}{3},z$; $\frac{2}{3},\frac{1}{3},\frac{1}{2}+z$; $(z\approx\frac{1}{4})$
in the space group $P6_3mc$, No. 186.

The small (probably correlated) displacements of the atoms produce several sorts of modulated structures (see sec. 4.4.).

6.5.2. Structural type: hP3–CdI_2

Hexagonal, space group $P\bar{3}m1$, No. 164.
Atomic positions:
1 Cd in a) 0,0,0
2 I in d) $\frac{1}{3},\frac{2}{3},z$; $\frac{2}{3},\frac{1}{3},-z$;
Coordination formula: $^{2}_{\infty}[CdI_{6/3}]$
For the prototype itself, CdI_2, a = 424.4 pm, c = 685.9 pm, c/a = 1.616 and z = 0.249.

Typical phases pertaining to this structural type are $CoTe_2$, HfS_2, PtS_2, etc. and also Ti_2O (which, owing to the exchange in the unit cell of the metal/non-metal positions may be considered to be a representative of the *CdI_2-antitype*).

6.5.3. Structural type: hP6–Ni_2In

Hexagonal, space group $P6_3/mmc$, No. 194.
Atomic positions:
2 Ni in a) 0,0,0; $0,0,\frac{1}{2}$;
2 In in c) $\frac{1}{3},\frac{2}{3},\frac{1}{4}$; $\frac{2}{3},\frac{1}{3},\frac{3}{4}$;
2 Ni in d) $\frac{1}{3},\frac{2}{3},\frac{3}{4}$; $\frac{2}{3},\frac{1}{3},\frac{1}{4}$;
Coordination formula: $^{3}_{\infty}[InNi_{6/6}Ni_{5/5}]$
For the prototype itself, a = 419 pm, c = 512 pm, c/a = 1.222.

Typical phases assigned to this structural type are, for instance: Zr_2Al, Co_2Ge, La_2In, Mn_2Sn, Ti_2Sn and several ternary phases such as: BaAgAs, CaCuAs, CoFeSn, LaCuSi,

VFeSb, KZnSb, etc.

A distorted variant of the $InNi_2$ type structure is the oP12–orthorhombic structure of the Co_2Si, (or $PbCl_2$) type: $\frac{3}{\infty}[SiCo_{6/5}Co_{4/5}]$, that is total coordination 10 of Co around Si with $\frac{6}{5}+\frac{4}{5}=\frac{10}{5}=2$ Co atoms for each Si atom). A ternary derivative of this type is the oP12–TiNiSi type (prototype of the so-called E phases).

6.5.4. Structural types: oP12–Co_2Si ($PbCl_2$) and oP12–TiNiSi

Orthorhombic, space group Pnma, N.62.

In these structural types the atoms are distributed in three groups of positions corresponding (obviously with different values of the x and z free parameters) to the same type of Wyckoff positions (Wyckoff position c).

Atomic positions:	in Co_2Si	in TiNiSi
c (1)) $x,\frac{1}{4},z$; $\frac{1}{2}-x,\frac{3}{4},\frac{1}{2}+z$; $-x,\frac{3}{4},-z$; $\frac{1}{2}+x,\frac{1}{4},\frac{1}{2}-z$;	4 Co	4 Ti
c (2)) $x,\frac{1}{4},z$; $\frac{1}{2}-x,\frac{3}{4},\frac{1}{2}+z$; $-x,\frac{3}{4},-z$; $\frac{1}{2}+x,\frac{1}{4},\frac{1}{2}-z$;	4 Co	4 Ni
c (3)) $x,\frac{1}{4},z$; $\frac{1}{2}-x,\frac{3}{4},\frac{1}{2}+z$; $-x,\frac{3}{4},-z$; $\frac{1}{2}+x,\frac{1}{4},\frac{1}{2}-z$;	4 Si	4 Si

For the prototypes:

Co_2Si: a = 491.8 pm, b = 373.8 pm, c = 710.9 pm, a/c = 0.692; $x_{c(1)}=0.038$, $z_{c(1)}=0.782$; $x_{c(2)}=0.174$, $z_{c(2)}=0.438$; $x_{c(3)}=0.702$, $z_{c(3)}=0.389$.

TiNiSi: a = 614.84 pm, b = 366.98 pm, c = 701.73 pm, a/c = 0.876; $x_{c(1)}=0.0212$, $z_{c(1)}=0.8197$; $x_{c(2)}=0.1420$, $z_{c(2)}=0.4391$; $x_{c(3)}=0.7651$, $z_{c(3)}=0.3771$.

Co_2Si is the prototype of a group of phases (also called $PbCl_2$ type) which can be subdivided into two sets according to the value of the axial ratio a/c which is in the range from 0.67 to 0.73 for one set (for instance, Co_2Si, Pd_2Al, Rh_2Ge, Pd_2Sn, Rh_2Sn, etc.) and in the range from 0.83 to 0.88 for the other set (for instance $PbCl_2$, BaH_2(h), Ca_2Si, Ca_2Pb, $GdSe_2$, ThS_2, TiNiSi, etc.) (PEARSON [1972]).

The ternary variant TiNiSi type is also called E-phase structure. Many ternary compounds belonging to a MeTX formula (Me = rare earth metal, Ti, Hf, V, etc., T = transition metal of the Mn, Fe, Pt groups, X = Si, Ge, Sn, P, etc.) have this structure.

6.5.5. Structural type: hP2–WC

Hexagonal, space group $P\bar{6}m2$, No. 187.

Atomic positions:

1 W in a) 0,0,0,;

1 C in d) $\frac{1}{3},\frac{2}{3},\frac{1}{2}$;

For the prototype itself, a = 290.6 pm, c = 283.7 pm, c/a = 0.976.

This structure type with the axial ratio c/a close to 1 is an example of the Hägg interstitial phases formed when the ratio between non-metal and metal radii is less than about 0.59. The structure can be described as a tridimensional array of trigonal prism of W-atoms (contiguous on all the faces). Alternate trigonal prisms are centered by C-atoms.

References: p. 363.

Compounds belonging to this structure type, for instance, are: IrB, OsB, RuB, MoC, WC (compare, however, with the NaCl type phase), NbN, WN, MoP, etc.

6.5.6. Structural types: hP3–AlB_2 and hP3–BaPtSb; hP3-ω, Cr-Ti phase

Structural type: hP3–AlB_2
Hexagonal, space group P6/mmm, No. 191.
Atomic positions:
1 Al in a) 0,0,0;
2 B in d) $\frac{1}{3},\frac{2}{3},\frac{1}{2}$; $\frac{2}{3},\frac{1}{3},\frac{1}{2}$;
Coordination formula: $\underset{\omega\omega}{3}\underset{\omega}{2}\underset{\omega}{3}[Al_{8/8}][B_{3/3}]_{12/6}$
For the prototype itself, a = 300.5 pm, c = 325.7 pm, c/a = 1.084.

The structure can be considered a filled-up WC structure type. The B-atoms form a hexagonal net and center all the Al trigonal prisms. The arrangement of the boron atoms in their layers is the same as that in graphite (see fig. 9 and sec. 6.3.4). (See sec. 6.5.10. for a comparison between the planar graphitic net and similar threedimensional networks).

Several B, Si, Ge, Ga, etc., binary and ternary compounds have been described as pertaining to this structure or, possibly, to its variants (many of them deficient in the second component and corresponding to different stoichiometries in the 1:2 to 1:1.5 range). The axial ratio of phases with this structure varies between very wide limits. The relationships between axial ratio, atomic radii ratio of the elements involved and the role of the different bonds have been discussed by PEARSON [1972]. In the specific case of AlB_2 ($c/a \approx 1.08$) the important role of the graphite-like net of B-atoms in determining the phase stability has been evidenced.

A disordered, AlB_2 type, ternary phase ($\approx Ce_2NiSi_3$) has been presented in table 3.

A variant (ordered derivative structure) of the hP3–AlB_2 type, previously discussed in sec. 4.1 and presented in fig. 17, is the hP3–BaPtSb type, hexagonal, space group $P\bar{6}m2$, No. 187. Another compound with this structure is, for instance, ThAuSi. The atomic positions are the following:

1 Ba (or Th) in a): 0,0,0;
1 Pt (or Au) in d) $\frac{1}{3},\frac{2}{3},\frac{1}{2}$;
1 Sb (or Si) in f): $\frac{2}{3},\frac{1}{3},\frac{1}{2}$.

The layer-stacking sequence symbols of the three previously mentioned structures are:

WC type, triangular (T) nets;
$W_O^A C_{0.5}^B$;
AlB_2 type, triangular, hexagonal (T, H) nets:
$Al_0^A B_{0.5}^a$;
ThAuSi type, triangular, hexagonal (T,H) nets:
$Th_0^A Au_{0.5}^B Si_{0.5}^C$.

Another ordered derivative structure of the AlB_2 type is the Er_2RhSi_3 type, hexagonal, space group $P\bar{6}2c$, No. 190 with the following atomic positions:

2 Er in b): $0,0,\frac{1}{4}$; $0,0,\frac{3}{4}$;
4 Rh in f): $\frac{1}{3},\frac{2}{3},z$; $\frac{1}{3},\frac{2}{3},\frac{1}{2}-z$; $\frac{2}{3},\frac{1}{3},-z$; $\frac{2}{3},\frac{1}{3},\frac{1}{2}+z$;
6 Er in h): $x,y,\frac{1}{4}$; $-y,x-y,\frac{1}{4}$; $y-x,-x,\frac{1}{4}$; $y,x,\frac{3}{4}$; $x-y,-y,\frac{3}{4}$; $-x,y-x,\frac{3}{4}$
12 Si in i): x,y,z; $-y,x-y,z$; $y-x,-x,z$; $x,y,\frac{1}{2}-z$; $-y,x-y,\frac{1}{2}-z$; $y-x,-x,\frac{1}{2}-z$;
$y,x,-z$; $x-y,-y,-z$; $-x,y-x,-z$; $y,x,\frac{1}{2}+z$; $x-y,-y,\frac{1}{2}+z$; $-x,y-x,\frac{1}{2}+z$.
(with $z_{Rh}=0$; $x_{Er}=0.481$; $y_{Er}=0.019$; $x_{Si}=0.167$; $y_{Si}=0.333$; $z_{Si}=0$).

The different ordering relationships between these structures have been discussed in sec. 4.1. (see also fig. 17).

Finally, while considering the structural characteristics of the AlB_2 type phases, we may mention that boron-centered triangular metal prisms are the dominating structural building elements in the crystal structures of simple and complex metal borides. Building blocks of centered triangular prisms as base units for classification of these substances have been considered by ROGL [1985, 1991] in a systematic presentation of the crystal chemistry of borides.

We may mention here, also as an example of "modular" description, that several structures may be described in terms of cyclic translations about a 6_3 axis of blocks of AlB_2 type columns: see fig. 36.

Structural type: hP3–ω,Cr-Ti

The ω-phase, a ubiquitous metastable phase in Ti (or Zr or Hf)-transition metal systems, is approximately isotypic with AlB_2. (The axial ratio of the unit cell, however, instead of being close to unity, is very much smaller and has a value of about 0.62.) The components are randomly arranged. One third of the atoms are distributed in a triangular net at $z=0$ forming trigonal prisms. Two thirds of the atoms are placed near the centers of the prisms (slightly displaced alternately up and down) forming a rumpled 6^3 net at $z\approx\frac{1}{2}$. (The space group is $P\bar{3}m1$.)

6.5.7. Structural type: hP6–$CaIn_2$

Hexagonal, space group $P6_3/mmc$, No. 194.
Atomic positions:
2 Ca in b) $0,0,\frac{1}{4}$; $0,0,\frac{3}{4}$;
4 In in f) $\frac{1}{3},\frac{2}{3},z$; $\frac{2}{3},\frac{1}{3},\frac{1}{2}+z$; $\frac{2}{3},\frac{1}{3},-z$; $\frac{1}{3},\frac{2}{3},\frac{1}{2}-z$;
Layer stacking symbol:
Triangular (T) nets:
$In^{B}_{1/20}\,Ca^{A}_{1/4}\,In^{B}_{9/20}\,In^{C}_{11/20}\,Ca^{A}_{3/4}\,In^{C}_{19/20}$
For the prototype itself, $a=489.5$ pm, $c=775.0$ pm, $c/a=1.583$ and $z=0.455$.

This structure can be described as a distortion (a derivative form) of the AlB_2 type structure. Ca-atoms form trigonal prisms alternatively slightly off-centered up and down by In-atoms.

In fig. 37 the normalized interatomic distances and the equidistant neighbours are shown for the NiAs and $CaIn_2$ structures.

References: p. 363.

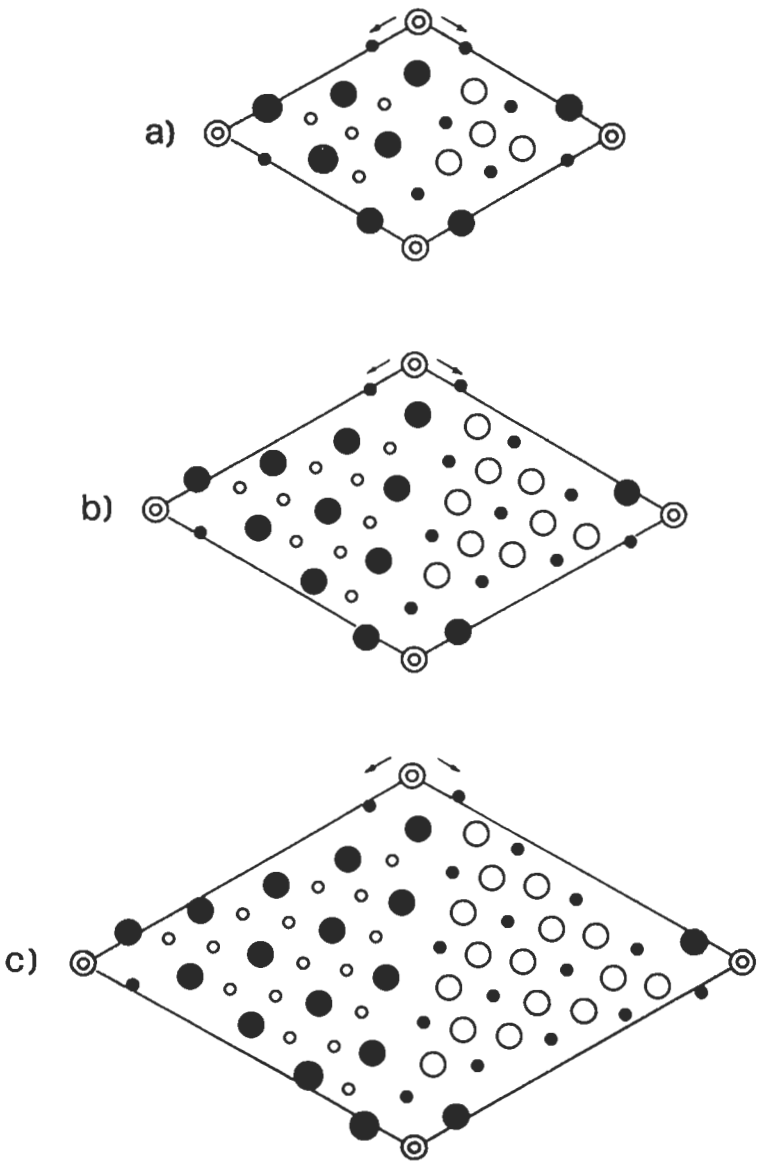

Fig. 36a,b,c. AlB_2–type derivative structures generated by cyclic translation of blocks of AlB_2–type columns. The projections of the unit cells (all having the same c value) on the x,y plane are shown.

a) hP22–$Ce_6Ni_2Si_3$ structure (a = 1211.2 pm, c = 432.3 pm).

b) hP40–≈$Ce_5Ni_2Si_3$ structure (a = 1612.0 pm, c = 430.9 pm).

c) hP64–≈$Pr_{15}Ni_7Si_{10}$ structure (a = 1988.1 pm, c = 425.5 pm)

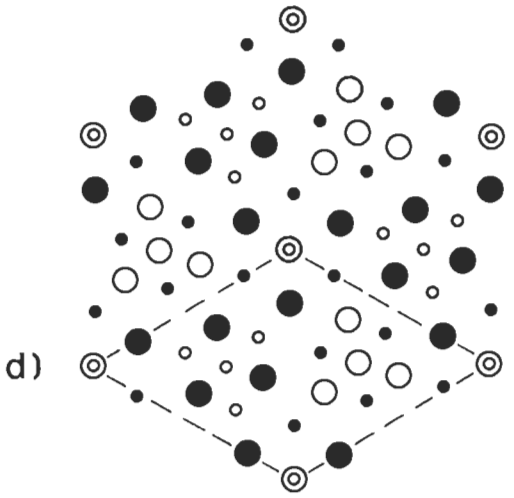

Fig. 36d. AlB_2–type derivative structures generated by cyclic translation of blocks of AlB_2–type columns. The projections of the unit cells (all having the same c value) on the x,y plane are shown.

d) hP22–$Ce_6Ni_2Si_3$ structure (compare with a)): the arrangement of the building blocks around the z-axis (6_3 symmetry axis) is shown.

Black circles represent the rare earth atoms (Ce or Pr), open circles Si (and Si + Ni); small circles are atoms at level $\frac{1}{4}$, large circles at level $\frac{3}{4}$. Double circles (at cell origin) represent Ni atoms at level 0 and at level $\frac{1}{2}$.

6.5.8. Structural type: hP9–Fe_2P

Hexagonal, space group $P\bar{6}2m$, No. 189.

Atomic positions:

1 P in b) $0,0,\frac{1}{2}$

2 P in c) $\frac{1}{3},\frac{2}{3},0$; $\frac{2}{3},\frac{1}{3},0$;

3 Fe in f) x,0,0; 0,x,0; $-x,-x,0$;

3 Fe in g) $x,0,\frac{1}{2}$; $0,x,\frac{1}{2}$; $-x,-x,\frac{1}{2}$;

For the prototype itself, a = 586.5 pm, c = 345.6 pm, c/a = 0.589 and x (f) = 0.256 and x (g) = 0.594.

In the Fe_2P type structure there are 4 different groups of equipoints. The distribution of P and Fe atoms in different groups of positions is reported. A number of isostructural binary compounds are known. To the same structure, however, ternary (or even more complex) phases may be related if different atomic species are distributed in the different sites.

This structure can be considered as an example of more complex structures built up by linked triangular prisms of Fe-atoms.

Several ordered ternary phases have structures related to the Fe_2P type.

6.5.9. Structural types: tI8–NbAs, tI8–$AgTlTe_2$ and tI10–$BaAl_4$ ($ThCr_2Si_2$)

The three structural types tI8–NbAs, tI8–$AgTlTe_2$ and tI10–$BaAl_4$ (with its ordered ternary variants such as the tI10–$ThCr_2Si_2$) belong to a group of interrelated structures.

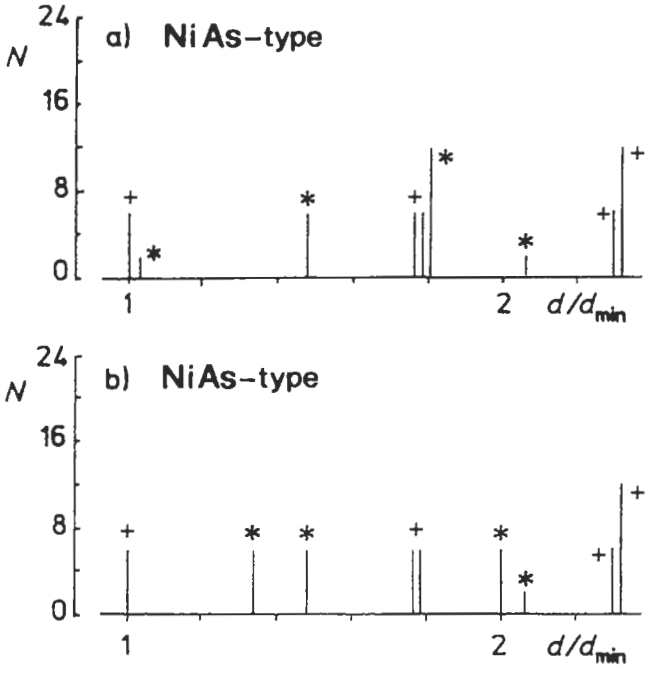

Fig. 37a,b. Distances and coordinations in the hP4–NiAs and hP6–$CaIn_2$ types structures.
a) hP4–NiAs type structure. Coordination around Ni:
(+) Ni–As; (*) Ni–Ni.
b) hP4–NiAs type structure. Coordination around As:
(+) As–Ni; (*) As–As.

All these structures contain among their building parts layers of (metal atoms) triangular prisms with specific distributions of the (non-metal) atoms centering the prisms (PEARSON [1972]). The prisms are parallel to the basal planes of the tetragonal unit cells.

Features of the hP2–WC type structure (characterized by an array of trigonal prisms alternatively centered by C-atoms) are, therefore, present in the aforementioned structures. (In the hP2–WC structure, of course, the prism axes are lying in the *c*-direction of the hexagonal cell.)

Another convenient description of these group of structures may be in term of 4^4 net layer stacking. The corresponding square net symbols for the 8–layers stacks are the following ones:

tI8–NbAs:
$Nb_0^1\, As_{0.17}^2\, Nb_{0.25}^3\, As_{0.42}^1\, Nb_{0.5}^4\, As_{0.67}^3\, Nb_{0.75}^2\, As_{0.92}^3$
tI8–$AgTlTe_2$:
$Tl_0^1\, Te_{0.13}^4\, Ag_{0.25}^3\, Te_{0.37}^1\, Tl_{0.5}^4\, Te_{0.63}^1\, Ag_{0.75}^2\, Te_{0.87}^4$
tI10–$ThCr_2Si_2$:
$Th_0^1\, Si_{0.13}^4\, Cr_{0.25}^5\, Si_{0.38}^1\, Th_{0.5}^4\, Si_{0.63}^1\, Cr_{0.75}^5\, Si_{0.88}^4$

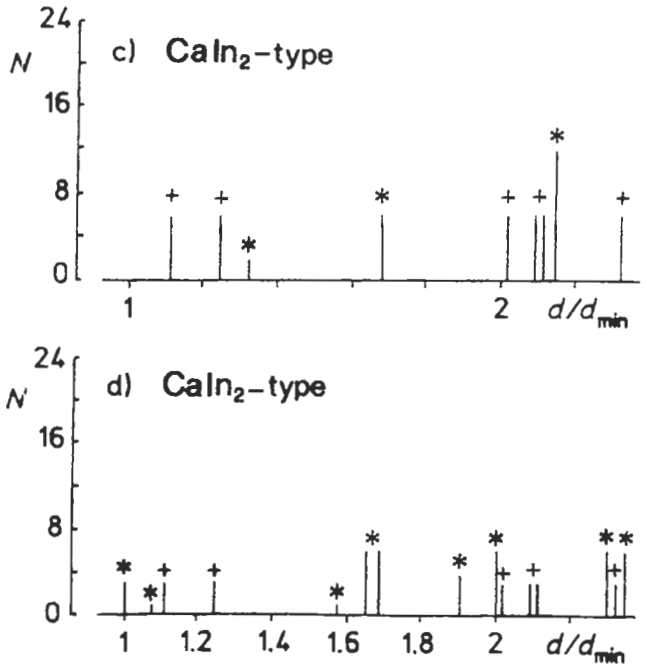

Fig. 37c,d. Distances and coordinations in the hP4–NiAs and hP6–$CaIn_2$ types structures.
c) hP6–$CaIn_2$ type structure. Coordination around Ca:
(+) Ca–In; (*) Ca–Ca;
d) hP6–$CaIn_2$ type structure. Coordination around In:
(+) In–Ca; (*): In–In.

Structure type: tI8–NbAs
Body-centered tetragonal, space group $I4_1md$, No. 109.
4 Nb in a(1): $0,0,z;\ 0,\frac{1}{2},\frac{1}{4}+z;\ \frac{1}{2},\frac{1}{2},\frac{1}{2}+z;\ \frac{1}{2},0,\frac{3}{4}+z;$
4 As in a(2): $0,0,z;\ 0,\frac{1}{2},\frac{1}{4}+z;\ \frac{1}{2},\frac{1}{2},\frac{1}{2}+z;\ \frac{1}{2},0,\frac{3}{4}+z;$
For the prototype itself a = 345.2 pm, c = 1168 pm, c/a = 3.384, z(Nb) = 0, z(As) = 0.416.

Structural type: tI8–$AgTlTe_2$
Body-centered tetragonal, space group $I\bar{4}m2$, No. 119.
2 Tl in a): $0,0,0,;\ \frac{1}{2},\frac{1}{2},\frac{1}{2};$
2 Ag in c): $0,\frac{1}{2},\frac{1}{4};\ \frac{1}{2},0,\frac{3}{4};$
4 Te in e): $0,0,z;\ 0,0,-z;\ \frac{1}{2},\frac{1}{2},\frac{1}{2}+z;\ \frac{1}{2},\frac{1}{2},\frac{1}{2}-z;$
For the prototype itself, a = 392 pm, c = 1522 pm, c/a = 3.883 and z(Te) = 0.369.

Structural type: tI10–$BaAl_4$ and tI10–$ThCr_2Si_2$
The $ThCr_2Si_2$ is one of the ordered ternary variant of the $BaAl_4$ type, frequently found in several ternary compounds.

The two structures may be described by the following occupation of the same atomic positions in the space group I4/mmm (No. 139).

References: p. 363.

	in $BaAl_4$	in $ThCr_2Si_2$
a) 0,0,0; $\frac{1}{2},\frac{1}{2},\frac{1}{2}$	2 Ba	2 Th
d) $0,\frac{1}{2},\frac{1}{4}$; $\frac{1}{2},0,\frac{1}{4}$; $\frac{1}{2},0,\frac{3}{4}$; $0,\frac{1}{2},\frac{3}{4}$;	4 Al	4 Cr
e) 0,0,z; 0,0,−z; $\frac{1}{2},\frac{1}{2},\frac{1}{2}+z$; $\frac{1}{2},\frac{1}{2},\frac{1}{2}-z$;	4 Al	4 Si

For the prototypes themselves:
$BaAl_4$, a = 453.9 pm, c = 1116 pm, c/a = 2.459 , z = 0.38
$ThCr_2Si_2$: a = 404.3 pm, c = 1057.7 pm, c/a = 2.616, z = 0.37$_5$
The unit cell is presented in fig. 38.

Normalized interatomic distances and numbers of equidistant neighbours are reported in fig. 39 for the ternary $ThCr_2Si_2$ type.

Many ternary alloys MeT_2X_2 (Me = Th, U, alkaline-earth, rare earth metal, etc., T = Mn, Cr, Pt family metal, X = element of the fifth, fourth and occasionally third main group) have been systematically prepared and investigated (PARTHE and CHABOT [1984], ROSSI *et al.* [1979]). A few hundreds of them resulted in the $ThCr_2Si_2$ (or other Al_4Ba derivatives) structure. The peculiar superconductivity and magnetic properties of these materials have been reported. The $ThCr_2Si_2$ type structure, can be described as formed by T_2X_2 layers interspersed with Me layers. The bonding between Me and T_2X_2 layers has been considered as largely ionic. In the T_2X_2 layers T–X (covalent) and some T–T bonding have to be considered. A detailed discussion of this structure and of the bonding involved has been reported by HOFFMANN [1987].

In the specific case of the RET_2X_2 phases (RE = rare earth metal) the data concerning

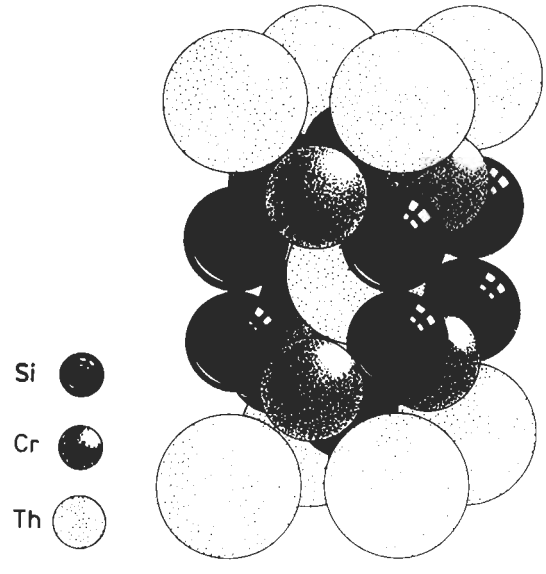

Fig. 38. Unit cell of the tI10–$ThCr_2Si_2$ type structure (a derivative structure of the tI10–$BaAl_4$ type).

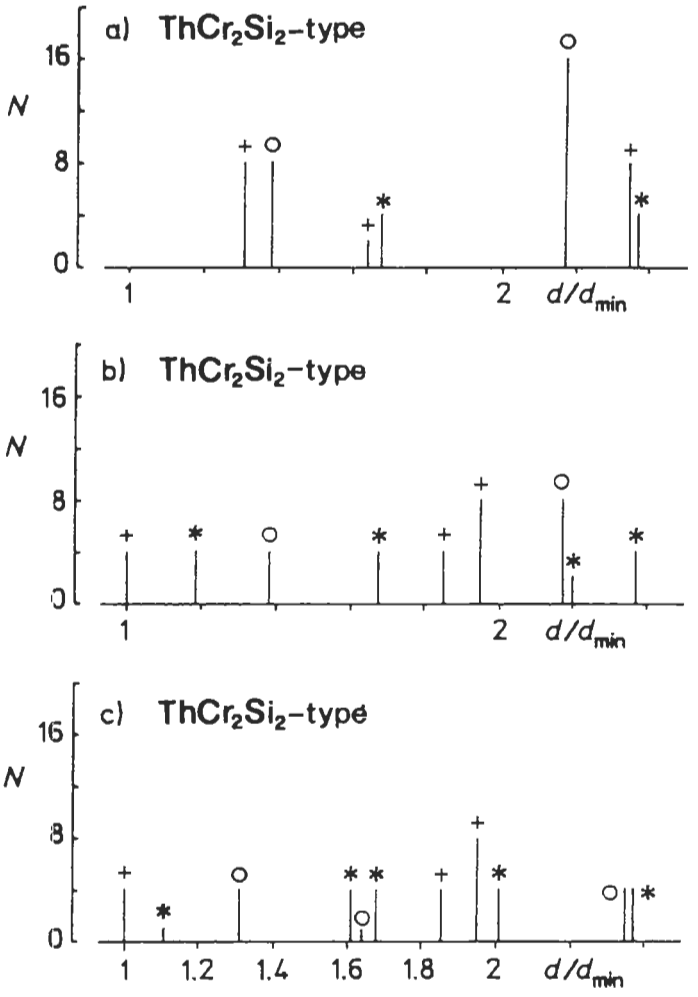

Fig. 39. Distances and coordinations in the tI10–$ThCr_2Si_2$ type structure.
a) Coordination around Th:
(+) Th-Si; (*) Th–Th; (o) Th–Cr;
b) Coordination around Cr:
(+) Cr–Si; (*) Cr–Cr; (o) Cr–Th.
c) Coordination around Si:
(+) Si–Cr; (*) Si–Si; (o) Si–Th.

ten series (T = Mn, Fe, Co, Ni, Cu; X = Si, Ge) have been analysed by PEARSON [1985a]. It has been observed that the cell dimensions are generally controlled by RE–X contacts. In the case of Mn, however, the RE-Mn contact has to be assumed to control the cell dimensions (see sec. 7.2.5.).

Magnetic phase transition in RET_2X_2 phases have been described by SZYTULA [1992].

References: p. 363.

Structural distortions in some groups of RET_2X_2 phases ($REPt_2Sn_2$), leading to less symmetric cells, have been reported by LATROCHE *et al.* [1992].

An interesting compound belonging to the RET_2X_2 family is $EuCo_2P_2$. In a neutron diffraction investigation of this phase carried out by REEHUIS *et al.* [1992] the positional (nuclear) and the magnetic structures were determined. The ordering of the magnetic moments of the Eu-atoms and the relation (commensurability) between this ordering and that of the atomic positions were studied (see sec. 4.4.).

6.5.10. Structural types: tI12–$\alpha ThSi_2$ and tI12–LaPtSi

The $\alpha ThSi_2$ type structure, and its lattice-equivalent ternary LaPtSi type derivative can be considered, filled up tI8–NbAs type derivative. These structures can be described in terms of layers of (metal atoms) triangular prisms parallel to the basal planes of the tetragonal cells, the prism axes in one layer being rotated 90° relative to those of the layers above and below.

In the NbAs type structure the As atoms only center alternate Nb prisms. In the $\alpha ThSi_2$ type structure all the Th-prisms are centered by Si instead of only half of them (PEARSON [1972]).

We may also compare the three structures in terms of 4^4 net layer stacking (along the c-direction of the tetragonal cells): See also fig. 40.

tI8–NbAs:
$Nb_0^1\ As_{0.17}^2\ Nb_{0.25}^3\ As_{0.42}^1\ Nb_{0.5}^4\ As_{0.67}^3\ Nb_{0.75}^2\ As_{0.92}^4$
tI12–$\alpha ThSi_2$:
$Th_0^1\ Si_{0.08}^4\ Si_{0.17}^2\ Th_{0.25}^3\ Si_{0.33}^2\ Si_{0.42}^1\ Th_{0.5}^4\ Si_{0.58}^1\ Si_{0.67}^3\ Th_{0.75}^2\ Si_{0.83}^3\ Si_{0.92}^4$
tI12–LaPtSi:
$La_0^1\ Pt_{0.08}^4\ Si_{0.17}^2\ La_{0.25}^3\ Pt_{0.33}^2\ Si_{0.42}^1\ La_{0.5}^4\ Pt_{0.58}^1\ Si_{0.67}^3\ La_{0.75}^2\ Pt_{0.83}^3\ Si_{0.92}^4$

Structural type: tI12–$\alpha ThSi_2$
body-centered, tetragonal, space group $I4_1/amd$, No. 141.
4 Th in a): 0,0,0; $0,\frac{1}{2},\frac{1}{4}$; $\frac{1}{2},\frac{1}{2},\frac{1}{2}$; $\frac{1}{2},0,\frac{3}{4}$;
8 Si in e): 0,0,z; $0,\frac{1}{2},\frac{1}{4}+z$; $\frac{1}{2},0,\frac{3}{4}-z$; $\frac{1}{2},\frac{1}{2},\frac{1}{2}-z$; $\frac{1}{2},\frac{1}{2},\frac{1}{2}+z$; $\frac{1}{2},0,\frac{3}{4}+z$; $0,\frac{1}{2},\frac{1}{4}-z$; 0,0,−z.
For the prototype itself a = 412.6 pm, c = 1434.6 pm, c/a = 3.477 and $z(Si) = 0.416_5$.

Structural type: tI12–LaPtSi
body-centered, tetragonal, space group $I4_1md$, N.109.
4 La in a(1): 0,0,z; $0,\frac{1}{2},\frac{1}{4}+z$; $\frac{1}{2},\frac{1}{2},\frac{1}{2}+z$; $\frac{1}{2},0,\frac{3}{4}+z$;
4 Pt in a(2): 0,0,z; $0,\frac{1}{2},\frac{1}{4}+z$; $\frac{1}{2},\frac{1}{2},\frac{1}{2}+z$; $\frac{1}{2},0,\frac{3}{4}+z$;
4 Si in a(3): 0,0,z; $0,\frac{1}{2},\frac{1}{4}+z$; $\frac{1}{2},\frac{1}{2},\frac{1}{2}+z$; $\frac{1}{2},0,\frac{3}{4}+z$.
For the prototype itself a = 424.90 pm, c = 1453.9 pm, c/a = 3.422 and z(La) = 0 (fixed conventionally), z(Pt) = 0.585 and z(Si) = 0.419.
The unit cells of the two structures are presented in fig. 40.

The $ThSi_2$ type structure according to PEARSON [1972] is primarily controlled by the Th-Si contacts, with the Si-Si contacts exerting a certain influence. Each Si atom has three close Si neighbours resulting in the three dimensionally connected framework schematically shown in fig. 40d. This framework (and the Si–Si coordination) can be compared

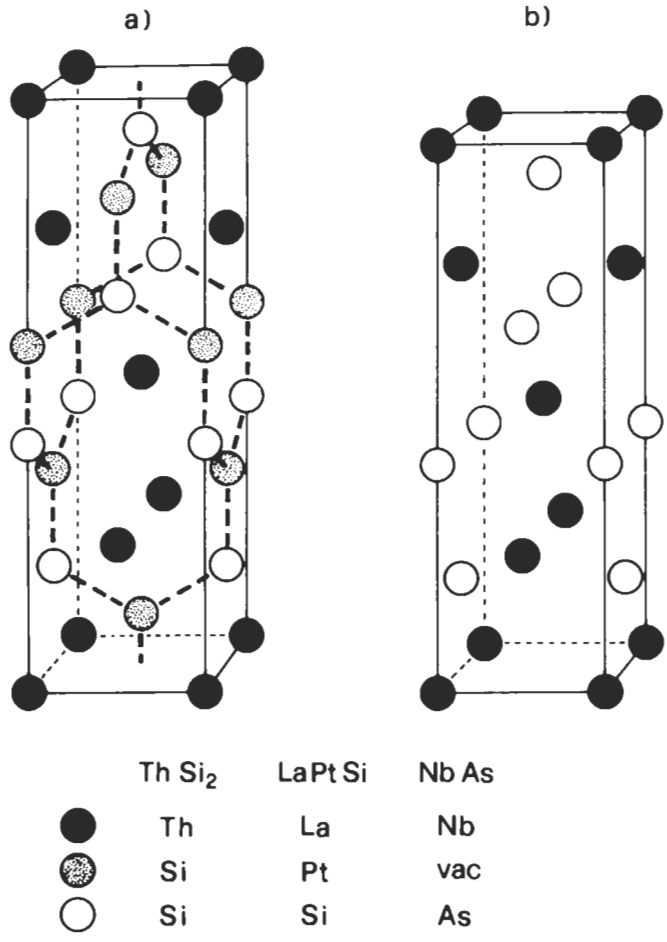

Fig. 40a,b. Crystal structures of $ThSi_2$ and LaPtSi (a) and NbAs (b) with the indication of the atoms which, in the three structures, occupy the different sites. (Notice the defective character of the NbAs type structure in comparison with the $ThSi_2$ type.) In c) different sections of the LaPtSi structure unit cell are presented with the indication of the heights along the z-direction and of the codes used for the different atomic position in a square net (compare with fig. 11). In the NbAs structure, the sections at $z = 0.08$, 0.33, 0.58 and 0.83 are not occupied by any atoms. The dotted lines in a) show a part of the three-connected framework of Si (or Pt,Si) atoms. A larger portion of the framework is presented in d).

with the planar graphite hexagonal nets and therefore with, for instance, the hP3–AlB_2 type structure (and its ordered variants). In the case of $ThSi_2$, however, one vertex of each hexagon is always missing and we have parallel sets of planar chains interconnected to similar perpendicular sets.

It may be interesting to mention that the characteristic structure of this network described as "*hinged*" *network* should have the peculiar feature that the entire framework could undergo reorganisation by a nearly barrierless twisting type motion. According to

References: p. 363.

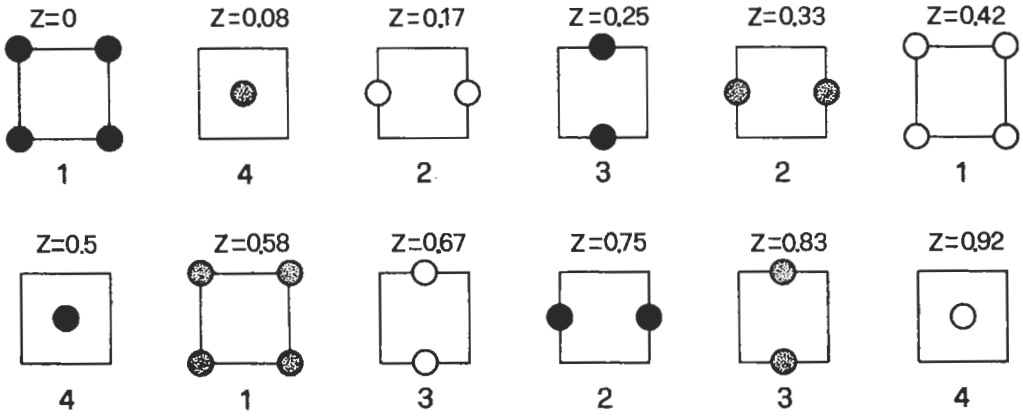

c)

d)

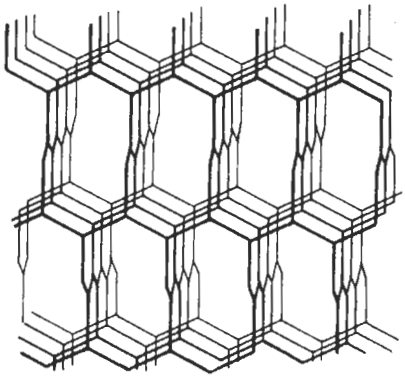

Fig. 40c,d.

BAUGHMAN and GALVAO [1993] and MOORE [1993], unusual mechanical and thermal properties may be predicted for substances having all their atoms arranged in such a framework. These special properties, therefore, may be envisaged for hypothetical compounds such as polyacetylene, polydiacetylene, polyphenylene, $(BN)_x$ phases, etc. and perhaps for substances containing the hinged network as a part of their structure (*"crowded" hinged network* crystals) such as $ThSi_2$ compounds.

Finally considering the AlB_2 and the $\alpha ThSi_2$ type structures we may notice that the similarity of their bonding arrangements may be further confirmed by the existence of the AlB_2 structure also for a different form of $ThSi_2$ (β form, high temperature form) and (as a defective structure) for $\approx Th_3Si_5$. Following the description presented by BAUGHMAN and GALVAO [1993]) the AlB_2 type structure could be called a "crowded" graphitic network structure.

6.6. Tetrahedrally close-packed, Frank–Kasper structures, Laves phases, Samson phases

6.6.1. General remarks

A number of structures of several important intermetallic phases can be classified as tetrahedrally close-packed structures. As an introduction to this subject we may remember, according to SHOEMAKER and SHOEMAKER [1969] that in packing spheres of equal sizes the best space filling is obtained in the cubic or hexagonal close-packed structures (or in their variants). In those arrangements there are tetrahedral and octahedral holes (see the comments on this point reported in the description of the cF4–Cu type structure in sec. 6.2.2). The local mean atomic density (the average space filling) is somewhat higher at the tetrahedral holes than in the larger octahedral ones. A more compact arrangement might, therefore, be obtained if it were be possible to have only tetrahedral interstices. It is, however, *impossible to fill space* with *regular tetrahedra* throughout. By introducing some variability in the sphere dimensions it is possible to obtain packing containing only tetrahedral holes. The tetrahedra are now no longer regular: the ratio of the longest tetrahedron edge to the shortest, however, needs not exceed about $\frac{4}{3}$ in a given structure. The corresponding crystal structure can be considered to be obtained from the space filling of these tetrahedra (which share faces, edges and vertices). In structures containing atoms of approximately the same size and within the aforementioned limits of edge-length ratio, the sharing of a given tetrahedron edge (i.e. an interatomic link ligand) either among 5 or 6 tetrahedra has to be considered the most favored situation (according to the systematic analysis of these structures carried out by FRANK and KASPER [1958, 1959]). On the assumption that only 5 or 6 tetrahedra may share a given edge the number of tetrahedra that share a given vertex is limited to the values 12, 14, 15 and 16. The 12 (or 14, 15, 16) tetrahedra sharing a given vertex form, *around this point*, a coordination polyhedron with triangular faces. The radii of this polyhedron are the edges shared among 5 or 6 component tetrahedra and connect the central atom with the polyhedron vertices, five-fold or six-fold vertices, that is vertices in which 5 or 6 faces meet.

The four possible coordination polyhedra are shown in fig. 41 and correspond to the following properties:

coordination 12 (regular, or approximately regular, icosahedron): 12 vertices (12 five-fold vertices) and 20 faces.
coordination 14: 14 vertices (12 five-fold and 2 six-fold) and 24 faces.
coordination 15: 15 vertices (12 five-fold and 3 six-fold) and 26 faces.
coordination 16: 16 vertices (12 five-fold and 4 six-fold) and 28 faces.
(For symbols used in the coding of the vertex-characteristics see sec. 7.2.7).

Several structures (*Frank–Kasper structures*) can be considered in which all atoms have either 12 (icosahedral), 14, 15 or 16 coordinations. These can be described as resulting from the polyhedra presented in fig. 41. These polyhedra interpenetrate each other so that every vertex atom is again the center of another polyhedron. All structures in this family contain icosahedra and at least one other coordination type.

Frank and Kasper demonstrated that structures formed by the interpenetration of the four polyhedra contain planar or approximately planar layers of atoms. (*Primary layers* made up by tessellation of triangles with hexagons and/or pentagons were considered,

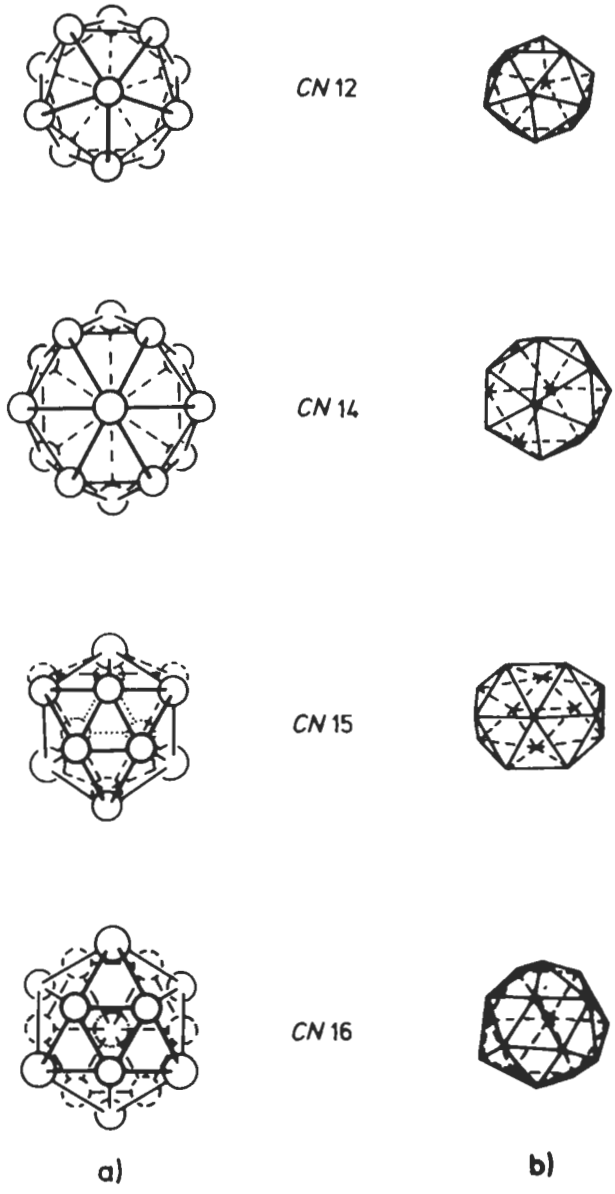

Fig. 41. The coordination polyhedra of the Frank–Kasper structures, are shown in two different styles.

a) the relative positions of the coordinating atoms are shown (the central atoms are not reported). (For the coordination numbers (CN) 12 and 14, one atom of the coordination shell is not visible).

b) the corresponding triangulated polyhedra are shown. Vertices in which 5 or 6 triangles meet are easily recognizable.

and intervening *secondary layers* of triangles and/or squares). For a classification and coding of the nets and of their stacking see PEARSON [1972] and also SHOEMAKER and SHOEMAKER [1969] or FRANK and KASPER [1958, 1959].

A short summary of structural types pertaining to this family is reported in table 6; for a few of them, some details or comments are reported in the following.

6.6.2. cP8–Cr_3Si type structure

This structure is also called W_3O or β-W type (it was previously believed to be a W modification instead of an oxide) or A15 type (see section 3.4).
Cubic, space group $Pm\bar{3}n$, No. 223.
Atomic positions:
2 Si in a) 0,0,0; $\frac{1}{2},\frac{1}{2},\frac{1}{2}$;
6 Cr in c) $\frac{1}{4},0,\frac{1}{2}$; $\frac{3}{4},0,\frac{1}{2}$; $\frac{1}{2},\frac{1}{4},0$; $\frac{1}{2},\frac{3}{4},0$; $0,\frac{1}{2},\frac{1}{4}$; $0,\frac{1}{2},\frac{3}{4}$.

This structure type is observed for many phases formed in the composition ratio 3:1 by several transition metals with elements from the III, IV, V main groups (or with Pt metals or Au). Phases having this structural type are, for instance, Mo_3Al, Nb_3Al, V_3Al, Ta_3Au, Ti_3Au, Cr_3Pt, Cr_3Os, Cr_6AlSi, V_6AlSn, Nb_6GaGe, etc. A number of compounds with this structure have been found to have significantly high superconducting transition temperature, T_c (among the highest known, before the discovery of the families of superconducting complex oxides, such as $Ba_2YCu_3O_{7-x}$ or $\approx Bi_2(Ca,Sr)_3Cu_2O_{9-x}$, etc.). Examples of superconducting, Cr_3Si type, phases are:

Nb_3Ge ($T_c = 23.2$ K, sputtered films), Nb_3Ga ($T_c = 20.7$ K, bulk), Nb_3Sn ($T_c = 18.1$ K), V_3Si ($T_c = 16.8$ K), V_3Ga ($T_c = 14.1$ K), Nb_3Au ($T_c = 11.5$ K), Nb_3Pt ($T_c = 9.2$ K), Mo_3Ir ($T_c = 8.8$ K), etc.

The Cr_3Si type structure does not always remain stable in these materials down to 0 K, yet the change in crystal structure, when it occurs (for instance, with a tetragonal structure formed at low temperature as a result of a martensitic transformation) seems not correlated with T_c. Solid solutions in general have lower T_c values than the stoichiometric compounds. (Other superconducting intermetallic phases belonging to different structural types are, for instance, $LuRh_4B_4$ ($T_c = 11.7$ K, $YPd_5B_3C_x$ ($T_c = 23$ K), quaternary lanthanum nickel boro-nitrides, etc. See CAVA *et al.* [1994a, 1994b]).

6.6.3. σ phase type structure, (tP30–σCr-Fe type)

In the space group $P4_2/mnm$, No. 136, the two atomic species, Cr and Fe, are distributed in several sites with a nearly random occupation. Different atom distributions have been proposed in the literature (also owing to different preparation methods and heat treatments). The following distribution is one of those reported in DAAMS *et al.* [1991]: two atoms in sites a) (with a 12% probability for Cr and 88% for Fe), 4 atoms (75% Cr, 25% Fe) in sites f), 8 atoms (62% Cr, 38% Fe) in a set i) of sites, 8 atoms (16% Cr, 84% Fe) in another set i) and 8 atoms (66% Cr, 34% Fe) in j). The structure can be considered as made up of primary hexagon–triangle layers containing $3636 + 3^26^2$ and 6^3 nodes (in a 3:2:1 ratio) at height ≈ 0 and $\frac{1}{2}$ separated (at height $\approx \frac{1}{4}$ and $\frac{3}{4}$) by secondary 3^2434 layers (that is layers, in which every node is surrounded, in order, by 2

Table 6
Examples of tetrahedral close-packed structures.

Structural types	Unit cell dimensions (rounded values) for the reported prototype [pm]	% of atoms in the center of a polyhedron with CN 12	14	15	16
cP8–Cr_3Si (also called W_3O or ß-W type or A15 type phase).	a = 456	25	75		
tP30–σ-$Cr_{46}Fe_{54}$* σ phases	a = 880 c = 456	33	53	13	
hR39– W_6Fe_7 μ phases	a = 476 c = 2562	55	15	15	15
hP7–Zr_4Al_3	a = 543 c = 539	43	28	28	
oP52 ≈ $Nb_{48}Ni_{39}Al_{13}$* M phases	a = 930 b = 493 c = 1627	55	15	15	15
oP56 ≈ $Mo_{21}Cr_9Ni_{20}$* P phases	a = 1698 b = 475 c = 907	43	36	14	7
hR159 ≈ $Mo_{31}Cr_{18}Co_{51}$* R phases	a = 1090 c = 1934	51	23	11	15
cI162–$Mg_{11}Zn_{11}Al_6$*	a = 1416	61	7	7	25
Laves Phases:					
cF24–Cu_2Mg	a = 704	67	33		
hP12–$MgZn_2$	a = 522 c = 856	67	33		
hP24–Ni_2Mg	a = 482 c = 1583	67	33		

* For these phases the reported formulae generally correspond to an average composition within a solid solution field. This also in relation with a (partially) disordered occupation of the different sites.

triangles, 1 square, 1 triangle and 1 square).

As pointed out by Pearson (by studying the near-neighbours diagram: see sec. 7.2.5.a) the σ-phase structure is a good example of a structure which is controlled by the coordination factor: all the known phases are closely grouped around the intersection of lines corresponding to high coordination numbers. (The most favorable radius ratio for the component atoms is included between 1.0 and 1.1.) It is also possible that the electron concentration plays some role in controlling the phase stability. The different phases are grouped in the range 6.2 to 7.5 electrons (s, p and d) per atoms.

6.6.4. Laves phases: cF24–Cu_2Mg (and cF24–Cu_4MgSn and cF24–$AuBe_5$), hP12–$MgZn_2$ (and hP12–U_2OsAl_3) and hP24–Ni_2Mg types

General remarks

The Laves phases form a *homeotect structure type set* (a family of polytypic structures). In all of them (described in terms of a hexagonal cell) three closely spaced 3^6 nets of atoms are followed (in the z direction of the same cell) by a 3636 net (see figs. 8 and 10). The 3^6 nets are stacked on the same site as the kagomé 3636 nets which they surround (for instance: β-BAC–γ-CAB in the "two slabs" $MgZn_2$ type (h) structure, β-BAC–γ-CBA–α-ACB in the "three slabs" $MgCu_2$ type (c) structure, α-ABC–γ-CBA–α-ACB–β-BCA in the "four slabs (hc)" Ni_2Mg type structure, etc.: see sec. 4.3. on homeotect structure type). The Laves phases, as Frank–Kasper structures, (see table 6), can also be described by alternative stacking of pentagon–triangle main layers of atoms and secondary triangular layers (parallel to (110) planes of the hexagonal cell). The importance of the geometrical factor in determining the stability of these phases has been pointed out (PEARSON [1972]). The role of the electron concentration in controlling the differential stability of the different Laves phase types has been also observed. By studying, for instance, solid solutions of Cu_2Mg and $MgZn_2$ with Ag, Al, Si (LAVES and WITTE [1936], KLEE and WITTE [1954]) it was observed that for an average VEC (valence electron concentration) between 1.3 and 1.8 e/a (electrons per atom) the Cu_2Mg structure is generally formed, for VEC values in the range from ≈ 1.8 to 2.2 e/a generally the $MgZn_2$ type structure is obtained. The Ni_2Mg type can be observed for intermediate values of VEC between 1.8 and 2.0.

It may be useful, however, to mention that depending, for instance, on the temperature different Laves type structures may be observed in the same chemical system. An example may be the Ti–Cr system for which 3 different structures have been described: α-$TiCr_2$ ($MgCu_2$ type, homogeneous in the composition range $\approx$ 63–65 at% Cr), stable from room temperature up to $\approx$ 1220°C; β-$TiCr_2$ ($MgZn_2$ type, homogeneous from 64 to 66 at% Cr), high temperature phase stable from 800°C up to $\approx$ 1270°C; and γ-$TiCr_2$ (Ni_2Mg type, $\approx$ 65–66 at% Cr), high temperature phase stable from 1270°C up to the melting point (1370°C). Notice that the α and β forms, which can coexist in the temperature range from 800°C up to 1220°C have slightly different compositions.

Many (binary and complex solid solutions) Laves phases are known. Typically Laves compounds XM_2 are formed in several systems of X metals such as alkaline-earths, rare earths, actinides, Ti, Zr, Hf, etc, with M = Al, Mg, VIII group metals, etc.

Before passing to a detailed description of the principal Laves types, a few more remarks can be made concerning the *Laves polytypes*. An interesting example may be given by the Li–Mg–Zn alloys (MELNIK [1974], MALLIK [1987]). This system is one of the richest in the Laves phases among the known ternary systems. It contains, besides $MgZn_2$, eight ternary compounds L_n (the index n denotes the number of slabs) in the following sequence:

L_2: $MgZn_2$ (hP), a = 521.4 pm; c = 856.3 pm ($\equiv 2*428.1$)
L_8: $Mg(Li_{0.07}Zn_{1.93})$ (hP), a = 521.3 pm; c = 3422 pm ($\equiv 8*427.8$)
L_{14}: $Mg(Li_{0.11}Zn_{1.89})$ (hP), a = 521.5 pm; c = 5989 pm ($\equiv 14*427.8$)
L_9: $Mg(Li_{0.20}Zn_{1.80})$ (hR), a = 522 pm; c = 3841 pm ($\equiv 9*426.8$)

L_{10}: $Mg(Li_{0.23}Zn_{1.77})$ (hP), a = 522.3 pm; c = 4278 pm (≡ 10 * 427.8)
L_4: $Mg(Li_{0.25}Zn_{1.75})$ (hP), a = 522.7 pm; c = 1709 pm (≡ 4 * 427.3)
L'_4: $Mg(Li_{0.50}Zn_{1.50})$ (hP), a = 1046 pm; c = 1705 pm (≡ 4 * 426.3)
L'_3: $Mg(Li_{0.56}Zn_{1.44})$ (hR), a = 1051 pm; c = 1285 pm (≡ 3 * 428.3)
L_3: $Mg(Li_{0.77}Zn_{1.23})$ (cF), a = 522.6 pm; c = 1290 pm (≡ 3 * 430)

Notice that the structures with n = 3 and 4 exist not only in an ordinary form L_4, Ni_2Mg, and L_3, $MgCu_2$ type cubic, (a = 744.8 pm, here described in terms of an equivalent set of hexagonal axes) but also with doubled unit cell edge *a* (Ni_2Mg type and $MgCu_2$ type superstructures L'_4 and L'_3).

Structural type: cF24–Cu_2Mg and derivative structures
Face-centered cubic cF24–Cu_2Mg, space group $Fd\bar{3}m$, No. 227.
Atomic positions:
8 Mg in a) 0,0,0; $0,\frac{1}{2},\frac{1}{2}$; $\frac{1}{2},0,\frac{1}{2}$; $\frac{1}{2},\frac{1}{2},0$; $\frac{3}{4},\frac{1}{4},\frac{3}{4}$; $\frac{3}{4},\frac{3}{4},\frac{1}{4}$; $\frac{1}{4},\frac{1}{4},\frac{1}{4}$; $\frac{1}{4},\frac{3}{4},\frac{3}{4}$;
16 Cu in d) $\frac{5}{8},\frac{5}{8},\frac{5}{8}$; $\frac{5}{8},\frac{1}{8},\frac{1}{8}$; $\frac{1}{8},\frac{5}{8},\frac{1}{8}$; $\frac{1}{8},\frac{1}{8},\frac{5}{8}$; $\frac{3}{8},\frac{7}{8},\frac{1}{8}$; $\frac{3}{8},\frac{3}{8},\frac{5}{8}$; $\frac{7}{8},\frac{7}{8},\frac{5}{8}$; $\frac{7}{8},\frac{3}{8},\frac{1}{8}$; $\frac{7}{8},\frac{1}{8},\frac{3}{8}$; $\frac{7}{8},\frac{5}{8},\frac{7}{8}$; $\frac{3}{8},\frac{1}{8},\frac{7}{8}$; $\frac{3}{8},\frac{5}{8},\frac{3}{8}$; $\frac{1}{8},\frac{3}{8},\frac{7}{8}$; $\frac{1}{8},\frac{7}{8},\frac{3}{8}$; $\frac{5}{8},\frac{3}{8},\frac{3}{8}$; $\frac{5}{8},\frac{7}{8},\frac{7}{8}$;
Coordination formula: $3\frac{3}{\infty}3\,[Mg_{4/4}][Cu_{6/6}]_{12/6}$
For the prototype itself, Cu_2Mg, a = 704 pm.
Fig. 42 shows the $MgCu_2$ packing spheres structure.
Normalized interatomic distances and numbers of equidistant neighbours are shown in fig. 43.

Ordered variants of this type of structure are the *Cu_4MgSn* type structure and the *$AuBe_5$* type structure. The packing spheres structure of $AuBe_5$ is shown in fig. 44. The atomic positions of the two structures correspond to the following occupation of the same equipoints in the space group $F\bar{4}3m$ (No. 216).

	in Cu_4MgSn	in $AuBe_5$
a) 0,0,0; $0,\frac{1}{2},\frac{1}{2}$; $\frac{1}{2},0,\frac{1}{2}$; $\frac{1}{2},\frac{1}{2},0$	4 Sn	4 Au
c) $\frac{1}{4},\frac{1}{4},\frac{1}{4}$; $\frac{1}{4},\frac{3}{4},\frac{3}{4}$; $\frac{3}{4},\frac{1}{4},\frac{3}{4}$; $\frac{3}{4},\frac{3}{4},\frac{1}{4}$;	4 Mg	4 Be
e) x,x,x; −x,−x,x; −x,x,−x; x,−x,−x $x,\frac{1}{2}+x,\frac{1}{2}+x$; $-x,\frac{1}{2}-x,\frac{1}{2}+x$; $-x,\frac{1}{2}+x,\frac{1}{2}-x$; $x,\frac{1}{2}-x,\frac{1}{2}-x$; $\frac{1}{2}+x,x,\frac{1}{2}+x$; $\frac{1}{2}-x,-x,\frac{1}{2}+x$; $\frac{1}{2}-x,x,\frac{1}{2}-x$; $\frac{1}{2}+x,-x,\frac{1}{2}-x$; $\frac{1}{2}+x,\frac{1}{2}+x,x$; $\frac{1}{2}-x,\frac{1}{2}-x,x$; $\frac{1}{2}-x,\frac{1}{2}+x,-x$; $\frac{1}{2}+x,\frac{1}{2}-x,-x$. ($x \cong 0.625 = \frac{5}{8}$)	16 Cu	16 Be

We can see that the 8-atom equipoint of the Cu_2Mg type structure has been subdivided into two different, ordered, 4-point subsets in the two derivative structures.

Layers stacking symbols, triangular, kagomé (T,K) nets:

Cu_2Mg:
$Mg_0^A\ Cu_{0.13}^{\alpha}\ Mg_{0.25}^A\ Cu_{0.29}^C\ Mg_{0.33}^B\ Cu_{0.46}^{\beta}\ Mg_{0.58}^B\ Cu_{0.63}^A\ Mg_{0.67}^C\ Cu_{0.79}^{\gamma}\ Mg_{0.92}^C\ Cu_{0.96}^B$
Cu_4MgSn:
$Mg_0^A\ Cu_{0.13}^{\alpha}\ Sn_{0.25}^A\ Cu_{0.29}^C\ Mg_{0.33}^B\ Cu_{0.46}^{\beta}\ Sn_{0.58}^B\ Cu_{0.63}^A\ Mg_{0.67}^C\ Cu_{0.79}^{\gamma}\ Sn_{0.92}^C\ Cu_{0.96}^B$
$AuBe_5$:
$Au_0^A\ Be_{0.13}^{\alpha}\ Be_{0.25}^A\ Be_{0.29}^C\ Au_{0.33}^B\ Be_{0.46}^{\beta}\ Be_{0.58}^B\ Be_{0.63}^A\ Au_{0.67}^C\ Be_{0.79}^{\gamma}\ Be_{0.92}^C\ Be_{0.96}^B$

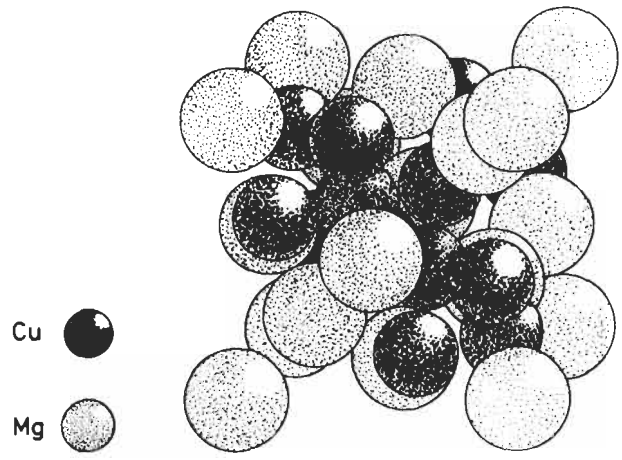

Fig. 42. cF24–$MgCu_2$ type structure (1 unit cell is shown).

Structural type: hP12–$MgZn_2$
Hexagonal, space group $P6_3/mmc$, N. 194,
Atomic positions:
2 Zn in a) 0,0,0; $0,0,\frac{1}{2}$;
4 Mg in f) $\frac{1}{3},\frac{2}{3},z$; $\frac{2}{3},\frac{1}{3},\frac{1}{2}+z$; $\frac{2}{3},\frac{1}{3},-z$; $\frac{1}{3},\frac{2}{3},\frac{1}{2}-z$;
6 Zn in h) $x,2x,\frac{1}{4}$; $-2x,-x,\frac{1}{4}$; $x,-x,\frac{1}{4}$; $-x,-2x,\frac{3}{4}$; $2x,x,\frac{3}{4}$; $-x,x,\frac{3}{4}$;
For the prototype itself, $MgZn_2$, a = 522 pm, c = 856 pm, c/a = 1.640, $z_{Mg} = 0.062$ and $x_{Zn} = 0.830$.
Coordination formula: $3^3_\infty 3\,[Mg_{4/4}][Zn_{6/6}]_{12/6}$
Layer stacking symbols, triangular, kagomé (T,K) nets:
$Zn_0^A\ Mg_{0.06}^B\ Zn_{0.25}^\beta\ Mg_{0.44}^B\ Zn_{0.50}^A\ Mg_{0.56}^C\ Zn_{0.75}^\gamma\ Mg_{0.94}^C$
Fig. 45 shows the packing spheres structure for the $MgZn_2$ compound.

A ternary ordered variant of this structure corresponds to three different atomic species in the three equipoint set. An example may be U_2OsAl_3 (2 Os in a), 4 U in f) and 6 Al in h)).

Structural type: hP24–Ni_2Mg
Hexagonal, space group $P6_3/mmc$, No. 194.
Atomic positions:
4 Mg in e) $0,0,z$; $0,0,\frac{1}{2}+z$; $0,0,-z$; $0,0,\frac{1}{2}-z$;
4 Mg in f) $\frac{1}{3},\frac{2}{3},z$; $\frac{2}{3},\frac{1}{3},\frac{1}{2}+z$; $\frac{2}{3},\frac{1}{3},-z$; $\frac{1}{3},\frac{2}{3},\frac{1}{2}-z$;
4 Ni in f) $\frac{1}{3},\frac{2}{3},z$; $\frac{2}{3},\frac{1}{3},\frac{1}{2}+z$; $\frac{2}{3},\frac{1}{3},-z$; $\frac{1}{3},\frac{2}{3},\frac{1}{2}-z$;
6 Ni in g) $\frac{1}{2},0,0$; $0,\frac{1}{2},0$; $\frac{1}{2},\frac{1}{2},0$; $\frac{1}{2},0,\frac{1}{2}$; $0,\frac{1}{2},\frac{1}{2}$; $\frac{1}{2},\frac{1}{2},\frac{1}{2}$;
6 Ni in h) $x,2x,\frac{1}{4}$; $-2x,-x,\frac{1}{4}$; $x,-x,\frac{1}{4}$; $-x,-2x,\frac{3}{4}$; $2x,x,\frac{3}{4}$; $-x,x,\frac{3}{4}$;
For the prototype itself, Ni_2Mg, a = 482 pm, c = 1583 pm, c/a = 3.284 and z (e_{Mg}) = 0.094, z (f_{Mg}) = 0.8442, z (f_{Ni}) = 0.1251, and x (h_{Ni}) = 0.1643.

References: p. 363.

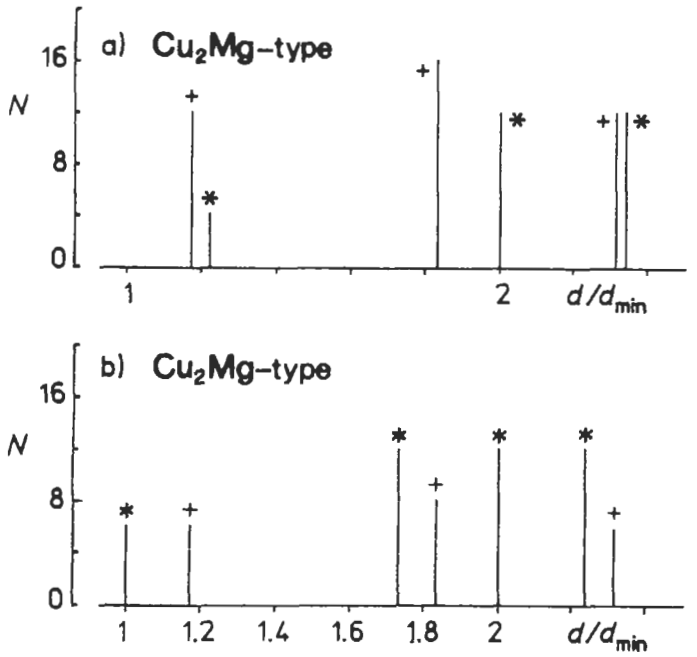

Fig. 43. Distances and coordinations in the cF24–$MgCu_2$ type structure.
a) Coordination around Mg:
(+) Mg–Cu; (*) Mg–Mg.
b) Coordination around Cu:
(*) Cu–Cu; (+) Cu–Mg.

The structure can be described by the following layer stacking sequence triangular, kagomé (T,K) nets:
$Ni_0^{\alpha}\, Mg_{0.09}^{A}\, Ni_{0.13}^{B}\, Mg_{0.16}^{C}\, Ni_{0.25}^{\gamma}\, Mg_{0.34}^{C}\, Ni_{0.37}^{B}\, Mg_{0.41}^{A}\, Ni_{0.50}^{\alpha}$
$Mg_{0.59}^{A}\, Ni_{0.63}^{C}\, Mg_{0.66}^{B}\, Ni_{0.75}^{\beta}\, Mg_{0.84}^{B}\, Ni_{0.87}^{C}\, Mg_{0.91}^{A}$
Coordination formula:
$3^3_{\infty}3\,[Mg_{4/4}][Ni_{6/6}]_{12/6}$

6.6.5. Structures based on frameworks of fused polyhedra, Samson phases

In addition to the Frank–Kasper phases, other structures may be considered in which the same four coordination polyhedra prevail although some regularity is lost. Many of these structures and, in particular the giant cell structures studied by SAMSON [1969] can be described as based on frameworks of fused polyhedra rather than the full interpenetrating polyhedra. Among the most important polyhedra we may mention the truncated tetrahedron: it is shown in fig. 46. It can be related to the CN 16 polyhedron (Friauf polyhedron) of fig. 41. The two polyhedra can be transformed into each other by removing (adding) the 4 six-fold vertices of the CN 16 polyhedron (corresponding to positions out from the center of each of the 4 hexagons of the truncated tetrahedron).

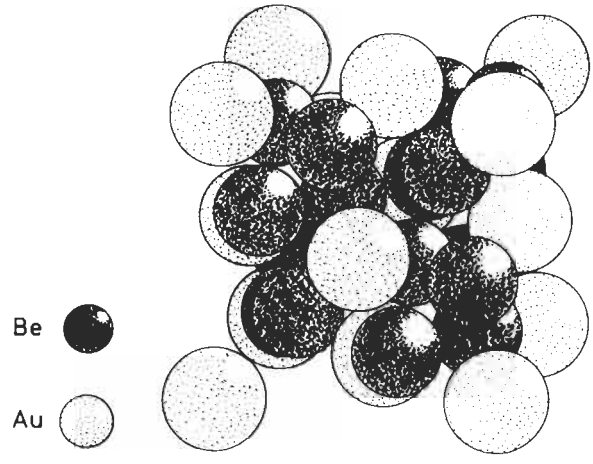

Fig. 44. Unit cell of the cF24–$AuBe_5$ type structure. (Compare with the cF24–$MgCu_2$ type structure, fig. 42.)

Several other coordination polyhedra occur in giant cell structures in addition to the Frank–Kasper polyhedra and to the truncated tetrahedron. (The most important are polyhedra corresponding to CN between 11 and 16).

The following phases represent a few examples of structures to which the aforementioned considerations specially apply:

cI58–α-Mn (a = 891.4 pm) type structure (and its binary variants, cI58–Ti_5Re_{24} or χ-phase and cI58–γ-$Mg_{17}Al_{12}$), cF1124–Cu_4Cd_3 type (a = 2587.1 pm); cF1192–$NaCd_2$ type (a = 3056 pm); cF1832–Mg_2Al_3 (a = 2823.9 pm), etc. (In the giant cell structures partial disorder and/or partial occupancy in some atomic positions have been generally reported, for cF1124–Cu_4Cd_3, for instance, the structure was described as corresponding to the occupation, in several Wyckoff positions, of 388 atomic sites by Cd-atoms, 528 by Cu-atoms and of 208 by Cu- and Cd-atoms in substitutional disorder.)

7. *On some regularities in the intermetallic compound formation and structures*

7.1. Preliminary remarks

As already mentioned in the previous sections, several thousands of binary, ternary and quaternary intermetallic phases have been identified and their structures determined. In a comprehensive compilation such as that by VILLARS and CALVERT about 2200 (in the first edition, [1985]) or about 2700 (second edition, [1991]) different structural types have been described. The specific data concerning about 17500 different intermetallic phases (pertaining to the aforementioned structural types) have been reported in the 1st edition and 26000 in the 2nd one.

As an introductory remark, a little *statistical information* about the *phase* and *structure type distributions* may be interesting.

References: p. 363.

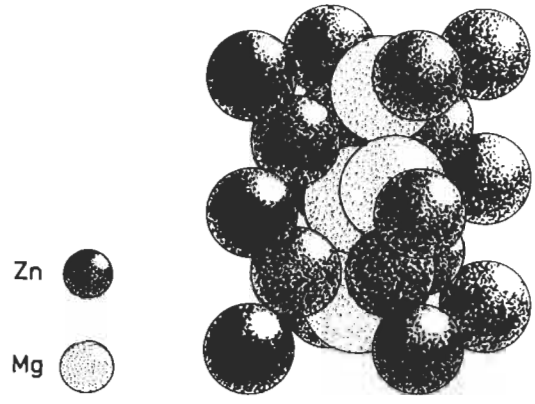

Fig. 45. Unit cell of the hP12–$MgZn_2$ type structure.

For this purpose, we may consider the group of phases described in the compilation by VILLARS and CALVERT [1991]. This, in fact may be considered a fairly representative sample even if the number of new intermetallic phases (and structural types) is constantly increasing.

As a first observation we may notice that the number of phases pertaining to each structural type is not at all constant. Table 7 shows that a very high number of phases crystallize in a few more common structure types. About 25% of the known intermetallic phases belong to the first 12 more common structure types and about 50% of the phases belong to 44 types (that is less than 2% of the known structural types).

This kind of distribution seems to be significant even if table 7 contains only an approximate list. (Some changes may actually be obtained by a more accurate attribution of different phases to a certain structural type or to its degenerate or derivative variants).

The distribution of the phases among the different types is summarized in fig. 47, where (in a double logaritmic scale) the number of phases belonging to each structural type is plotted against the rank order of the type itself. According to a suggestion of the authors of this chapter, in the same figure a curve is presented which has been computed by fitting the reported data by means of eq. (1):

$$N_f = A(r + r_O)^{-B} \tag{1}$$

where N_f is the number of phases corresponding to the structure type having rank r (A, B and r_0 are empirical constants whose values have been determined by the fitting (see also FERRO *et al.* [1995]).

It may be interesting to point out that the aforementioned equation is that suggested by MANDELBROT [1951] as a generalization of ZIPF's law [1949] (which corresponds to the special case of $r_0 \approx 0$ and B = 1). This law, in linguistics, relates for a given text the recurrence frequency (N_f) of a word to its rank (recurrence order). The formula had been deduced to define a cost function for the transmission of linguistic information and minimizing the average cost. (The word "cost" was considered to be related to the complexity of the word

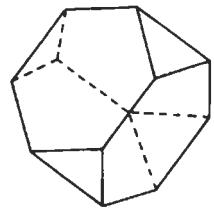

Fig. 46. Truncated polyhedron (12 vertices) related, by the addition of 4 more coordinate atoms out from the centers of the hexagonal faces to the Friauf polyhedron (CN 16), reported in fig. 41.

itself). (Eq. (1) may be considered a special case of a general "Rank Size Rule".)

We note, moreover, the larger numbers of phases having highly symmetric structures (cubic, hexagonal or tetragonal structures). The most frequent orthorhombic and monoclinic structures are the 6th and the 58th respectively in a general list such as reported in table 7. This may be partially related to a certain greater ease in solving highly symmetric structures but probably also contains an indication of a stability criterion. The Laves' stability principles (presented in sec. 7.2.3.) and, specially, the "symmetry principle" may be mentioned.

Considering then the phase composition as a significant parameter, we obtain the histogram shown in fig. 48 for the distribution of the structural types and of the intermetallic phases (as obtained from the 2nd edition of Villars–Calvert) according to the *stoichiometry* of *binary prototypes* (that is, for instance, the binary and ternary Laves phases, the AlB_2, $CaIn_2$, etc., type phases are all included in the number reported for the 66 to 67.99 stoichiometry range, even if the real stoichiometry of the specific phase is different). We may note the overall prevalence of phases and (to a certain extent) of structural types, which, at least ideally, may be related to simple (1:2, 1:1, 1:3, 2:3, etc.) stoichiometric ratios.

The restriction of the phases concentration to a limited number of stoichiometric ratios is also valid (and, perhaps, more evident) for the ternary phases. We may notice in fig. 49 (adapted from a paper by RODGERS and VILLARS [1993]) that seven stoichiometric ratios (1:1:1, 2:1:1, 3:1:1, 4:1:1, 2:2:1, 3:2:1, 4:2:1) are the most prevalent. According to Rodgers and Villars they represent over 80% of all ternary known compounds.

We have, however, to remark that, considering only selected groups of (binary or ternary) alloys, quite different stoichiometric ratios may be predominant. As an example we may mention the binary alloys formed by an element such as Ca, Sr, Ba, rare earth metals, actinides, etc., with Be, Zn, Cd, Hg and, to a certain extent, Mg. Many compounds are generally formed in these alloys. Among them, phases having very high stoichiometric ratios are frequently observed, such as, for instance: $CaBe_{13}$, $LaBe_{13}$, $BaZn_{13}$, $BaCd_{11}$, $BaHg_6$, $BaHg_{11}$, $BaHg_{13}$, La_2Zn_{17}, $LaZn_{13}$, La_2Cd_{17}, $LaCd_{11}$, Th_2Zn_{17}, Pu_3Zn_{22}, Ce_5Mg_{41}, La_2Mg_{17}, $LaMg_{12}$, etc.

7.2. On some factors which control the structure of intermetallic phases

A systematic description of bond characterization from thermodynamic properties in intermetallic compounds (and considerations concerning the stability of intermetallic

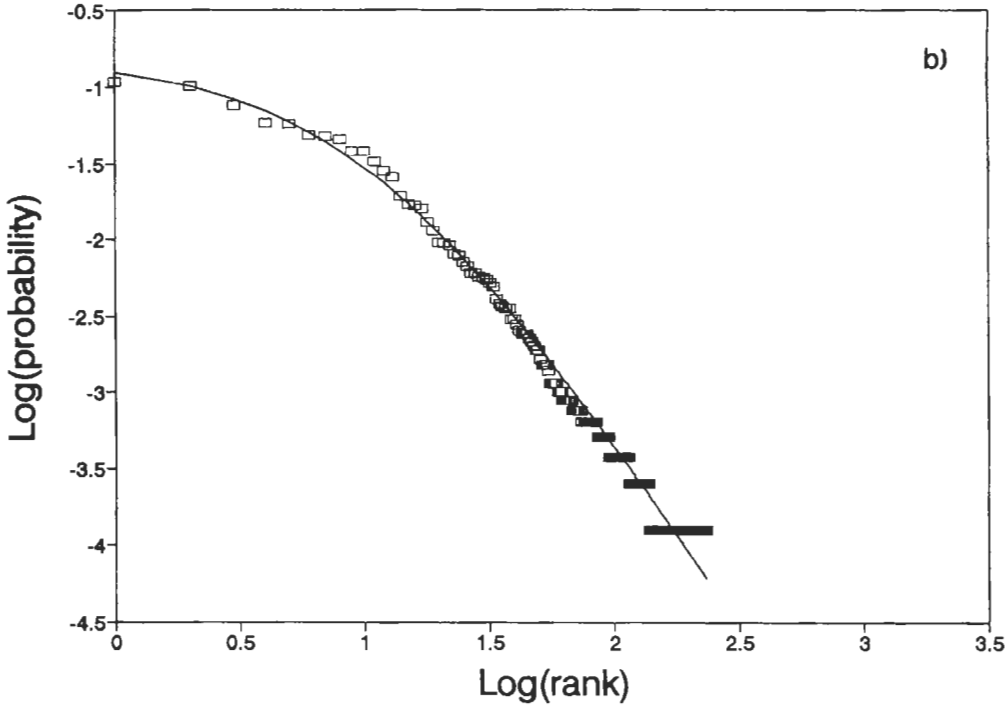
b)
Log(probability)
-0.5
-1
-1.5
-2
-2.5
-3
-3.5
-4
-4.5
0
0.5
1
1.5
2
2.5
3
3.5
Log(rank)

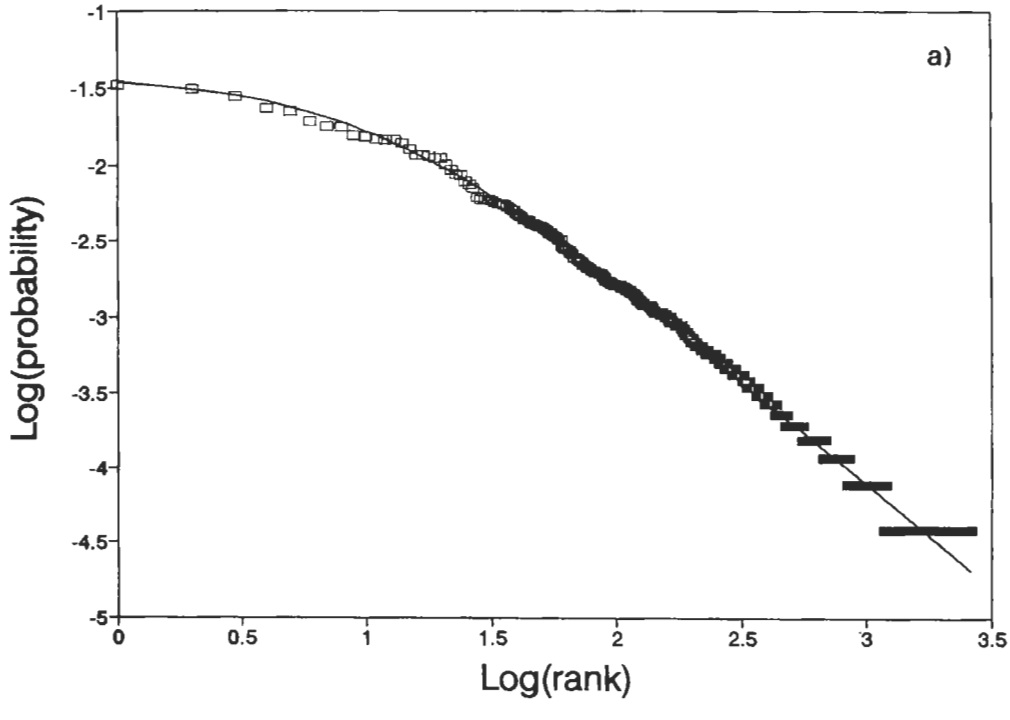
a)
Log(probability)
-1
-1.5
-2
-2.5
-3
-3.5
-4
-4.5
-5
0
0.5
1
1.5
2
2.5
3
3.5
Log(rank)

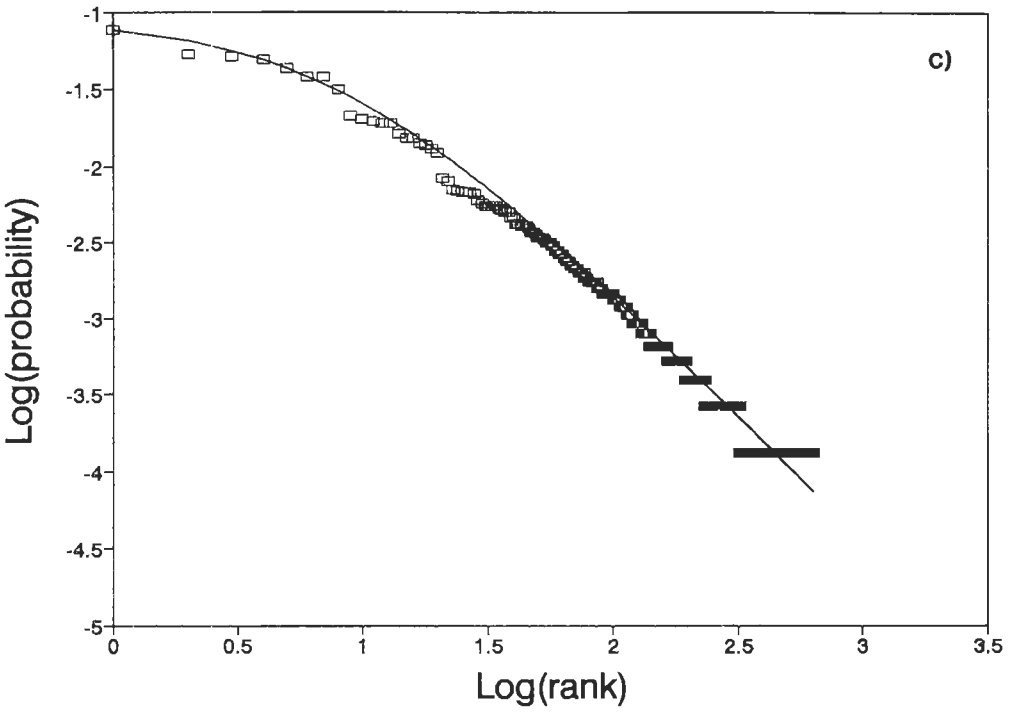

Fig. 47c. Distribution of the intermetallic phases among the structural types. In a double logarithmic diagram the phase numbers (expressed as ratios to the total number) are plotted versus the rank order of the structural type. The continuous line corresponds to the Mandelbrot's equation.
a) Number of phases belonging to the overall different structural types. (Compare with Table 6).
b) Number of phases belonging to the cubic structural types.
c) Number of phases belonging to the hexagonal structural types.

phases) has been reported by ELLNER and PREDEL [1994]. Some information about the computation of the enthalpy of formation of alloys according Miedema's model will be given in sec. 8.5. On this subject we may mention the peculiar properties of alloys of extraordinary stability formed by elements such as Al, Ti, Zr, Hf with the transition metals Re, Ru, Os, Rh, Ir, Pd, Pt, characterized by very high formation heats and discussed by BREWER [1973, 1990] as example of generalized Lewis acid–base interactions in metallic systems.

A general presentation and discussion of the origin of structure of crystalline solids and the structural stability of compounds and solid solutions have been given by Pettifor (see chapter 2 of this book).

In this section and in the following one a brief sampling of some *semiempirical* useful *correlations and, respecively, of methods of predicting phase* (and structure) *formation* will be summarized. The search for regularities and criteria for the synthesis of new representatives of particular structure types has been carried out by many authors. Several factors

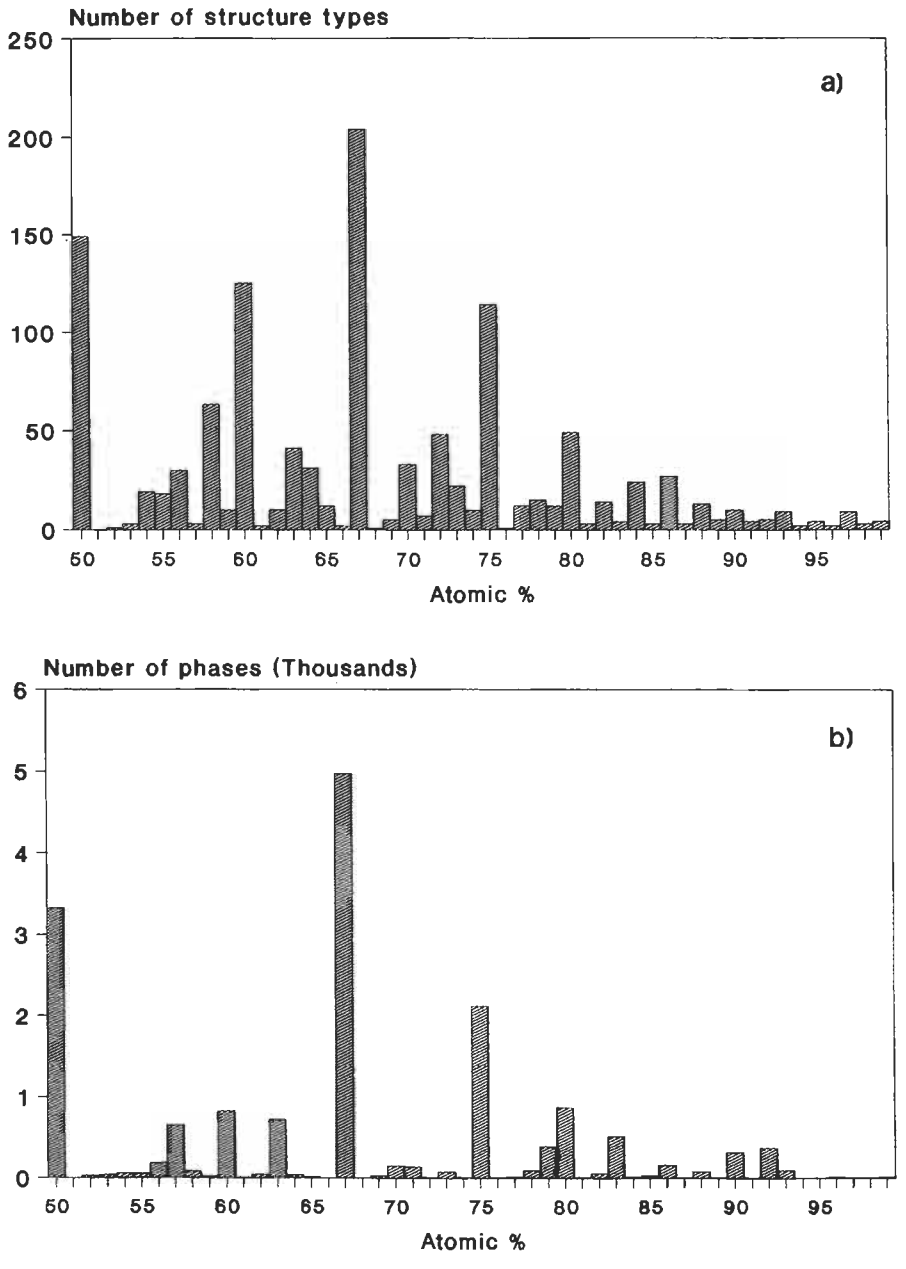

Fig. 48. Distribution of binary intermetallic phases and structural types, according to the stoichiometry.
a) Distribution of the structural types.
b) Distribution of the intermetallic phases.

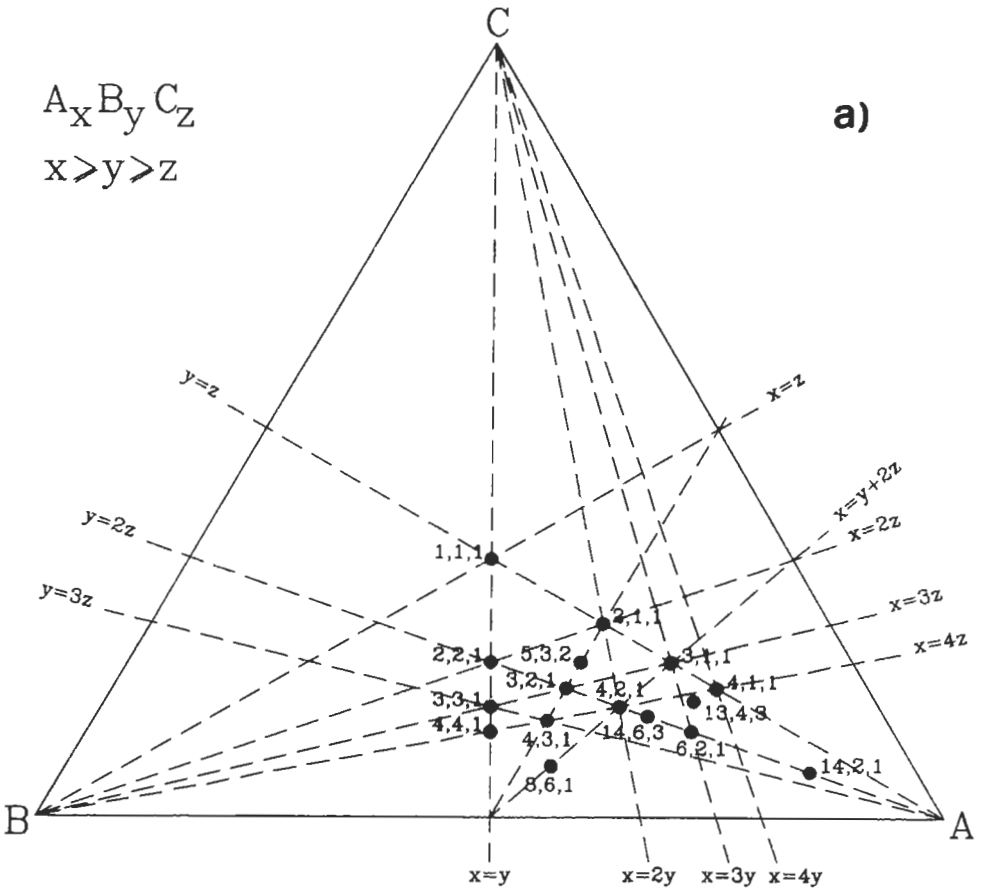

Fig. 49. Distribution of the known ternary intermetallic phases according to their stoichiometry.
a) In a representative portion of a general composition triangle, the more common stoichiometries are shown.

were recognized to be important in controlling the structural stability and some of them were used as coordinates for the preparation of "*classification and prediction maps*", in which various compounds can be plotted and separated into different structure domains.

Intermetallic phases, therefore, could be classified following the most important factor which controls their crystal structure (PEARSON [1972], WESTBROOK [1977], GIRGIS [1983], HAFNER [1989]).

According to PEARSON [1972], following factors may be evidenced:

— *Chemical bond factor,*
— *Electrochemical factor, (electronegativity difference)*
— *Energy band factor, electron concentration*
— *Geometrical factor*
— *Size factor*

References: p. 363.

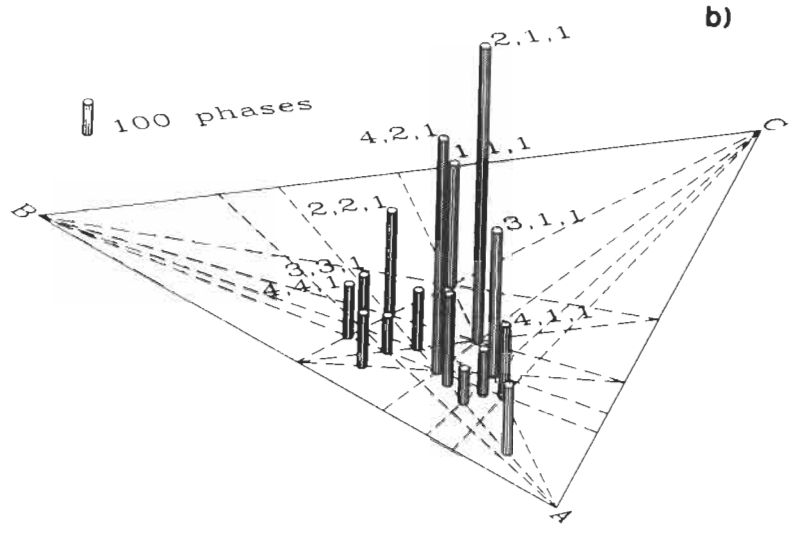

Fig. 49. Distribution of the known ternary intermetallic phases according to their stoichiometry.
b) For the same compositions shown in a), an indication is given of the number of phases.

In the following paragraphs a few comments will be reported on this matter. Emphasis, however, will be given only to those aspects which are more directly related to a description of the "geometrical" characteristics of the phases. For the other questions reference should be made to other parts of this volume.

For an introduction to the electronic structure of extended systems, see HOFFMANN [1987, 1988].

7.2.1. Chemical bond factor and electrochemical factor

A *chemical bond factor* can be said to control the structure when interatomic distances (and as a consequence unit cell dimensions) can be said to be determined by a particular set of chemical bonds. Two different situations can be considered: bonds having high *ionic characteristics* (largely non-directional, the larger anions tend to form symmetrical coordination polyhedra subjected to the limitation related to the anion/cation atomic size ratio) or bonds having *covalent character* (the directional characteristic of which tend to determine the structural arrangement in the phase).

To an increasing weight of the chemical bond factor (ionic and/or covalent bonding) will, of course, correspond, in the limit, the formation of *valence compounds*. According to PARTHE [1980b] a compound C_mA_n can be called a *normal valence compound* if the number of valence electrons of cations (e_C) and anions (e_A) correspond to the relation (normal valence compound rule):

$$m\,e_C = n(8 - e_A) \tag{2}$$

Table 7
Intermetallic phases: The most common structural types
(from the data reported in VILLARS and CALVERT [1991]).

Structural type	Number of phases belonging to each type			Relative Frequency		
	Total	Binary	Ternary	Specific	Cumulative	Rank order
cF8–NaCl	863	318	545	0.0332	0.0332	1
cF24–Cu_2Mg	806	243	563	0.0310	0.0642	2
tI10–$BaAl_4$	723	19	704	0.0278	0.0921	3
cF4–Cu	605	520	85	0.0233	0.1154	4
hP12–$MgZn_2$	580	148	432	0.0223	0.1377	5
oP12–Co_2Si	495	95	400	0.0191	0.1567	6
cP2–CsCl	461	307	154	0.0177	0.1745	7
cP4–$AuCu_3$	454	266	188	0.0175	0.1920	8
hP6–$CaCu_5$	405	106	299	0.0156	0.2076	9
hP2–Mg	393	362	31	0.0151	0.2227	10
cI2–W	382	309	73	0.0147	0.2374	11
cF16–BiF_3	379	39	340	0.0146	0.2520	12
hP9–Fe_2P	375	11	364	0.0144	0.2664	13
cI28–Th_3P_4	358	117	241	0.0138	0.2802	14
hP3–AlB_2	327	122	205	0.0126	0.2928	15
cF8–ZnS	302	40	262	0.0116	0.3044	16
cF56–$MgAl_2O_4$	301	11	290	0.0116	0.3160	17
tI26–$ThMn_{12}$	296	38	258	0.0114	0.3274	18
hP16–Mn_5Si_3	290	177	113	0.0112	0.3385	19
hP24–$Ce_6Al_3S_{14}$	288	0	288	0.0111	0.3496	20
cP8–Cr_3Si	260	82	178	0.0100	0.3596	21
hP4–NiAs	241	101	140	0.0093	0.3689	22
tP6–Cu_2Sb	227	74	153	0.0087	0.3777	23
cP5–$CaTiO_3$	225	3	222	0.0087	0.3863	24
cF116–Th_6Mn_{23}	202	49	153	0.0078	0.3941	25
oC8–CrB	193	120	73	0.0074	0.4015	26
tP68–$BFe_{14}Nd_2$	185	0	185	0.0071	0.4086	27
hR57–Th_2Zn_{17}	160	36	124	0.0062	0.4148	28
oP8–MnP	156	33	123	0.0060	0.4208	29
oP16–Fe_3C	155	101	54	0.0060	0.4268	30
hP6–Ni_2In	154	54	100	0.0059	0.4327	31
cP12–FeS_2	152	50	102	0.0059	0.4385	32
hP6–$CaIn_2$	149	11	138	0.0057	0.4443	33
hP38–$Ni_{17}Th_2$	145	62	83	0.0056	0.4499	34
oI12–$CeCu_2$	145	61	84	0.0056	0.4554	35
hR12–$NaCrS_2$	144	9	135	0.0055	0.4610	36
tI16–$FeCuS_2$	139	0	139	0.0053	0.4663	37
cF12–AlLiSi	135	1	134	0.0052	0.4715	38
cF12–CaF_2	133	87	46	0.0051	0.4767	39
cP40–$Pr_3Rh_4Sn_{13}$	126	0	126	0.0048	0.4815	40
hR36–Be_3Nb	122	49	73	0.0047	0.4862	41
oP8–FeB	121	73	48	0.0047	0.4909	42
hR45–Mo_6PbS_8	115	0	115	0.0044	0.4953	43
hP5–La_2O_3	115	22	93	0.0044	0.4997	44
tP2–AuCu	112	82	30	0.0043	0.5040	45

References: p. 363.

If we consider only the s and p block elements, the number of valence electrons of the elements correspond to their traditional group number) In this case (considering that no anions are formed from the elements of groups I, II and III) following formulae can be deduced for the *normal valence compounds* (formed in binary systems with large electronegativity difference between elements):

$-\ 1_4 4 - 2_2 4 - 3_4 4_3 - 1_3 5 - 2_3 5_2 - 35 - 4_3 5_4$
$-\ 1_2 6 - 26 - 3_2 6_3 - 46_2 - 5_2 6_3 - 17 - 27_2$
$-\ 37_3 - 47_4 - 57_5 - 67_6$

(in these formulae each element is indicated by a number corresponding to its number of valence electrons; for instance:
17 represent NaCl, KCl, etc, $3_2 6_3$ Al_2O_3, etc.)

In the more general case where some electrons are also considered to be used for bonds between cations and anions we have (general valence compound rule):

$$m(e_C - e_{CC}) = n(8 - e_A - e_{AA}) \tag{3}$$

In this formula, which can only be applied if all bonds are two-electron bonds and additional electrons remain inactive in non-bonding orbitals (or, in other words, if the compound is semiconductor and has not metallic properties) e_{CC} is the average number of valence electrons per cation which remain with the cation either in non-bonding orbitals or (in polycationic valence compounds) in cation–cation bonds; similarly e_{AA} can be assumed to be the average number of anion-anion electron pair bonds per anion (in polyanionic valence compounds).

In a more limited field than that of the previously considered general octet rule, it may be useful to mention the "*tetrahedral structures*" which form a subset of the general valence compounds. According to PARTHE [1963, 1964, 1991], if each atom in a structure is surrounded by 4 nearest neighbours at the corner of a tetrahedron, the structure is called "*normal tetrahedral structure*". The general formula of this structure, for the compound C_mA_n, is (*normal tetrahedral structure*):

$$(m\,e_C + n\,e_A) = 4(m + n) \tag{4}$$

(This may be considered a formulation of the so-called GRIMM–SOMMERFELD [1926] Rule).

For the same elements previously mentioned the possible combinations are:

$4_X 4_Y$ (all compositions, for instance, C, Ge, SiC)
35 (BP, AlSb, etc.), 26 (BeO, MgTe, ZnS), 17 (CuBr, AgI),
$3_2 6$, $3_3 7$, 25_2 (ZnP_2, $ZnAs_2$), $2_3 7_2$, 15_3 and $1_2 6_3$.
(ternary or more complex combinations may be obtained by a convenient addition of different binary formulae; for instance:
$14_2 5_3 = (15_3 + 44)$: for instance $CuGe_2P_3$
$136_2 = (1_2 6_3 + 3_2 6)/2$: $CuAlS_2$, $CuInTe_2$, etc.
$1_2 246_4 = (1_2 6_3 + 26 + 4)$: for instance Cu_2FeSnS_4 (Fe^{II}), etc.)

The aforementioned rule may be extended to include the "*defect tetrahedral structures*" where some atoms have less than four neighbours (*general tetrahedral structure*):

$$(m e_C + n e_A) = 4(m+n) + N_{NBO}(m+n) \tag{5}$$

In this formula N_{NBO} is the *average number of non-bonding orbitals* per atom.

By adding the *symbol 0* (zero) to the described notation, *vacant tetrahedral sites* can be represented. Examples of formulae of defect tetrahedral structures are:

40_37_4 (SiI_4, SnI_4); 406_2 (GeS_2); $3_60_5 4_6 3_6$ ($Ga_6As_4Se_3$), $1_2 5_2 0 6_4$ ($CuSbS_2$); etc.

Notice that the aforementioned compositional scheme is a *necessary condition* for building the tetrahedral structures, but *not* every compound that fulfills this condition is a tetrahedral compound. The influence of other parameters, such as the electronegativity difference, has been pointed out. By means of a diagram as shown in fig. 50, the separation of tetrahedral structures from other structures may be evidenced (MOOSER and PEARSON [1959]).

As a final comment to this point, we may mention that when one component in a binary alloy is very electropositive relative to the other, there is a strong tendency to form compounds of high stability in which valence rules are satisfied (PEARSON [1972]). Such alloys are considered to show a strong *electrochemical factor.*

7.2.2. Energy band factor, electron concentration

The properties of a solid on principle could be calculated on the basis of the states of the electrons in the crystal. The status of the understanding of the structures of the solids and indications on the technical and computational problems have been presented in other chapters.

We may mention here that if the stable crystal structure may be described as controlled by the number of electrons per atoms, the phase is called an "*electron compound*". An important class of electron compounds (generally showing rather wide homogeneity ranges) are the *Hume–Rothery phases.*

These include several groups of isostructural phases, each group corresponding to a given value of the so-called valence electron concentration (VEC). Three categories of Hume–Rothery phases are generally considered: those corresponding to VEC values of 3/2 (that is three valence electrons every two atoms), 21/13 and 7/4, respectively.

Representatives of the Hume–Rothery phases are the following:

VEC ≈ 3/2, body centered cubic, (cI2–W type): CuZn, ≈ Cu_3Al, ≈ Cu_5Sn, etc.
VEC ≈ 3/2, complex cubic, (cP20–β Mn type): Cu_5Si, Ag_3Al, Au_5Si, etc.
VEC ≈ 21/13, complex cubic, 52 atoms in the unit cell (or superstructures)
(cP52: ≈ Cu_9Al_4, ≈ Cu_9Ga_4, Ag_9In_4, ≈ Co_5Zn_{21}, etc.; cI52: ≈ Cu_5Zn_8, γ-brass, ≈ Ag_5Cd_8, Ag_5Zn_8, Ru_3Be_{10}, etc.; cF408: $Fe_{11}Zn_{39}$, etc.)
VEC ≈ 7/4, hexagonal close-packed, (hP2–Mg type or superstructures): ≈ $AgZn_3$, ≈ Au_3Ge, ≈ Ag_5Al_3, etc.

The VEC in all the aforementioned cases, for which approximate "ideal" formulae have been indicated, were calculated assuming the following "valence": transition elements with non-filled d-shells: 0; Cu,Ag,Au: 1; Mg and Zn,Cd,Hg: 2; Al,Ga,In: 3; Si,Ge,Sn: 4; Sb: 5.

The given ratios indicate ranges (which can even overlap). It has to be noted, moreover, that the number of electrons to be considered may be uncertain. The VEC

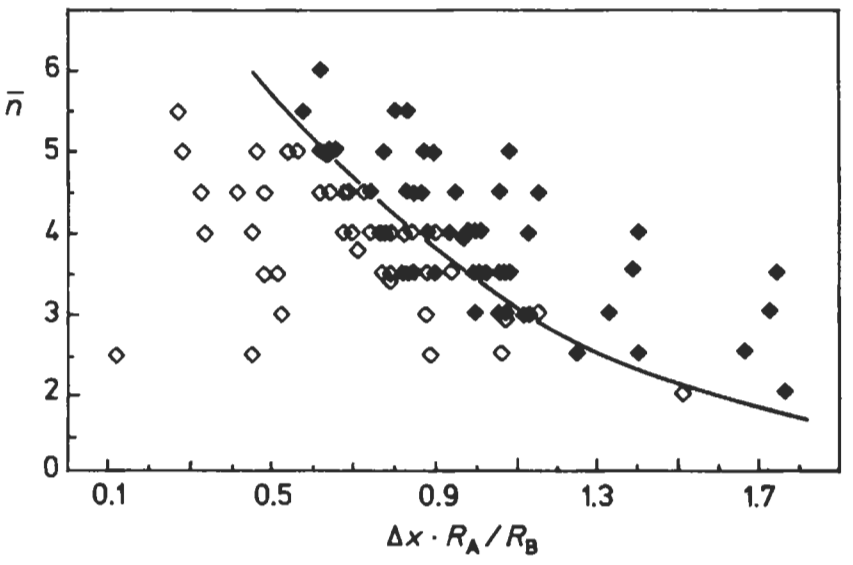

Fig. 50. Mooser–Pearson diagram separating AB compounds into covalent (◊) and ionic (♦) types after HUME–ROTHERY [1967]. The representative points of the different components are plotted in the map $\bar{n}$, average quantum number, versus the electronegativity difference multiplied by the radius ratio. (R_A and R_B radii of the anion and cation elements).

values, therefore, indicate only a composition range where one of the aforementioned structure types *may* occur.

According to GIRGIS [1983] the existence field of the electron phases may be especially related to the combinations of d elements with the elements of the Periodic Table columns from 11 to 14 (from Cu to Si groups).

7.2.3. Geometrical principles and factors, Laves' stability principles

LAVES [1956], when considering the factors which control the structures of the metallic elements, presented three principles that are interrelated and mainly geometric in character.

a) The principle of efficient (economical) use of space (*space-filling principle*).
b) The principle of *highest symmetry*.
c) The principle of the *greatest number of connections* (connection principle).

These principles may be considered to be valid to a certain extent for the intermetallic phase structures and not only for the metallic elements.

(See also some comments on this point as a result of the atomic-environment analysis of the structure types summarized in sec. 7.2.7.)

a) Space-filling principle

The *tendency to use the space economically* (to form structures with the best space-filling) which is especially exemplified by the closest-packing of spheres is considered to be the

result of a specific principle which operates in the metal structures (and also in ionic and, to a lesser degree, in van der Waals structures). This principle is less applicable to covalent crystals because the characteristic interbond angles are not necessarily compatible with an efficient use of the space. Among the metallic elements, 58 metals possess a close-packed arrangement (either cubic or hexagonal) which, in the assumption that the metal atoms are indeformable spheres having fixed diameters, corresponds to the best space-filling; 23 of the remaining metals crystallize in another highly symmetric structure, the body-centered cubic, which corresponds to a slightly less efficient space-filling.

(The space-filling concept has been analysed and discussed by several authors: we may mention LAVES [1956], PARTHE [1961], PEARSON [1972]. A short summary of this discussion will be reported in the following, together with some considerations on the atomic dimension concept itself).

b) The principle of highest symmetry (symmetry principle)

According to Laves a *tendency to build configurations with high symmetry* is evident and is called the symmetry principle. This tendency is particularly clear in metallic structures, especially in the simple ones.

However, according to HYDE and ANDERSSON [1989], for instance, the validity extension of this principle is difficult to evaluate. As time passes, crystallographers are able to solve more and more complex crystal structures and these tend to have low symmetry. The symmetry principle could perhaps be restated by observing that a crystal structure has the highest symmetry compatible with efficient use of space and the specific requirements of chemical bonding between nearest neighbours.

For a discussion on the "symmetry principles", its alternative formulations and the history of its development, papers by BRUNNER [1977] and by BÄRNIGHAUSEN [1980] may be consulted. In these papers a number of statements have been reported which perhaps may be considered equivalent. When considering close sphere packings, the following statements are especially worthy of mention.

a) A tendency to form arrangements of high symmetry is observable.
b) Points are disposed around each point in the same way as around every other.
c) Atoms of the same type tend to be in equivalent positions.

c) The principle of the greatest number of connections (connection principle)

To understand the meaning of this principle it may be at first necessary to define the *concept of connection*. To this end we may consider a certain crystal structure and imagine connecting each atom with the other atoms present in the structure by straight lines. There will be a *shortest segment* between any two atoms. We will then delete all links except the shortest ones. After this procedure, the atoms that are still connected constitute a "*connection*". The connection is *homogeneous* if it consists of structurally equivalent atoms, otherwise it is a *heterogeneous connection.*

Such connections may be finite or 1, 2, 3 dimensionally infinite and are respectively called *islands*, *chains*, *nets* or *lattices*. Symbols corresponding to the letters I, C, N, L (homogeneous connections) or i, c, n, l (heterogeneous connections) have been proposed. (see also the dimensionality indexes reported in sec. 3.5.1.).

As pointed out by Laves (for instance, LAVES [1967]) metallic elements and

intermetallic phases show a tendency to form multidimensional (possibly homogeneous) connections (*connection principle*).

7.2.4. Atomic dimensions and structural characteristics of the phases

a) Atomic radii and volumes

A few comments about the atomic dimension concept may be useful also in order to present a few characteristic parameters and diagrams (such as space-filling parameters, reduced strain parameters, near-neighbours diagrams, etc.).

Quoting from a comprehensive review on this subject (SIMON [1983]) we may remember that ever since it has been possible to determine atomic distances in molecules and crystals experimentally, efforts have been made to draw conclusions from such distances about the nature of the chemical bonding and to compare interatomic distances (dimensions) in the compounds with those in the chemical elements. Distances between atoms in an element can be measured with high precision. As such, however, they cannot be simply used in predicting interatomic distances in the compounds. In rational procedure, reference values (atomic radii) have to be "extracted" from the individual (interatomic distances) measured values. Various functions have been suggested for this purpose. In the specific case of the metals it has been pointed out that interatomic distances depend primarily on the number of ligands and on the number of valence electrons of the atoms (PEARSON [1972]).

Pauling's rule (PAULING [1947]):

$$R_n = R_1 - 30 \log n \,(pm) \tag{6}$$

relating radii for bond order (bond strength) n (number of valence electron per ligand) to that of strength 1, gives a means of correcting radii for coordination and/or for effective valencies. It has been shown (PEARSON [1972], SIMON [1983]) that, no matter what the limitations may be of any particular set of metallic radii (or valencies) that is adopted, the Pauling's relation appears to be reliable, giving a basis for comparing interatomic distances in metals. According to SIMON [1983] slightly better results could be obtained changing the Pauling's formula to:

$$R_n = R_1(1 - A \log n) \tag{7}$$

where A is not constant but can be represented as a function of the element valency.

The subsequent point is to select some system of (a set of) atomic radii which can be used when discussing interatomic distances.

The radii given by TEATUM *et al.* [1968] (and reported in table 8, together with the assumed "valencies") are probably the most useful for discussing metallic alloys. These radii have been reported for a coordination number of 12; they were taken from the observed interatomic distances in the fc cubic (cF4–Cu type) structure and in the hexagonal close-packed hP2–Mg type structure (averaging the distances of the first two groups of 6 neighbours, if the axial ratio has not the ideal 1.633.. value) or from the bc cI2–W type. Since the coordination is 8 in the cI2–W type structure, for the elements having this structure the observed radii were converted to coordination 12 by using a correction given by the formula:

Table 8
Radii (CN 12) of the Elements (from TEATUM *et al.* [1968])[a)]

Element	"Valence"	Radius (pm)	Element	"Valence"	Radius (pm)
H	−1	77.9	Sb	5	157.1
Li	1	156.2	Te	6	164.2
Be	2	112.8	Cs	1	273.1
B	3	92.0	Ba	2	223.6
C	4	87.6	La	3	187.7
N	−3	82.5	Ce	3	184.6
O	−2	89.7	Ce	4	167.2
Na	1	191.1	Pr	3	182.8
Mg	2	160.2	Nd	3	182.2
Al	3	143.2	Pm	3	180.9
Si	4	132.2	Sm	3	180.2
P	−3	124.1	Eu	2	204.1
S	−2	125.0	Eu	3	179.8
K	1	237.6	Gd	3	180.1
Ca	2	197.4	Tb	3	178.3
Sc	3	164.1	Dy	3	177.5
Ti	4	146.2	Ho	3	176.7
V	5	134.6	Er	3	175.8
Cr	6	128.2	Tm	3	174.7
Mn	5	130.7	Yb	2	193.9
Mn	7	125.4	Yb	3	174.1
Fe	8	127.4	Lu	3	173.5
Co	9	125.2	Hf	4	158.0
Ni	10	124.6	Ta	5	146.7
Cu	1	127.8	W	6	140.8
Zn	2	139.4	Re	7	137.5
Ga	3	135.3	Os	8	135.3
Ge	4	137.8	Ir	9	135.7
As	5	136.6	Pt	10	138.7
Se	6	141.2	Au	1	144.2
Rb	1	254.6	Hg	2	159.4
Sr	2	215.1	Tl	3	171.6
Y	3	177.3	Pb	4	175.0
Zr	4	160.2	Bi	5	168.9
Nb	5	146.8	Po	6	177.4
Mo	6	140.0	Fr	1	280
Tc	7	136.5	Ra	2	229.4
Ru	8	133.9	Ac	3	187.8
Rh	9	134.5	Th	4	179.8
Pd	10	137.6	Pa	5	162.6
Ag	1	144.5	U	6	154.3
Cd	2	156.8	Np	6	152.8
In	3	166.6	Pu	~4.8	164
Sn	2	163.1	Pu	5	159.2
Sn	4	158.0	Am	4	173.0

a) The elements are arranged according to their atomic number.
Noble gases and halogens are not included.

References: p. 363.

$$R_{CN\,12} = 1.0316\ R_{CN\,8} - 0.532\ \ (pm) \tag{8}$$

which was empirically obtained from the properties of elements having at least two allotropic modifications, cI2–W type and either cF4–Cu type or hP2–Mg type. The radii in the two structures (calculated at the same temperature by means of the known expansion coefficients) were compared and used to construct the reported equation. For the other metals (that is for the more general problem of the radius conversion from any coordination to coordination number 12) a percentage correction was applied (by using a curve which ranges from about +3% for the conversion from CN 8 to CN 12 to about +20% for the conversion from CN 3 to CN 12) as suggested by LAVES [1956] in a detailed paper dealing with several aspects of crystal structure and atomic sizes.

While dealing with atomic dimension concepts, *atomic volumes* may also be considered. A value of the volume per atom, V_{at} in a structure may be obtained from the room temperature lattice parameter data by calculating the volume of the unit cell and dividing by the number of atoms within the unit cell. See also the table reported by KING [1983].

An equivalent atomic radius could be obtained by computing, on the basis of the space-filling factor of the structure involved, the corresponding volume of a "spherical atom" using the relationship $V_{sph} = (4\ \pi\ R^3/3)$.

In the cP2–W type (CN 8) structure we have $V_{sph} \approx 0.68\ V_{at}$ (only a portion of the available space is occupied by the atomic "sphere", see the following paragraph b). In the cF4–Cu type, and in the "ideal" hP2–Mg type (CN 12) structures we have $V_{sph} \approx 0.74\ V_{at}$. Considering now the previously reported relationship between $R_{(CN\ 12)}$ and $R_{(CN\ 8)}$ we may compute for a given element, very little volume (V_{at}) changes in the allotropic transformation from a form with CN 12 to the form with CN 8. (The radius variation is nearly counterbalanced by the change in the space filling).

This generally is in agreement with the experimental observations (PEARSON [1972]).

We will see that on the basis of the atomic dimensions of the metals involved (expressed, for instance, as R_X–R_Y or R_X/R_Y) many characteristic structural properties of an X_nY_m phase may be conveniently discussed and/or predicted (*size factor effect*). As a further comment to this point we may mention here two "rules", the *Vegard's* and the *Biltz–Zen's rules*, which have been formulated for solid solutions and to a certain extent for ordered compounds. These rules, mutually incompatible, are very seldom obeyed; they may, however, be useful either as approximations or for defining reference behaviours. The first one, VEGARD's rule [1921], corresponds to an additivity rule for interatomic distances (or lattice parameters or "average" atomic diameters). For a solid solution A_xB_{1-x} (x = atomic fraction) between two components of similar structure it takes the form:

$$d_{AB} = x\,d_A + (1 - x)d_B \tag{9}$$

The BILTZ [1934], (or ZEN [1956]) rule has been formulated as a volume additivity rule:

$$V_{AB} = x\,V_A + (1 - x)V_B \tag{10}$$

These rules are only roughly verified in the general case (for the evaluation of interatomic distances weighted according to the composition and for a discussion on the calculation and prediction of the deviations from Vegard's rule see PEARSON [1972] and SIMON [1983]).

As contributions to the general question of an accurate prediction of the variation of the average atomic volume in alloying we may mention a few different approaches. MIEDEMA and NIESSEN [1982] calculated atomic volumes and volume contractions on the basis of the same model and parameters used for the evaluation of the formation enthalpy of the alloy (see sec. 8.5). In a simple model proposed by HAFNER [1985] no difference of electronegativity and no charge transfer were considered. Volume (and energy) changes in the alloy formation were essentially related to elastic effects. Good results have been obtained for alloys formed between s and p block-elements. An empirical approach has been suggested by MERLO [1988]. Deviations from Biltz–Zen trend have been discussed and represented as a function of a "charge transfer atomic parameter" which correlates with Pauling's electronegativity. This approach has been successfully employed for groups of binary alloys formed by the alkaline earths and the bivalent rare earth elements.

Negative experimental deviations from Vegard's rule (and values of the volume contractions) have been sometimes considered as an approximate indication of the formation of strong bonds and related to more or less negative enthalpies of formation (KUBASCHEWSKII [1967]). This indication is only very poor in the general case. For selected groups of alloys, however, the existence of a correlation between the formation volume and enthalpy ($\Delta_{form}V$ and $\Delta_{form}H$) has been pointed out (even if only as an evaluation of relative trends). This is the case of the rare earth (RE) alloys. As noticed by GSCHNEIDNER [1969] considering the trivalent members of the lanthanide series, we may compare the atomic volume decreasing observed in the metals (RE) (lanthanide contraction) with the decreasing of the average atomic volume measured in a series of $REMe_x$ compounds. If this diminution is more (less) severe in the compounds than in the RE metal series, this is considered an indication that the bonding strength in the $REMe_x$ compounds increases (decreases) as we proceed along the series from La to Lu; the heats of formation are expected to increase (decrease) in the same order. To make this comparison the unit cell volumes of the compounds are divided by the atomic volumes of the pure metals. The volume ratio for the series of compounds are then divided for that corresponding to a selected rare earth, this giving a relative scale. If the resultant values increase, with the atomic number of the rare earth, then the lanthanide contraction is less severe in the compounds (in comparison to the rare earth element) and a decrease of the heat of formation is expected (conversely if the relative volume ratio decreases, an increase of the heat of formation (more negative enthalpy of formation) is expected).

(Examples of this correspondence will be examined in sec. 8.6., see also fig. 59.)

b) Space-filling parameter (and curves)

The *space-filling parameter* introduced by LAVES [1956] and by PARTHE [1961] gives a means of studying the relationships between atomic dimensions and structure. For a compound, it is defined by the ratio between the volume of atoms in a unit cell and the volume of unit cell.

$$\varphi = \frac{(4\pi / 3)\left(\Sigma_i n_i R_i^3\right)}{V_{cell}} \tag{11}$$

(n_i, R_i number and radius of type i atoms).

References: p. 363.

To calculate the space filling value for a specific compound, one has to know the radii of the atoms and the lattice constant. Neither of these is needed for the construction of a *space filling curve* of a crystal *structure type*: it is sufficient to know the point positions of the atoms and the axial ratios. The curve is based on a *hard sphere model* of the atoms: the cell edges are expressed as functions of the atomic radii (R_X and R_Y for a binary system) for the special cases of X–X, X–Y and Y–Y contacts. The parameter can then be given (and plotted) as a function of the R_X/R_Y ratio.

Considering, for instance, the cF8–ZnS-sphalerite type structure (PARTHÉ [1964]) the space filling can be given by:

$$\phi = \left[4\pi/3\left(4R_X^3 + 4R_Y^3\right)\right]/a^3 \tag{12}$$

where a is the cubic cell edge and R_X and R_Y are the radii of the atoms in the a) and c) positions (4 Zn and 4 S, respectively) in the unit cell. (See the description of the structure in sec. 6.3.2.).

In the case that the two atoms (or, more accurately, the hard spheres) occupying the Zn and S sites are touching each other, then the sum of the two radii must be equal to one-quarter of the cubic cell diagonal.

$$R_X + R_Y = a\sqrt{3}/4 \tag{13}$$

By expressing the unit cell volume as a function of the sum of the radii we obtain:

$$\varphi = \frac{(4\pi/3)\left(4R_X^3 + 4R_Y^3\right)}{\left(4^3/3\sqrt{3}\right)\left(R_X + R_Y\right)^3} \tag{14}$$

Introducing the radius ratio $\varepsilon = R_X/R_Y$ one obtains:

$$\varphi = \left(\sqrt{3}\pi/4\right)\frac{\varepsilon^3 + 1}{(\varepsilon + 1)^3} \tag{15}$$

This equation describes the middle section ($0.225 < \varepsilon < 4.44$) of the space-filling curve for the sphalerite type structure plotted (with log scales) in fig. 51.

(The other sections, $0 < \varepsilon < 0.225$ and $4.44 < \varepsilon < \infty$ correspond to the cases in which Y–Y atoms or X–X atoms are touching.)

In the φ versus ε diagram every structure type is generally characterized by its own individually shaped *space-filling curve*. The space-filling curves, however, of all binary structures belonging to one *homeotect structure set* coincide with one curve (see sec. 4.3).

By assuming appropriate values for the radii R_X and R_Y it is possible to compare, with the specific curve of a given structure, the points representing actual compounds. Generally a good agreement is found for ionic structures (and/or compounds) while it is often observed that the φ versus ε points for particular metallic phases lie above the space-filling curves, indicating a denser packing and emphasizing the lack of unique radii associated with X–X, X–Y, etc. contacts (compressible atom model) (PEARSON [1972]).

In the specific case of unary structures (element structures), providing that there are no

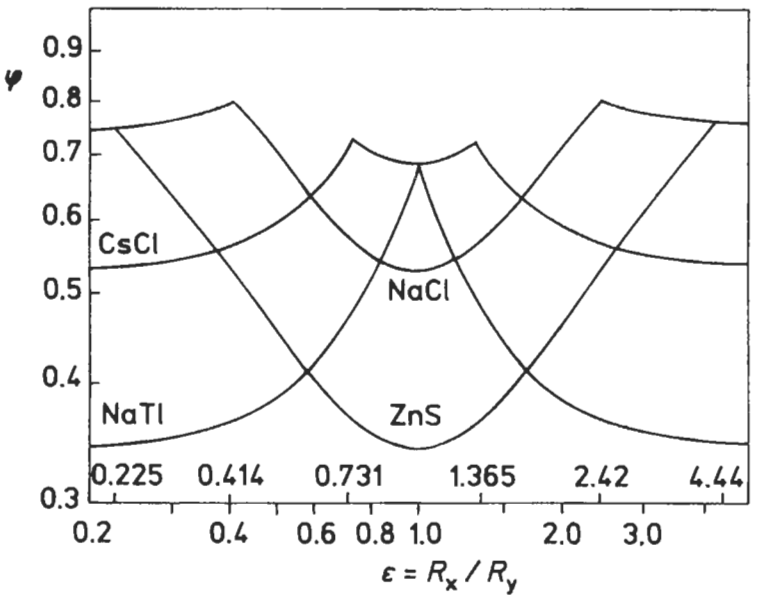

Fig. 51. Space filling diagram for the CsCl, NaCl and ZnS structures (from PARTHE [1961]).

variable atomic positional parameters or axial ratios, there is a unique space-filling parameter (independent of atomic size for every structure type). For the cF4–Cu type structure, for instance,

$$\varphi = (4\pi/3)(4R^3/a^3) \tag{16}$$

Assuming the atoms to be hard spheres $a = 2\sqrt{2}$ R, then $\varphi = 0.740$ (which is the highest value for an infinite collection of close-packed hard spheres of the same radius). Typical *space-filling parameters* of *elemental structures* are the following:

cF4–Cu type	0.740	
hP2–Mg type	0.740	(for the "ideal" value, $c/a = 1.633..$, of the axial ratio. It is $\varphi = 0.65$ in the case, for instance, of Zn, for which $c/a = 1.86$).
cI2–W type	0.680	
tI4–β-Sn type	0.535	
cP1–Po type	0.524	
cF8–Diamond	0.340	

Several other considerations and applications of the space filling concept may be found in PARTHE [1961], for instance: space-filling diagrams of ternary structures, applications of space-filling concept for discussing and predicting possible pressure structures, etc.

A similar treatment has been made by LIU and BASSETT [1986] defining a special "*volumetric index*" α, considering that the molar volume V of a crystal must be a linear function of the cube of the nearest neighbor interatomic distance d_{min}

References: p. 363.

$$V = \alpha d_{min}^3 \tag{17}$$

where α is a function of the axial ratio, axial angle(s) and positional parameters of a crystal structure.

Within a group of isostructural substances small variations are therefore generally observed in the α-value. If d_{min} is given in nm and V in cm^3/mol (moles of atoms or moles of formulae) the following α-values may be mentioned:

425.9 (cF4–Cu); 425.9 to 485.0 (hP2–Mg for $1.633 \leq c/a \leq 1.86$; 463.6 (cI2–W); 589.7 (tI4–βSn, $c/a = 0.5456$); 602.2 (cP1–Po); 927.2 (cF8–diamond); 927.1 (cP2–CsCl); 1204.4 (cF8–NaCl); $\approx$ 1843 (hP4–C graphite); etc.

The α-values are the slopes in the plots of the molar volume versus the cube of the interatomic distances for given types of structures such as those illustrated in fig. 52a. These indexes (as the space-filling parameters) may be useful, for instance, in a systematic description of the effect of pressure on the phase transformations which may be observed for a given compound. In a discussion of high-pressure phases (of elements, oxides and silicates) with implications for the Earth's interior, LIU and BASSETT [1986] presented data relevant to several families of compounds in a number of graphs such as those of fig. 52b. The transformations at increasing pressure from C graphite to diamond, from Si and Ge diamond type to βSn type, the modifications of a number of 1:1 compounds from NaCl to CsCl type structure and also for elements, such as Cd and Zn, the preservation of the same structure but with c/a approaching the "ideal" 1.633 value can all be effectively summarized in these type of graphs.

7.2.5. Reduced dimensional parameters

a) Reduced strain parameter and near-neighbours diagrams

By means of the comparison between the space-filling theoretical curves and the actual values of intermetallic phases it has been observed that an incompressible sphere model of the atom is unsuitable when discussing metallic structures.

PEARSON [1972] suggested the use of a model which allows the atoms of a binary X–Y alloy to be compressed until subsequently (and according to the structure geometry) X–X, X–Y, Y–Y contacts are established. The contacts are considered to occur when the X–X, X–Y and Y–Y interatomic distances in the compound structure, d_X, d_{XY} and d_Y are equal to 2 R_X ($=D_X$), $R_X + R_Y$ and 2 R_Y($=D_Y$) (R_X, R_Y, D_X, D_Y atomic radii and diameters, respectively). According to Pearson, the metallic radii choosen are those appropriate for the coordination of the atoms (compare with sec. 7.2.4.). The distances between all the close atoms in the structure may be expressed in terms of the cell (and atomic site) parameters. (As an example see, for instance, the phases XY_3, $AuCu_3$ type, described in sec. 3.5.5. and in figs. 12, 13, 14. In these phases around each X atom there are 6 X atoms at a distance equal to the unit cell edge $d_X = a$. Around the X atoms there are 12 Y atoms at a distance $d_{XY} = a\sqrt{2}/2$), and around the Y atoms at the same distance $d_Y = a\sqrt{2}/2$). All these distances may thence be expressed as a function of one of them, selected as a reference. (In the case of the $AuCu_3$ type phase, for instance:

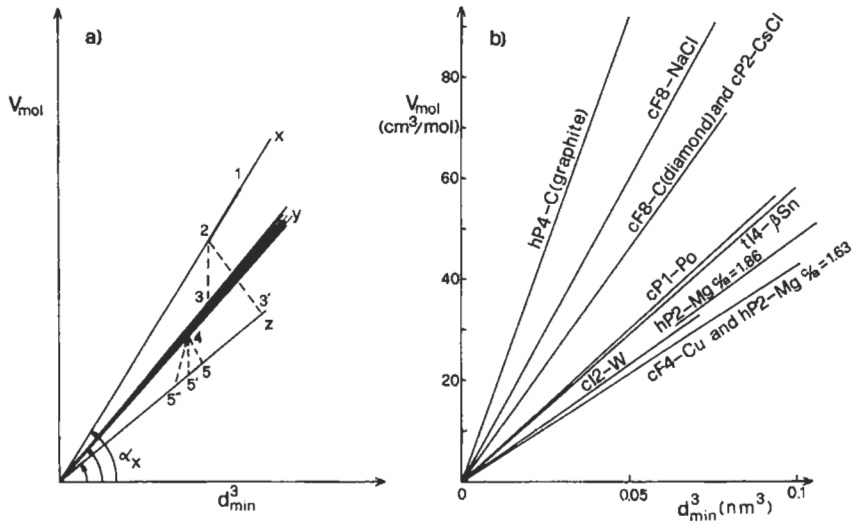

Fig. 52. Trends of the molar volumes of selected groups of phases as a function of the nearest neighbours interatomic distances.

a) Schematic trends for X, Y, Z, etc., structural types. (Y may represent a structure type for which, for instance, owing to different c/a ratios, several volume values may correspond to the same d_{min}). The hyphens 1 → 2, 2 → 3 (or 2 → 3'), etc. from 1 to 2 etc., represent different behaviours (and transformations) that may be observed by increasing pressure.

b) Actual trends for a group of common crystal structure types.

$$d_{XY} = d_X\sqrt{2}/2,\ d_Y = d_X\sqrt{2}/2 \tag{18}$$

A *reduced strain parameter* is then defined with reference to a arbitrarily selected set of contacts. With reference to the d_X distances the strain parameter may be defined as $S = (D_X - d_X)/D_Y$. This parameter gives an indication of the atomic dimension compression. It is computed, as a function of the ratio $\varepsilon = D_X/D_Y = R_X/R_Y$, for the different kinds of interatomic contacts.

In the aforementioned $AuCu_3$ type phases, we have 3 cases corresponding to X–X, X–Y and Y–Y contacts.

If X–X atoms are touching $d_X = D_X$, then the strain parameter S_{X-X} will be $(D_X - D_X)/D_Y = 0$ for all the ε-values.

If X–Y atoms are considered to be in contact $d_{XY} = d_X\sqrt{2}/2$ will be equal to $\frac{1}{2}(D_X + D_Y)$ so we will have:

$$S_{X-Y} = \frac{D_X}{D_Y} - \frac{d_X}{D_Y} = \frac{D_X}{D_Y} - \frac{d_{XY}\sqrt{2}}{D_Y} = \frac{D_X}{D_Y} - \frac{\frac{1}{2}\sqrt{2}D_X + \frac{1}{2}\sqrt{2}D_Y}{D_Y} \tag{19}$$

If, on the other hand, the Y–Y atoms are those which are considered to be in contact we will have:

References: p. 363.

$$d_Y = d_X\sqrt{2}/2 = D_Y; d_X = D_Y\sqrt{2} \text{ and} \tag{20a}$$

$$S_{Y-Y} = \frac{D_X}{D_Y} - \frac{\sqrt{2}D_Y}{D_Y} = \frac{D_X}{D_Y} - \sqrt{2} \tag{20b}$$

The values of the strain parameters are then plotted, according to PEARSON [1972], as a function of $\varepsilon = R_X/R_Y$. Several straight lines are obtained (see figs. 53, 54, 55) the lines corresponding to the reference contacts are horizontal and set at zero. What matters is only the *relative position* of the different straight lines (which does not change by taking another contact as the reference one: a rotation will only be obtained of the whole diagram). The diagram is called *Near-Neighbour Diagram*. In the diagram, points may also be plotted which represent actual phases. (To this end the experimental d_X, d_{XY}, etc., values will be used).

According to PEARSON [1972], when a point representing a specific phase has a larger value of the strain parameter than that of a particular contact line, then the contacts corresponding to that line are to be considered (on the basis of the D_X and D_Y assumed for the components) compressed. If, on the other hand, the experimental points lie below a line then those contacts have not been established.

Figs. 53 to 55 represent the data and the trend for a few structure types. For compounds having the cF8–ZnS sphalerite structure (see sec. 6.3.2.) it can be seen that the X–Y (Zn–S) bonds (corresponding to a tetrahedral coordination) are the most important in controlling the structural characteristics. The different points, representing actual compounds, are very close indeed, for a wide range of diameter ratio and of electronegativity differences to the line corresponding to the X–Y contacts. (The X–X and Y–Y contacts are not formed). The structure can, therefore, be considered as formed by a skeleton of presumably covalent (and directional in character) X–Y bonds. An X–Y chemical bond can similarly be recognized as important in several compounds having cF12–CaF_2 type (or antitype), cF16–Li_3Bi, hP3–CdI_2, hP8–Na_3As, etc., type structures. The different behaviours of more "metallic" phases can be seen in fig. 53 and fig. 55.

The $AuCu_3$ type near-neighbour diagram (fig. 53) shows the importance of contacts corresponding to high coordinations. A similar trend can be observed for the XY_2 Laves phases (see fig. 55 for the $MgCu_2$ type) for which, moreover, a certain compression of the X–X contacts generally results. (The X–X curve is, for $\varepsilon > 1.25$, far below the data points).

Many near-neighbour diagrams have been presented by PEARSON (1972) and systematically discussed for several structure types in order to show the importance of factors such as geometrical or chemical bond factors in controlling occurrence and structural characteristics of different phases.

For an analysis of the meaning and the applications of these diagrams see also SIMON [1983]. A representation, in generalized near neighbour diagrams, of structure families for alloy phases with given XY_n compositions has been presented and discussed.

b) Unit-cell dimension analysis

While discussing the interest in an analysis of the dimensional characteristics of phases with given structures and reconsidering advantages and limitations of the near-neighbour

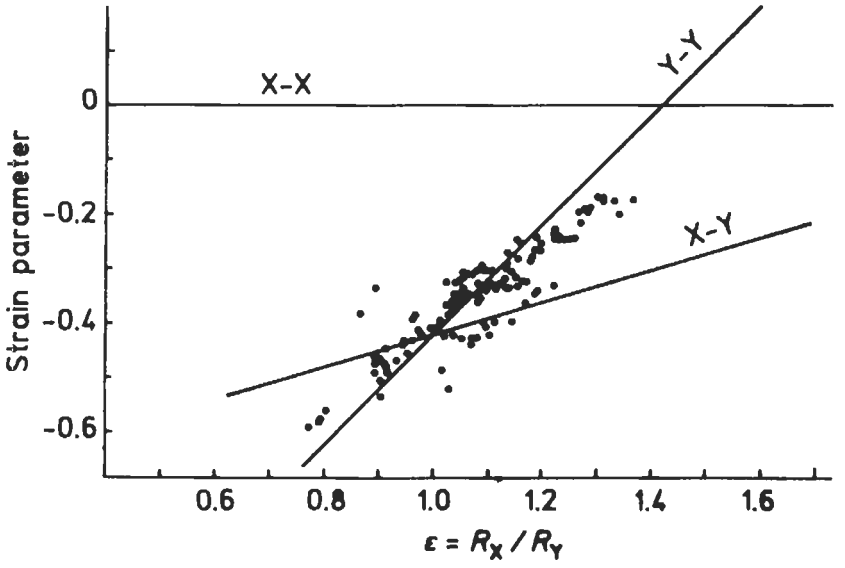

Fig. 53. Near neighbour diagram for binary phases with XY_3 formula belonging to the cP4–$AuCu_3$ structural type (according to PEARSON [1972]). The lines corresponding to the different contacts are shown.

diagrams, Pearson himself has proposed [1985a] a new analytical method based on plots as functions of the CN 12 atomic diameters determined from elemental structures and in which attention is paid to the group and period of the component elements in the selection of subsets of the data of phases to be considered together.

As an example of such an analysis we may consider the data reported in fig. 56. Phases are considered which pertain to the tI10–$ThCr_2Si_2$ type; the structure contains three different position sets, as described in sec. 6.5.9. It is one of the most populous of the different structure types. In particular, there are ten almost complete groups of data for RET_2X_2 phases given by rare earth metals (RE) with T = Mn, Fe, Co, Ni, Cu and X = Si or Ge. The data reported in fig. 56 are those concerning the $RENi_2Ge_2$ compounds. According to PEARSON [1985a] and PEARSON and VILLARS [1984] the contacts of interest between pairs (i,j) of the three components (RE, T, X) are defined by the relation:

$$\Delta_{ij} = \tfrac{1}{2}\left(D_i + D_j\right) - d_{ij} \tag{21}$$

where D_i, D_j are the atomic diameters and d_{ij} is the interatomic distance between i and j atoms (obtained from the experimental structure data). Generally it has been observed (see fig. 56) that Δ_{ij} varies linearly with D_{RE} (for series with different RE but the same T and X components).

A parameter f_{ij} may thus be defined by:

$$\Delta_{ij} = f_{ij} D_{RE} + k_{ij} \tag{22}$$

If a specific f_{ij} is of the order of zero (see, for instance, $\Delta_{RE\text{–}Ge}$ in fig. 56) this can be

References: p. 363.

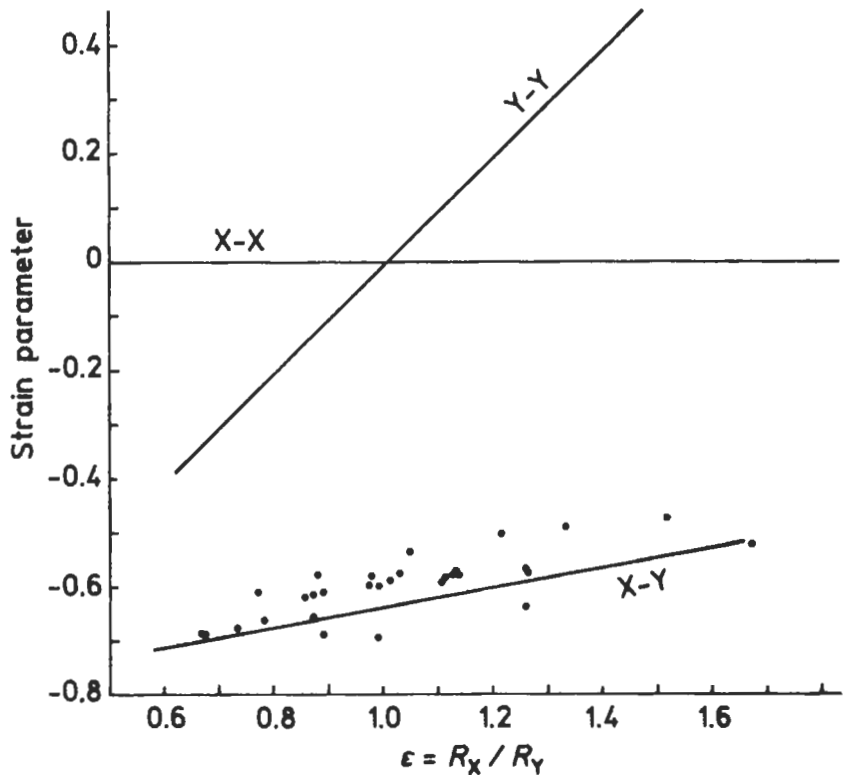

Fig. 54. Near neighbour diagram for binary phases with XY formula belonging to the cF8–ZnS structural type (according to PEARSON [1972]).

considered an indication that the particular ij contact is independent of change in D_{RE} and therefore it can be assumed to control the cell dimensions (as the size of RE changes in the series of phases having the same T and X components). For the different RET_2X_2 phases it was observed that $f_{RE-X} \approx 0$ for T = Fe, Co, Ni, Cu and X = Si, Ge, whereas $f_{RE-T} \approx 0$ for T = Mn.

Structural aspects of chemical bonding in another family of phases formed by similar groups, RE–T–X, of elements (1:1:1, RETX compounds) have been analysed by BAZELA [1987] using the same technique.

For a general discussion on the dimensional analysis of the structures of the metallic phases with special reference to the hR57–Th_2Zn_{17}, tI26–$ThMn_{12}$ and hP6–$CaCu_5$ type structures see also PEARSON [1980].

7.2.6. Alternative definitions of coordination numbers

We have seen in the previous sections that the determination of the coordination number of an atom in a structure is clearly recognized as an important point in the

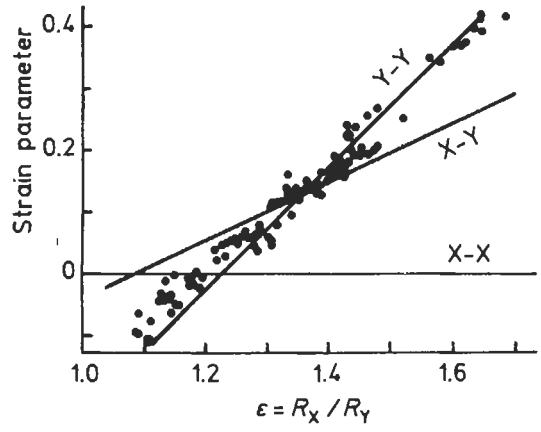

Fig. 55. Near neighbour diagram for binary phases with XY_2 formula belonging to the cF24–$MgCu_2$ structural type (according to PEARSON [1972]).

definition of that atom's contribution to the bulk material properties and in the characterization of the structure itself. Several properties (for instance, atomic size, atomic valence and magnetic properties and species stability and reactivity) are know to be coordination number dependent.

In many cases the coordination number (or ligancy) of a central atom is readily obtained by enumerating the number of neighbours; we have seen, however, that there are numerous cases where the criteria for the enumeration procedure may be ambiguous. As an introductory summary of this point see, for instance, CARTER [1978], O'KEEFFE [1979]).

As already pointed out by FRANK and KASPER [1958] the term "*coordination number*" *has been used in two ways* in crystallography. According to the first (more precisely defined, in principle) the coordination number, (CN), is the *number of the nearest neighbours* to an atom. According to this definition in the hexagonal close-packed hP2–Mg type structure CN is 6 unless the axial ratio c/a has exactly the "ideal" value $\sqrt{\frac{8}{3}}$ (= 1.63299..), in which case it is 12. (see fig. 26). In this structure the mentioned definition is seldom applied with rigour, that is, the CN in the hP2–Mg type structure is generally regarded as 12, even with c/a slightly different from the "ideal" value; that is not only the first group but also the very close second group of distances are considered together. More difficulties arise in less symmetrical structures and when there is a high coordination number. Near neighbours with slightly different interatomic distances are often found and it may be difficult to determine (and to state in an unambiguous way) how many should be considered as coordinating the central atom. Several schemes for the calculation of an "*effective*" *coordination* have been proposed.

According to FRANK and KASPER [1958] the computation of the coordination number may be based on the definition of the "*domain*" *of an atom* in a structure. This is the space in which all points are nearer to the centre of that atom than to any other. It is a polyhedron, (Voronoi polyhedron, Voronoi cell, Wigner–Seitz cell), each face of which

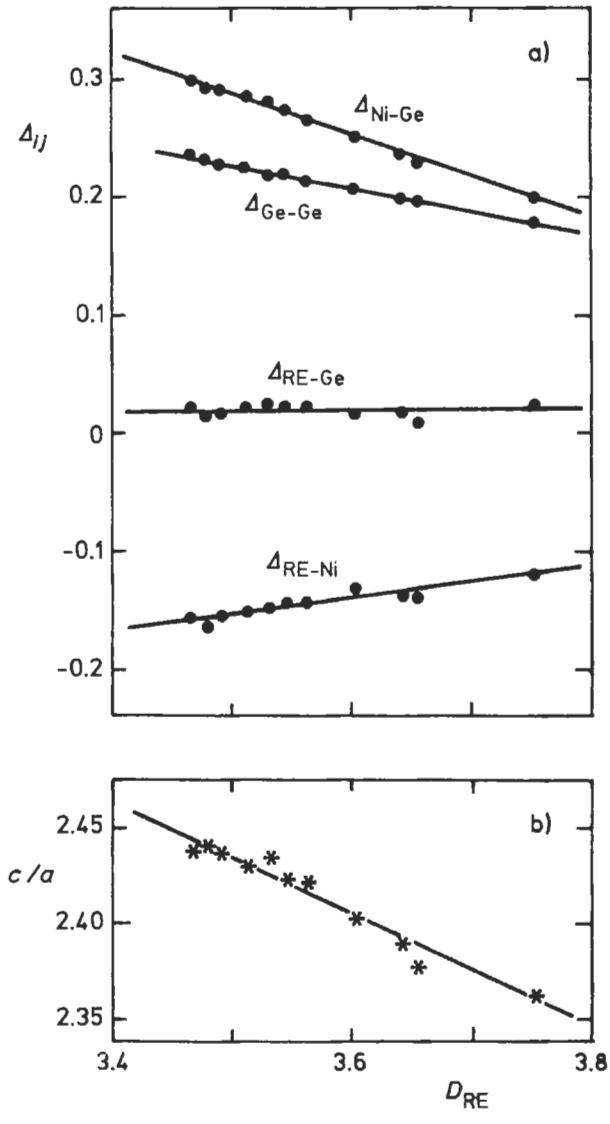

Fig. 56. $RENi_2Ge_2$ phases (RE=rare earth) with the tI10–$ThCr_2Si_2$ structure (from PEARSON [1985a]).
a) plot of Δ_{ij} ($= \frac{1}{2}(D_i + D_j) - d_{ij}$) versus D_{RE}.
b) plot of the c/a axial ratio of the cell versus D_{RE}.

is the plane equidistant between that atom and a neighbour. (Every atom whose domain has a face in common with the domain of the central atom is, by the Frank–Kasper definition, one of its neighbours). The counting of the faces of the *domain polyhedron* gives the number of neighbours: the set of neighbours is the "coordination shell". (The

coordination polyhedron, of course, is the polyhedron whose edges are the lines joining all the atoms in the coordination shell. The domain (Voronoi) polyhedron and the *coordination polyhedron*, therefore, stand in dual relationship, each having a vertex corresponding to each face of the other).

According to the Frank–Kasper definition the coordination number is unambiguously 12 in the hexagonal close-packed metals and assumes the value 14 in a body-centered cubic metal. Generally in several complex metallic structures this definition yields reasonable values such as 14, even when the nearest neighbour definition would give 1 or 2.

According, for instance, to O'Keeffe, however, this definition may lead to some difficulties (the value 14 for the bcc structure, higher than that of closest packing does not seem entirely reasonable, the difficulty becomes more acute in a structure as that of diamond for which a very high value, 16, is computed according to the mentioned definition).

For a better *quantification of the coordination number*, several alternative schemes have been proposed. For example, a simple procedure is based on the identification of a gap in the list of interatomic distances (and to add atoms up to this gap). A similar procedure (O'KEEFFE [1979]) may be to add atoms to the coordination polyhedron in order of increasing interatomic distances and to stop when the next addition would result in a non-convex polyhedron. BRUNNER and SCHWARZENBACH [1971] suggested *cutting off the coordinating atoms* at the *largest gap in the list of the interatomic distances* (see also sec. 7.2.7). According to BRUNNER [1977] the largest gap in the list of reciprocal interatomic distances is used to limit the coordination polyhedra. It has also been suggested to weight the contribution of the atoms according a weight that decreases with interatomic distances (BHANDARY and GIRGIS [1977]) or according to a bond strenghts of the Pauling type (BROWN and SHANNON [1973]). Non integral coordination numbers may of course be obtained.

In relation with the Frank–Kasper proposal, previously reported, O'KEEFFE [1979] suggested that coordinating atoms contribute faces to the Voronoi polyhedron around the central atom and their contributions are weighted in proportion to the solid angle subtended by that face at the center.

By using this definition increasing values of the (weighted) CN coordination number are obtained for the structures: diamond (4.54), simple cubic (6), body-centered cubic (10.16), face-centered cubic (12) (in agreement with the increasing packing density).

A more complex weighting scheme has been suggested by CARTER [1978] on the basis of the following assumptions:

The interactions of a central atom with its i^{th} neighbour is considered as being measured by a certain parameter A_i ($\Sigma A_i = A_{tot}$, finite).
The CN as a function of all the A_i should satisfy the following conditions:
— $CN(A_i)$ is dimensionless and ≥ 1 if any neighbours with non-zero A_i exists;
— $CN(A_i)$ is a continuous function of the A_i (its slope may not be);
— if N interactions exist such that $A_1 = A_2 = ... = A_N$, for all neighbours with non-zero A_i, then $CN(A_i) = N$;

References: p. 363.

— if some of the A_i are unequal, then $CN(A_i) < N$;
— if m of the A_i are equal and large and N-m equal are small, then $m < CN(A_i) < N$.

The formula proposed by Carter for the quantification is:

$$1 / CN = \Sigma_1^N \left(w_i A_i / \Sigma w_j A_j \right)^2 \tag{23}$$

(where w_i are finite weighting factors). Definitions and measures of A_i might include bond strenghts, bond energies, bond orders, etc.).

As an example, the structure of the CsCl type has been discussed by Carter using several criteria of evaluation of A_i. In a geometrical approach a weighted coordination number (varying from 8 to 14 to 6) as a function of atomic radii difference was described.

We may finally mention the so-called "effective coordination number" ECoN, proposed by HOPPE [1979] and HOPPE and MEYER [1980] computed by means of a rapidly converging function of the distances. According to Hoppe's scheme (which may be related to Brunner's suggestions previously mentioned), individual contributions $ECoN_j$, of all neighbours to the coordination number are summed together. Each contribution $ECoN_j$ quickly becomes vanishingly small with increasing atomic distances d_j according to an expression such as $ECoN_j = \exp(1-(d_j/d_m)^6)$, where d_m is a reference distance (the "mean fictive" atomic size) which has to be determined beforehand from the structure. The trend of the ECoN has, for instance, been discussed as a function of the axial ratio c/a for the hexagonal closest packing of spheres (hP2–Mg structure). Values of ECoN ranging from say 11.94 (for $c/a \approx 1.57$ as Ho or Er) to 12.02 (for the "ideal" c/a value, 1.633..,) and to 11.02 ($c/a = 1.856$, as for Zn) or to 10.74 ($c/a = 1.886$, as for Cd) have been computed. ECoN for different Laves phases have been presented. For a number of NaCl and CsCl type compounds, moreover, values have been given to show the dependence of ECoN as a function of varying ionic radii.

(For a discussion on the "effective coordination number" its relation with atomic size, bond-strength, Madelung constant, etc., see also SIMON [1983]. For a computation of the heats of formation based on the so-called effective coordination see a suggestion by KUBASCHEWSKI [1958], and for a discussion on the application and limits of this suggestion see BORZONE *et al.* [1993].).

7.2.7. Atomic-environment classification of the structure types

DAAMS *et al.* [1992] and DAAMS and VILLARS [1993, 1994] in a series of reviews have given an important contribution to the problem of the classification of intermetallic structural types, reporting a complete description of the *geometrical atomic environments* found in the structural types of cubic, rhombohedral and hexagonal intermetallic compounds, respectively. To *define* an *atomic environment* they used the maximum gap rule (see sec. 7.2.6.). The Brunner–Schwarzenbach method was considered, in which all interatomic distances between an atom and its neighbours are plotted in a histogram such as those shown in figs. 15, 23, 25, etc.. (The height of the bars is proportional to the number of neighbours, and all distances are expressed as reduced values relative to the shortest distance). In most cases a clear maximum gap is revealed (see, for instance, in

fig. 23 the gap between the second and the third bar). The atomic environment is then constructed with the atoms to the left of this gap (8+6 in the example of fig. 23). To avoid, in some particular cases, bad or ambiguous descriptions, however, a few additional rules have been considered. In those cases, for instances, where two (or more) nearly equal maximum gaps were observed, a selection was made in order to keep, in a given structure type, the number of different atomic environment types as small as possible. A convexity criterion for the environment polyhedron was also considered (the coordination polyhedron has to be defined as the maximum convex volume around only one central atom enclosed by convex faces with all coordinating atoms lying at the intersections of at least three faces). This rule was specially used where no clear maximum gap was detectable.

The different atomic environment types were characterized by a polyhedron code based on the number of triangles, squares, pentagons, hexagons, etc. that join each other in the different vertices (coordinating atoms). The *polyhedron code* gives the number of equivalent vertices with the number of faces in the above-mentioned sequence as an exponent. For example, a quadratic pyramid has four corners adjoining two triangles and one square (no pentagons or hexagons) and one corner adjoining four triangles: its code, therefore, is $4^{2.1.0.0}1^{4.0.0.0}$ (or briefly $4^{2.1}1^{4.0}$ with coordination number 5). The cube, 8 equivalent vertices, adjoining 3 squares, has the code $8^{0.3}$, the octahedron $6^{4.0}$ and the Frank–Kasper polyhedra have the codes $12^{5.0}$; $12^{5.0}2^{6.0}$; $12^{5.0}3^{6.0}$ and $12^{5.0}4^{6.0}$ (see sec. 6.6. and fig. 41).

DAAMS *et al.* [1992] have analysed all the *cubic structure types* reported in VILLARS and CALVERT [1985], after excluding all oxides and a few types with improbable interatomic distances, thus leaving 128 structure types representing 5521 compounds. Their analysis showed that these cubic structure types have 13917 atomic-environments (point sets). Of those environments 92% belong to one of the 21 most frequently occurring atomic-environment types, which are those reported in the following list:

$4^{3.0}$ (tetrahedron) – $4^{2.1}1^{4.0}$ – $6^{4.0}$ (octahedron) – $3^{5.0}3^{4.0}1^{3.0}$ – $8^{0.3}$ – $6^{5.0}3^{4.0}$ – $8^{5.0}2^{4.0}$ – $6^{6.0}4^{3.0}$ – $9^{2.2}2^{0.3}$ – $8^{5.0}2^{4.0}1^{6.0}$ – $12^{5.0}$ (icosahedron) – $12^{2.2}$ (cp. cubic) and $12^{2.2}$ (cp. hexagonal) (the same code describes the cubic as well as the hexagonal atomic environment of the ideal close-packing) – $10^{2.2}2^{5.0}$ – $10^{5.0}2^{6.0}1^{4.0}$ – $11^{2.2}2^{4.1}$ – $12^{5.0}2^{6.0}$ – $8^{0.3}6^{0.4}$ – $12^{5.0}3^{6.0}$ – $12^{5.0}4^{6.0}$ – $12^{6.0}6^{4.0}$.

Of the 5521 compounds crystallizing in the mentioned 128 structure types, 46% belong to a single-environment group (structures in which all atoms have the same type of environment), 37% have two environment types, 9% three and the rest four or more environments. (≈ 98% of the cubic compounds crystallize in structure types with 1, 2, 3 or 4 atomic environment types).

In a subsequent paper (DAAMS and VILLARS [1993]) the results of a similar classification of the rhombohedral intermetallic structure types were reported. The 195 *rhombohedral structure types* reported in VILLARS and CALVERT [1991] were analysed. 51 types have improbable interatomic distances or correspond to oxides with no intermetallic representatives and were excluded. The remaining 144 types (corresponding to 1324 compounds) were considered. It was observed that 14 atomic environment types are greatly preferred. Out of 6356 investigated point sets 71% belong to one of these 14 frequent atomic environment types which are those reported in the following list:

References: p. 363.

3 (loose triangle); $4^{3.0}$; $6^{4.0}$; $6^{1.2}$ (trigonal prism) $8^{0.3}$; $6^{5.0}3^{4.0}$; $6^{4.0}4^{3.0}$; $9^{2.2}2^{0.3}$; $12^{5.0}$; $12^{2.2}$ (cubic type); $10^{5.0}2^{6.0}1^{4.0}$; $12^{5.0}2^{6.0}$; $8^{0.3}6^{0.4}$; $12^{5.0}4^{6.0}$. (Compare this list with the previous one of the cubic compounds: notice that several atomic environment types are reported in both lists.)

Of the 1324 rhombohedral compounds crystallizing in one of the 144 types, 19% belong to a single-environment group, 15% combine two environment types, 25% three environments; 34% four and the rest , 7%, five or more environments ($\approx$ 94% of the rhombohedral compounds crystallize in structure types with 1, 2, 3 or 4 environment types).

The results of a similar analysis of the intermetallic *hexagonal structure types* have been reported by DAAMS and VILLARS [1994]. Of 442 structure types 315 (clearly intermetallic and correctly refined) were considered. In this case too it was observed that a small group of atomic environments is greatly preferred. The 23 atomic environment types most frequently occurring in the 315 hexagonal structure types are reported in the following list (to be compared with those previously reported for cubic and rhombohedral structure types):

3; $4^{3.0}$; 4; $6^{4.0}$; $6^{1.2}$; $3^{5.0}3^{4.0}1^{3.0}$; $8^{0.3}$; $6^{5.0}3^{4.0}$; $6^{4.0}4^{3.0}$; $6^{5.0}3^{4.0}1^{6.0}$; $9^{2.2}2^{0.3}$; $8^{5.0}2^{4.0}1^{5.0}$; $12^{5.0}$; $12^{2.2}$ (cubic); $12^{2.2}$ (hexagonal); $10^{5.0}2^{6.0}1^{4.0}$; $6^{4.1}3^{3.0}3^{2.2}1^{9.0}$; $12^{5.0}2^{6.0}$; $12^{2.2}2^{6.0}$; $6^{5.0}6^{3.0}2^{9.0}$; $12^{5.0}3^{6.0}$; $12^{5.0}4^{6.0}$; $12^{5.0}8^{6.0}$. (The 3 and 4 codes correspond to "irregular" atomic environment types. The reference atom is not included in the plane (volume) of the polygon (polyhedron) formed by the 3 (4) coordinating atoms.)

Out of 20131 poit sets investigated (belonging to 5646 compounds crystallizing in one of the aforementioned 315 hexagonal structure types), 81% (16392) belong to one of these 23 atomic environment types. Of the 5646 compounds, 14% belong to a single environment group; 35% combine two environment types; 32% three; 11% four and the rest (7%) five or more (93% of the hexagonal compounds crystallize in structure types with 1, 2, 3 or 4 atomic environment types).

As a result of these analysis several relations between structure types have been shown and discussed. Emphasis has been given to the fact that, in all the structure types considered (cubic, rhombohedral, hexagonal) it may be observed that: "Nature prefers one of the most symmetrical atomic environment types. Remarkably these atomic environment types (21 in the cubic structures, 14 in the rhombohedral and 23 in the hexagonal ones) are equally often found in single-environment up to poly-environment groups meaning that even in complex structures, symmetrical arrangements are preferred". The formation of the geometrically most simplest structure types containing a small number of different atomic environment types was also noticed.

As a comment, we may observe that the results of these analyses can be compared with the "*Stability Principles*" *stated by Laves* (see sec. 7.2.3.).

In conclusion to this section we may mention a paper by VILLARS and DAAMS [1993] concerning an atomic environment classification of the chemical elements. Critically evaluated crystallographic data for all element modifications (and recommended atomic volumes) have been reported. Special structural stability diagrams were used to separate atomic environment type stability domains and to predict the structure (in terms of